KAUNAS UNIVERSITY OF TECHNOLOGY

SOLVENTA KRAKAUSKAITĖ

ASSESSMENT OF A NON-INVASIVE ELECTRONIC CEREBROVASCULAR AUTOREGULATION MONITORING SYSTEM

Doctoral Dissertation

Technological Sciences, Electrical and Electronics Engineering (01T)

2017, Kaunas

The research for this dissertation was carried out over the period of 2013–2017 at the Health Telematics Science Institute of Kaunas University of Technology.

The doctoral dissertation was supported by the Research Council of Lithuania for scientific visits and by awarding with promotional scholarships.

Scientific supervisor:

Arminas RAGAUSKAS, Prof., DSc (Kaunas University of Technology, Technological Sciences, Electrical and Electronics Engineering – 01T).

Medical advisor:

Teodoro Forcht DAGI, MD, DMedSc (Harvard University, Biomedical Sciences, Medicine – 06B).

Editor:
Dovilė Dumbrauskaitė (Publishing House “Technologija”)

ISBN 978-609-02-1362-9

The bibliographic information about the publication is available in the National Bibliographic Data Bank (NBDB) of the Martynas Mažvydas National Library of Lithuania

KAUNO TECHNOLOGIJOS UNIVERSITETAS

SOLVENTA KRAKAUSKAITĖ

NEINVAZINĖS SMEGENŲ AUTOREGULIACIJOS STEBĖSENOS ELEKTRONINĖS SISTEMOS ĮVERTINIMAS

Daktaro disertacija
Technologijos mokslai, elektros ir elektronikos inžinerija (01T)

2017, Kaunas

Disertacija rengta 2013–2017 metais Kauno technologijos universiteto, Sveikatos telematikos mokslo institute.

Mokslinius tyrimus rėmė Lietuvos mokslo taryba, skiriant stipendiją už akademinius pasiekimus.

Mokslinis vadovas:

Prof. dr. Arminas RAGAUSKAS (Kauno technologijos universitetas, technologijos mokslai, elektros ir elektronikos inžinerija – 01T).

Medicinos konsultantas:

Teodoro Forcht DAGI, MD, DMedSc (Harvardo universitetas, biomedicinos mokslai, medicina – 06B).

Interneto svetainės, kurioje skelbiama disertacija, adresas:
http://ktu.edu

Redagavo:
Dovilė Dumbrauskaitė (leidykla „Technologija“)

ISBN 978-609-02-1362-9

Leidinio bibliografinė informacija pateikiama Lietuvos nacionalinės Martyno Mažvydo bibliotekos Nacionalinės bibliografijos duomenų banke (NBDB)

ACKNOWLEDGEMENTS

It is a distinct pleasure to express gratitude to those who made this thesis possible. First and foremost, I am grateful to my thesis supervisor Arminas Ragauskas, Prof., DSc. This work would not have been possible without his constant mentoring, advice, encouragement, our exchange of ideas, and discussions. Whenever there were any obstacles to overcome, Prof. Ragauskas dedicated his time to go over my concerns to get them completely resolved. I am immensely thankful for his support, on both the professional and personal level. He went above and beyond the regular responsibilities of a supervisor and kept me focused on my thesis and academic path. My sincere gratitude goes to professor Arminas Ragauskas.

I would like to express gratitude to an excellent advisor Theodoro Forcht Dagi, MD, DMedSc. I was touched by his impeccable standards of ethics which are simply exemplary. I feel that I have learned from him even more on this subject than about the objects of this dissertation. I have spent a sufficient amount of time with doctor Dagi during my fellowships at Harvard Medical School of Harvard University. He took time out of his day to meet and discuss various research facets that made an impact on my thesis.

Mr. Aidanas Preiksaitis, MD, and Mr. Saulius Rocka, MD, Prof., from Vilnius University generously provided the patients' data from traumatic brain injury patients study that was crucial for the assessment of the method presented in this thesis. Also, interesting and helpful discussions, ideas and support throughout the implementation of thesis guided me to explore the mechanism of cerebrovascular autoregulation and its evaluation capabilities. They shared their experience as neurosurgeons which was valuable for assessing the technology of cerebrovascular autoregulation monitoring on patients with severe brain injury. The role of both physicians was significant in fulfilling the tasks of this thesis.

Worldwide renowned and distinguished Dr. Rimantas Benetis, MD, Prof., and an internationally prominent anaesthesiologist Dr. Edmundas Sirvinskas, MD, Prof., with the team of brilliant doctors Birute Kumpaitiene, MD, and Milda Svagzdiene, MD, from the Lithuanian University of Health Sciences were remarkably cooperative by providing data from a study of patients undergoing cardiac surgery with cardiopulmonary bypass. Our fruitful collaboration inspired to advance the field of cerebrovascular autoregulation status monitoring with cardiopulmonary bypass. I owe my sincere gratitude to this amazing team of top-tier doctors for their kind generosity and contribution to my thesis.

I am honoured to have colleagues from Health Telematics Science Institute of Kaunas University of Technology who are top experts and professionals in the field of non-invasive brain monitoring. Without their contribution and support this thesis would not be as innovative and heavy as it is. They kept my attention on high standards by fostering challenging discussions, providing constructive criticism and advice, and giving me feedback during the execution of my thesis.

I would especially like to express my vast gratitude to Vytautas Petkus, DSc. He was a tremendous assistance in exploring the complex topic of cerebrovascular autoregulation. I am grateful for all intense and long discussions we had. He inspired me to dip into the object of this thesis. His passion and dedication to advance the cerebrovascular autoregulation monitoring technologies are tenacious, bold and champion. I feel blessed to have learned from him.

Finally, my huge gratitude for their contribution goes to the people in my personal life. My friends' support and understanding inspired me and kept me on track which made my life more balanced. I feel infinite gratefulness to my parents, especially my beloved Mother, for her love, patience and encouragement. They have raised me, nurtured me, and have given me the confidence to be bold and inquisitive and seek intelligence. My Mom always fostered me to grow intellectually, emotionally, spiritually above and beyond my own limits. I dedicate the rewards of my effort to my parents.

I am thankful to Neural Analytics, Inc. (Los Angeles, USA) for opening the attitude of diverse and volatile research experience. My appreciation to Research Council of Lithuania and Harvard Medical School for two fellowships. I also thank the Biomedical Engineering Institute of Kaunas University of Technology for laying the grounds in starting my doctorate path.

I hope the contributions of this thesis will eventually be helpful in saving lives and improving the quality of life of those who suffer from brain injury or are undergoing cardiac surgery.

CONTENT

ABBREVIATIONS

ABP	Arterial Blood Pressure
AUC	Area Under Curve
ASL	Arterial Spin Labeling
BP	Blood Pressure
BF	Blood Flow
CA	Cerebrovascular Autoregulation
CABG	Coronary Artery Bypass Graft
CBF	Cerebral Blood Flow
CBFV	Cerebral Blood Flow Velocity
CPB	Cardiopulmonary bypass – a replacement of the function of the heart and lungs during surgery. It sustains the circulation of blood and the oxygen of the body.
CPP	Cerebral Perfusion Pressure
CRV	Central Retinal Vein
CSF	Cerebrospinal Fluid
CT	Computed Tomography
CVR	Cerebrovascular Resistance
DCS	Diffuse Correlation Spectroscopy
DSC-MRI	Dynamic Susceptibility Contrast MRI
DPOAE	Distortion Product Otoacoustic Emission
DAI	Diffuse Axonal Injury
DC	Deterioration of Cognition
EVD	External Ventricular Drainage
EEG	Electroencephalography
EM	Electromagnetism
FV	Flow Velocity
FVEP	Flash Visual Evoked Potential

GCS	Glasgow Coma Scale – a neurological scale that gives the recording of conscious state of a person for initial and subsequent assessment. Brain injury is classified as follow: • Severe: GCS 3–8; • Moderate: GCS 9–12; • Mild: GCS 13–15.
GOS	Glasgow Outcome Score - a neurological scale of patients experienced brain injuries, allowing to divide them into groups for standardised descriptions of the degree of recovery.
IBV	Intracranial Blood Volume
ICP	Intracranial Pressure
IF	Impact factor refers to the journal citation frequency with which an average article has been cited in a year.
In Situ	In the normal location. An in Situ experiment is confined to site of origin in the body without touching other parts.
In Vivo	In a living organism. An in Vivo experiment is conducted in a living organism.
LCAI	Longest Cerebrovascular Autoregulation Impairment
LLA	Lower Limit of Autoregulation
MAP	Mean Arterial Pressure
MCA	Middle Cerebral Artery
MRI	Magnetic Resonance Imaging
Mx	Pearson's correlation coefficient between cerebral blood flow and arterial blood pressure.
NIR	Near-infrared
NIRS	Near-infrared Spectroscopy
OA	Ophtalmic Artery

OAE	Otoacoustic Emission
Observational study	An observational study draws to the independent variable of population (or sample) which is not under the control of the investigator because of ethical concerns or logistical constraints.
OCTR	Optical Coherence Tomography of Retina
ODM	Ophthalmodynamometry
ONSD	Optic Nerve Sheath Diameter
ONSU	Optic Nerve Sheath Ultrasonography
optCPP	Optimal CPP
OSASW	Width of the Orbital Subarachnoid Space
PI	Pulsatility Index
PET	Positron Emission Tomography
PCT	Perfusion Computed Tomography
POCD	Post-operative Cognitive Dysfunction
PRx	Pressure-reactivity index which is Pearson's correlation coefficient between intracranial pressure and arterial blood pressure.
Prospective study	A prospective study is a cohort study that is conducted over a certain timeframe with a group of similar subjects who differ to certain factors under the frame of study in order to determine how these factors affect the rates of a certain outcome.
PSG	Plethysmography
SD	Standard Deviation
SPECT	Single-photon Emission Computed Tomography
TBI	Traumatic Brain Injury
TCD	Transcranial Doppler
TDF	Thermal Diffusion Flowmetry

TMD	Tympanic Membrane Displacement
US	Ultrasound
VOP	Venous Outflow Pressure
vPRx1	Pearson's correlation coefficient between intracranial blood volume and arterial blood pressure.
vPRx2	Pearson's correlation coefficient between slow waves of intracranial blood volume and pulse waves of intracranial blood volume.

INTRODUCTION

Relevance of the research

The human brain has a great metabolic demand and requires adequate nutritional flow. The brain's vascular system must respond to changes in arterial blood pressure (ABP) or intracranial pressure (ICP) to sustain constant cerebral blood flow (CBF). By means of myogenic, neurogenic, or metabolic mechanisms cerebral blood vessels have an inherent ability to maintain CBF constant over a range of systemic ABP levels (Paulson et al, 1990; Chillon and Baumbach, 2002). A mechanism which maintains cerebral blood flow stable despite fluctuations of perfusion pressure is called cerebrovascular autoregulation (CA).

The importance of this research cannot be overstated. Traumatic brain injury (TBI) is the third most common cause of death in the United States of America (Faul et al, 2010). In the European Union, TBI is a major health problem of people under 40 years old (TBIcare project, 2014). It is important to emphasize that about 1,000 brain and nervous system disorders result in more hospitalizations than any other disease group, including heart disease and cancer. Neurological diseases affect more than 50 million Americans annually and cost $500 billion. Additionally, mental disorders affect 44 million adults each year at a cost of $148 billion. The advancement and headway in research and studies could diminish these costs, for example, by discovering how to save $50 billion in annual health care costs (Brain Facts, 2017).

Unfortunately, the impairment of CA has an impact on patients' outcome (Sviri and Newell, 2010; Czosnyka et al, 2007). CA status monitoring of these patients allows a physician to establish the optimal, individualized CA-targeted treatment, which is associated with better clinical outcomes and higher survival rates. The optimal cerebral perfusion pressure (optCPP) is a criterion for stabilizing the CA status in an individual patient (Aries et al, 2012; Steiner et al, 2002). Thus, it is essential to know the real-time status of CA and the individualized treatment strategy should be re-valuated regularly over the time-course of the CA status (Rasulo et al, 2012; Andrews et al, 2008). According to a statement for healthcare professionals from the Neurocritical Care Society and the European Society of Intensive Care Medicine, continuous bedside monitoring of CA is now accomplishable and should be a part of multimodality monitoring (Brain Trauma Foundation, 2007). The optimal CPP-targeted treatment strategy is also suggested for individualizing patients' treatment by Consensus Summary Statement of the International Multidisciplinary Consensus Conference on Multimodality Monitoring in Neurocritical Care in 2014 (Le Roux et al, 2014). The treatment is based on the identification of the optimum CPP value at which cerebrovascular reactivity works best (Aries et al, 2012; Steiner et al, 2002; Rasulo et al, 2012; Andrews et al, 2008), and maintaining CPP close to optimum over the treatment period.

Studies to support arterial blood pressure of 50 mmHg for the adult lower limit of autoregulation (LLA) based on a publication by Lassen (1959) were performed on different groups of subjects, including one study with pregnant women (McCall,

1953). The lower limit of Lassen's curve originated from this study. This hemodynamic management has been applied for years until, more recently, Drummond (Drummond, 1997) raised some ideas about the applicability of LLA of 50 mmHg by providing findings of ABP ability to manage LLA. It is not sensible to apply a single hemodynamic management strategy for patients with diverse states and physiology. Thus, a paradigm of individualized management by diminution in ABP as a percentage of a patient's baseline ABP has been proposed (Strandgaard, 1976; Finnerty et al, 1954).

CA monitoring outside of the boundaries of clinical neuroscience had not been applied previously until non-invasive measurements of CBF by using transcranial Doppler (TCD) and/or near-infrared spectroscopy were applied (Czosnyka et al, 1996; Brady et al, 2007). This individualized application allows to maintain ABP by ensuring CBF consummation according to cerebral metabolic demand.

Several approaches of the CA status estimation are known based on the measurement and analysis of cerebral perfusion pressure (CPP) and the slow fluctuations of cerebral blood flow velocity (Czosnyka et al, 1996; Eames et al, 2002; Czosnyka et al, 2012), and the measurement of cerebral vascular resistance in relation to the change in CPP (Czosnyka et al, 1997). However, a more clinically practical method for continuous CA assessment is performed by calculating the pressure reactivity index (PRx) proposed by Marek Czosnyka, PhD, Prof. (Cambridge University, UK) as correlation between ICP(t) and ABP(t).

The motivation of this research is to further our understanding of cerebrovascular autoregulation, including what processes are occurring and why; to discover the technological solutions to prevent from many devastating disorders of the brain; and to advance the enduring scientific quest to monitor the cerebrovascular autoregulation.

The object of this thesis is a fully non-invasive cerebrovascular autoregulation monitoring system based on the proposal of Prof. Arminas Ragauskas, DSc, and Vytautas Petkus, DSc. This CA monitoring technology is based on PRx calculation using non-invasively recorded intracranial blood volume fluctuations together with ABP slow waves (Eames et al, 2002) instead of ICP or CBF waves (Czosnyka et al, 1996; Reinhard et al, 2003). The results of prospective clinical trials by using a combination of apparatus showed significant correlation between PRx and outcomes of the patients. However, the adaptation of a CA monitoring system in clinical practice is still unavailable due to an unknown relationship between the technological solution and the diagnostic value rendered to physicians; and no existence of "Gold Standard" to compare the results with. One of the propositions to this issue would be to investigate the current system dedicated for non-invasive CA monitoring, which requires the accumulation of new scientific knowledge and the technological development of a fully non-invasive CA monitoring system.

Scientific-technological problem and work hypothesis

This thesis tackles a scientific-technological problem: *Can a non-invasive cerebrovascular autoregulation monitoring system based on intracranial blood volume measurement provide added value in clinical practice?*

This problem raised a hypothesis: *it is possible to obtain added value in clinical practice to diagnose impairments of cerebral autoregulation and to measure the duration of impairments by using the ultrasonic "time–of-flight" method and an electronic system, when its acoustic trajectory crosses the cerebral parenchyma where the capillaries and arterioles responsible for cerebrovascular autoregulation are located.*

To test this hypothesis and to assess or validate the ultrasonic "time-of-flight" CA monitor, it is methodologically necessary to have the "Gold Standard" CA monitor. However, such monitor does not exist, thus this thesis proposes to assess the ultrasonic "time–of-flight" CA monitoring method by prospectively accumulating CA status monitoring data from two extreme groups of patients': from severe TBI (it is highly possible that CA will be impaired due to severe brain injury) to healthy brain before cardiac surgery with CPB (it is much less possible that CA will be impaired).

The aim and objectives of the work

The aim of this research is to assess the clinical applicability and diagnostic value of a non-invasive electronic CA status monitoring system by performing experimental clinical studies and analysing new experimentally collected empirical data.

Tasks to accomplish the aim of this thesis:

1. To analyse the existing literature including latest patents, publications of measurement methods and techniques of cerebral blood flow, intracranial pressure, and arterial blood pressure. To produce conceptual foundations for understanding the physiological basis of cerebrovascular autoregulation processes through the analysis of theoretical approaches. To advance the understanding of complex, non-linear brain functions where human intuition fails through rigorous theory, modelling, and statistics. To determine the need of CA monitoring in different clinical applications.

2. To investigate innovative non-invasive CA monitoring technology proposed by A. Ragauskas and V. Petkus to understand cerebral autoregulation and treat its disorders. To establish new mechanisms to expand the set of empirical information.

3. To carry out a prospective comparative study of CA status indexes: invasive PRx vs non-invasive vPRx1 and vPRx2 derived from non-invasively monitored IBV waves using the investigated electronic CA monitoring system on traumatic brain injury patients. To produce a dynamic picture of the functioning cerebrovascular

autoregulation mechanism by developing and applying an improved non-invasive cerebrovascular autoregulation monitoring method.

4. To carry out an outcomes study of traumatic brain injury patients. Link TBI patients' outcomes with the performance of cerebrovascular autoregulation monitoring technology.

5. To perform an observational study of patients undergoing cardiac surgery with cardiopulmonary bypass. To collect empirical data and assess the conditions causing CA impairment and deterioration of cognitive abilities for patients undergoing cardiac surgery with cardiopulmonary bypass.

To integrate new scientific-technological and conceptual approaches produced in tasks 1–5 to explain why and how dynamic cerebrovascular autoregulation works by answering four key questions posed by Donnelly et al. (2015):

1) What is it?
2) How do we measure it?
3) Why is it important?
4) Can we use it as a basis for therapy?

Scientific novelty

For the first time, the non-invasive measurement system was assessed which derives parameters describing CA after non-invasive CA monitoring studies in subjects with different trauma levels – from healthy brain to severe TBI (Fig. 1.2.).

The diagnostic pressure reactivity index (PRx) used to assess CA was calculated in a conventional way; and by using in this thesis investigated non-invasive electronic monitoring system was statistically significant after the prospective clinical studies of the non-invasive CA monitoring sessions of severe traumatic brain-injured subjects and patients undergoing cardiac surgery with cardiopulmonary bypass.

The new scientific data which has been used to assess the technology needed for the method of non-invasive CA calculation from intracranial blood volume (IBV) signal was received.

Research methods and tools

The non-invasive CA monitoring system developed at the Health Telematics Science Institute of Kaunas University of Technology was used to perform the prospective clinical studies of severe traumatic brain-injured subjects and patients undergoing cardiac surgery with cardiopulmonary bypass as well as the study of healthy volunteers. The methodology of In Vivo and In Situ prospective experimental research was used.

The study of healthy volunteers was performed at the Health Telematics Science Institute of Kaunas University of Technology. The study of severe traumatic brain-injured patients was carried out at the Intensive Care Unit of the Republican Vilnius University Hospital. The study of patients undergoing cardiac surgery was

carried out at the Hospital of Lithuanian University of Health Sciences, Kaunas Clinics.

MATLAB software and ICM+ were used to process the data recorded during the studies.

MATLAB software was used to implement statistical analysis of the data.

Practical meaning of the thesis

A clinically assessed and experimentally tested non-invasive CA monitoring system.

It has been shown that the non-invasive CA monitoring system conforms with the invasive method (in clinical practice dominant CPP range of values) and the measurement duration of the procedure satisfies the requirements of clinical practice.

The results produced valuable scientific knowledge.

Statements submitted for defence

The study of effectiveness of the proposed cerebral autoregulation state index using the non-linear scale-forming method on 20 healthy volunteers shows dependence between the changes of ultrasonic "time-of-flight" pulse waveform and body position.

A comparative clinical study of 39 traumatic brain injury subjects shows a strong correlation between two different CA value calculation methods – with (vPRx1) and without (vPRx2) an arterial blood pressure reference signal.

The outcomes study of 39 traumatic brain injury subjects shows high a correlation between the calculated CA value and subjects' outcome.

A prospective clinical study of 65 patients undergoing cardiac surgery with cardiopulmonary bypass shows the relevance of monitoring CA, and regulating adjustable physiological parameters during operation according to its values to improve the post-operative outcome.

The non-invasive electronic CA monitor gives a reliable estimate of CA state to satisfy clinical requirements.

Dissemination of findings

- Four publications related to the doctoral thesis and published in the scientific journals with IF (see Publications on page 120).
- Three publications in reviewed journals (see Publications on pages 120, 121).
- Results presented at 14 international conferences in 10 countries: Sidney (Australia), New York (USA), Rome (Italy), Los Angeles (USA), Jaju Island (South Korea), Southampton (England), Hague (Netherlands), Miami (USA), Budapest (Hungary), Cambridge (USA), Warsaw (Poland), Berlin (Germany); and at a national conference in Vilnius (Lithuania) (see Publications on pages 121–123).

Structure of the dissertation

The dissertation consists of an introduction, five chapters, conclusions, a list of references, a list of scientific publications and an appendix.

Chapter one of the dissertation discusses the cerebrovascular autoregulation measurement and CA index calculation methods currently used in clinical practice and clinical research trials. The possibilities of validation and the necessary research of non-invasive CA value measurement system are highlighted. The problems of non-invasive CA value measurement system assessment are analysed and the requirements for successful problem solving are formulated.

Chapter two proposes and explains the technological combination of a non-invasive CA monitoring system. Comprehensive mathematical processing of data with examples on healthy volunteers are provided.

Chapter three presents the results of a comparative clinical study of severe traumatic brain-injured patients using the non-invasive CA monitoring system.

Chapter four introduces the findings of an outcomes study of severe traumatic brain injury subjects including GOS, age, optCPP, and the duration of impaired CA.

Chapter five presents the findings of a prospective clinical study of patients undergoing cardiac surgery with cardiopulmonary bypass.

The total volume of the thesis is 126 pages. There are 40 figures, 12 tables and 221 references in the text.

1. CEREBROVASCULAR AUTOREGULATION ASSESSMENT: METHODOLOGICALLY DIFFERENT MEASURING APPROACHES WITH(OUT) THE INFLUENCE ON RESULTS AND CLINICAL APPLICATION

In 1926, an American neurosurgeon Harvey Cushing formulated the doctrine still relevant today (Cushing, 1926) stating that the brain volume, the blood volume and cerebrospinal fluid volume are constant in an intact skull. An increase in one component influences a decrease in the other components. This interdependent relationship provides a compensatory reserve, also known as spatial compensation. For young people, it is 60–80 ml, for the elder it is 100–140 ml because of brain atrophy (Gjerris and Brennum, 2004).

In a normal physiological state, cerebral autoregulation maintains a constant blood flow supply to the brain: expanding or narrowing arterioles and capillaries (Fig. 1.1.). However, this autoregulation is effective when the mean arterial pressure (MAP) is from 60 to 160 mmHg which are the theoretical regular limits of a healthy subject. Normal intracranial pressure (ICP) is relatively low (7–15 mmHg). CPP theoretical regular limits are from 50 to 150 mmHg and it is principally dependent on the MAP; however, these limits vary for individual patients (Fig. 1.1. b)). The pressure above the upper limit of autoregulation can cause cerebral edema or hyperemia, while the pressure below the minimum threshold causes a lack supplement of blood flow and cerebral ischemia, thus the formation of an edema is induced, which ultimately leads to a poor condition of the patient. On the other hand, a brain injury can lead to vasomotor paralysis when autoregulation stops working and cerebral blood flow depends entirely on CPP (Gjerris and Brennum, 2004; Smith, 2008; Czosnyka et al, 2007; Bratton et al, 2007; Akopian et al, 2007; Knudsen et al 2004).

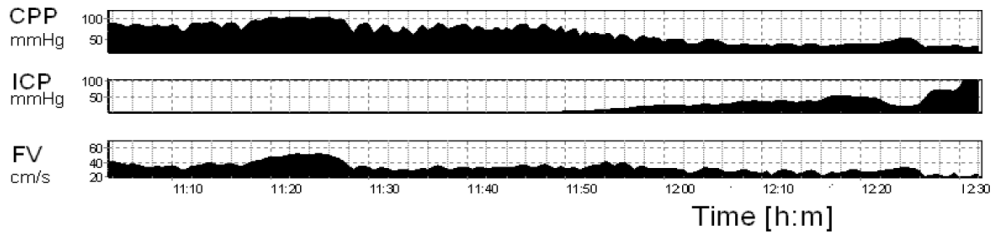

a)

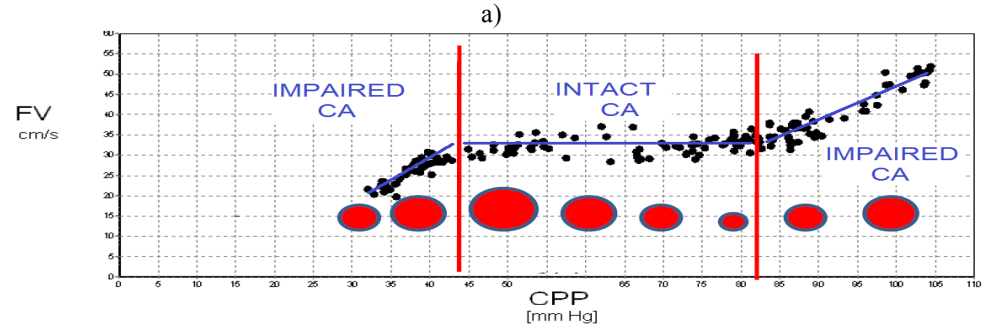

b)

Fig. 1.1. A graphical explanation of cerebral autoregulation status: a) graph shows dependencies of CPP, ICP, FV; b) the boundary of intact autoregulation: CPP lower limit is 44 mmHg and the upper limit is 82 mmHg; red circles show the changes of diameter of arterioles and capillaries when CA is intact and impaired. Adapted from Lazardis et al., 2013.

In case of intracranial hypertension or arterial hypotension when ICP rises, CPP is reduced. CPP is calculated:

$$CPP = ABP - ICP \tag{1}$$

In addition, elevated ICP can cause a hernia with irreversible brain damage and risk of death (Gjerris and Brennum, 2004; Smith, 2008; Bratton et al, 2007; Treggiari et al, 2007). Treatment to reduce ICP should be initiated at a pressure above 14.7–20 mmHg, depending on the reason of raised pressure. There are many causes of increased ICP; some are mentioned in Table 1.1. ICP monitoring is used in a variety of neurological and neurosurgical conditions.

Table 1.1. The clinical conditions in which ICP monitoring is used

Traumatic brain injury
Intracerebral hemorrhage
Subarachnoid hemorrhage
Malignant hydrocephalus
Malicious infarction
Cerebral edema
Ventricular encephalopathy
Central Nervous System infection

It is not enough to monitor the ICP, arterial blood pressure and cerebral perfusion pressure to optimize treatment decisions. It is essential to know the real-time status of CA.

During cardiac surgery with CPB when there is no brain injury and after brain injury (Fig. 1.2), cerebral blood flow and its regulation functions are rapidly impaired, intracranial pressure increases and tissues start swelling (Cipolla, 2009). The main clinical goal is to protect the brain from secondary damage, increased intracranial pressure and impaired cerebral autoregulation for healthy and injured brain, which is the object of this thesis. It is proven that continuous monitoring and regulation of adjustable parameters, such as CA, can significantly reduce the patient's post-operative disability or even the risk of death (Joshi, 2012). The measurements of these parameters are discussed in more detail below.

Fig. 1.2. Levels of brain trauma

1.1. Methods for testing dynamic cerebrovascular autoregulation

It is essential to evaluate the CA status by observing the response of cerebral perfusion to an alteration in blood pressure (BP). There are several potential methods to induce oscillations or rapid changes in BP (Beek et al, 2008).

Oscillations in ABP:

Breathing test (Diehl et al, 1995), squatting test (Birch et al, 1995), thigh cuff method (Aaslid et al, 2007), lower body negative pressure test (Birch et al, 2002; Hamner et al, 2004) produces sinusoidal oscillations in ABP. Cerebral blood flow velocity (CBFV) follows the oscillations after when ABP oscillations are forced at a determined frequency. These oscillations in BP and CBFV are used to assess dynamic CA.

Step decrease in ABP:

1. Aaslid et al (1989) presented the thigh cuff method. A rapid deflation of cuffs around both thighs after an inflation (duration approximately 2 min) induces BP step decreases.
2. Cold pressor test is based on placing a hand in ice water or on isometric exercise (for example, sustained hand grip) which result in augmented BP caused by the stimulation of sympathetic pathways for the assessment of CA (Micieli et al, 1994; Roatta et al, 1998; Giller et al, 2000). Unfortunately, the CBFV response to both tests is heterogeneous.
3. A head-up tilt test is a different stimulator of the sympathetic nervous system (Oblak et al, 2002). CBFV diminishes during head-up tilting, and this test has been used to assess dynamic CA (Schondorf et al, 1997).
4. The Valsalva maneuver is a simple and feasible technique which induces the elevation of intra-thoracic and intra-abdominal pressure by straining. These characteristic changes in BP (decrease) and CBFV are used for the assessment of CA (Tiecks et al, 1995).

5. Lower body negative pressure test causes a decrease of CBFV (Levine et al, 1994; Zhang et al, 2007). The exact mechanism which triggers the reduction of CBFV remains uncertain. Recently, it was proven that this CBFV decrease is not because of cerebral vasoconstriction caused by sympathetic activation (Zhang et al, 2007).
6. Sit-to-stand test is a straightforward method which affects a depressor change in BP and CBFV for the assessment of dynamic CA. Cardiopulmonary baroreflex mechanisms cause a decrease in peripheral resistance when standing which reduces the BP (Sprangers et al, 1991). This orthostatic hypotension that causes a decrease in BP does not exist in head-up tilt testing (Wieling et al, 2007).

1.2. The quantification of dynamic cerebral autoregulation

The relationship between CBF and ABP must be quantified when variations of ABP are caused. In this subchapter, the methods that approach the relationship between ABP and CBF are discussed as if they were used in clinical practise directly.

1. Gosling's pulsatility index (PI)

PI is used to reverberate cerebrovascular resistance (CVR) (Gosling et al, 1971). This index is defined as the difference between systolic and diastolic peaks of CBFV divided by the mean CBFV [mmHg per cm/sec]:

$$PI = \frac{CBFV_S - CBFV_D}{CBFV_{mean}} \quad (2)$$

2. Cerebrovascular resistance

CVR linear system analysis as a measure of autoregulation which examines the transfer of ABP oscillations to CBF. It quantifies the magnitude to which the input signal (ABP) is reverberated in the output signal (CBFV). The resistance of the arterioles is the regulator between the input and output. According to Ohm's law, this resistance is defined as mean BP/CBF [mmHg per mL/min]:

$$CVR = \frac{BP_{mean}}{CBF_{mean}} \quad (3)$$

3. Critical closing pressure

Another estimate for vasomotor resistance is the critical closing pressure, determined from the systolic–diastolic pressure–flow relationship within each heartbeat. The critical closing pressure of the cerebral circulation indicates the value of BP at which CBF is projected to approach zero (Panerai, 2003). This value is obtained by linear extrapolation of the BP and CBFV values in the systolic to diastolic range which were obtained within each cardiac cycle.

4. *Rate of recovery*

The time of CBFV recovery after a single pressor or depressor stimulus is taken as a measure for the efficiency of dynamic CA. The rate of recovery is defined as normalized changes in CVR per second during a BP decrease/increase (Aaslid et al., 1989) [CBFV/sec]:

$$Rate\ of\ recovery = \frac{\Delta CVR/\Delta T}{\Delta BP} \quad (4)$$

5. *Autoregulatory index*

Tiecks et al. (1995) introduced the autoregulatory index as variations in CVRi in relation to the change in ABP during thigh cuff inflation and deflation. A hypothetic CBFV curve without autoregulation is calculated. Then eight other different computer models of possible flow-velocity curves are calculated with a higher degree of CA. An autoregulatory index of 0 indicates that CBFV follows ABP. The index of 9 indicates that CBFV recovers faster than ABP.

Panerai et al. (1998) showed that this computer-based model might be used to grade cerebral autoregulation by using baseline recordings of ABP and CBFV and by calculating the impulse response function. This function implies the relationship between ABP and CBFV after a short disturbance in BP.

6. *Correlation index*

Czosnyka et al. (1996) proposed a Pearson's correlation coefficient between consecutive samples of averaged CPP and FV for every 3-min period calculating the correlation index Mx for subjects with head injury. Lang et al. (2003) showed that the estimation of this correlation index is valid for replacing CPP with ABP in traumatic brain injury patients. Fortunately, this eliminates the need for invasive measurement of intracranial pressure.

However, the Mx has not been validated in other patient groups. The proposed cut-off values were not valid in healthy subjects (Yam et al, 2005).

The same group of researchers led by M. Czosnyka proposed a derivative CA assessment pressure – reactivity index PRx which defines the relationship between ICP(t) and ABP(t). PRx is calculated from the continuous correlation between slow waves (20 s to 2 min periods) of ICP and ABP.

In this thesis, I will address the correlation index as a CA assessment tool. To evaluate the dynamic process of cerebrovascular autoregulation, monitoring of ABP, ICP and CBF with high temporal resolution are essential, as stated in formulas in Table 1.2. which presents the existing combinations of CA index Mx or PRx calculation. Various invasive and non-invasive technologies to monitor these parameters (CBF, ABP, ICP) are discussed in next sections of this chapter.

Table 1.2. Parameters used for Mx and PRx calculation

$\boldsymbol{PRx = r\{ICP_{SW}(t \ldots \Delta t); ABP_{SW}(t \ldots \Delta t)\}}$
$\boldsymbol{Mx = r\{CBF_{SW}(t \ldots \Delta t); ABP_{SW}(t \ldots \Delta t)\}}$

SW – slow waves; r – Pearson correlation coefficient; t – time moment; $\Delta t = 120…600$ sec – time window for calculation of correlation coefficient.

1.3. Cerebral blood flow measurements

Table 1.3. provides the existing invasive and non-invasive cerebral blood flow measurement techniques.

Table 1.3. Invasive and non-invasive CBF measurement methods

Invasive methods	**Non-invasive methods**
Direct measurements of intravascular tracers in the blood stream:	X-ray techniques:
• Kety–Schmidt arteriovenous difference method	• Xenon-enhanced computed tomography
• Jugular thermodilution	• Perfusion computed tomography
Nuclear methods:	Magnetic Resonance Imaging:
• Intra-arterial injection of a radioactive inert gas (^{133}Xe or ^{85}Kr)	• Dynamic susceptibility contrast/perfusion-weighted MRI
• Single-photon emission computed tomography	• Arterial spin labeling
• Positron emission tomography	Optical techniques:
Thermal Diffusion Flowmetry	• Diffuse correlation spectroscopy
	• Near-infrared spectroscopy
	Ultrasound technique

1.3.1. Invasive methods

1.3.1.1. Direct measurements of intravascular tracers in the blood

1. Kety–Schmidt arteriovenous difference method

Kety and Schmidt (1945) set the foundation for the development of various CBF measurements in the human brain, assuming nitrous oxide (N_2O) as diffusible intravascular tracer (Traystman, 2004). The dynamics of $[N_2O]^a$ (artery) and $[N_2O]^v$ (vein) were measured in blood drawn by the artery puncture and from a needle in the right internal jugular vein, respectively. The dynamic measurements were taken over a time interval $\Delta t = 10$ min. The beginning of N_2O inhalation – a time moment at which a steady state was approached ($[N_2O]^a = [N_2O]^v$). This steady state carries no information about CBF. The time necessary to approach it is reversely related to CBF. The measurement of CBF is based on the magnitude of N_2O delivered to the brain (per unit brain mass, over the entire time Δt (Δqx)), and the total arteriovenous difference integrated over time Δt, Eq. (1.1), written again here with the generic tracer x replaced by N_2O (Kety and Schmidt, 1945; Kety and Schmidt, 1948):

$$BF = \frac{\Delta q_{N_2O}}{\int_0^{\Delta t}([N_2O)]_a - [N_2O)]_v)(t)dt} \quad (5)$$

2. Jugular thermodilution

An alternative to intravascular tracers is the injection of cold fluid mixing with blood. Thermal perturbation directly measures blood FV within a large blood vessel that tiles the internal jugular vein (Wilson and Halsey, 1970). Jugular thermodilution method allows for continuous or repeated measurements. However, this technique requires jugular vein catheterization. It provides a local measurement of jugular venous flow (in units of ml_{blood}/min). The jugular blood flow measured continuously is expressed in (6). The temperatures are measured by using thermistors which are placed inside and outside of the catheter for injection of the indicator fluid (Mélot et al, 1996).

$$JBF = F_I \frac{\rho_I c_I}{\rho_B c_B}\left(\frac{T_M - T_I}{T_B - T_M}\right) \quad (6)$$

where F_I – the indicator fluid (ml/min); c_B , c_I – the specific heat of blood and indicator (cal/(g°C)); ρ_B, ρ_I – the densities of blood and indicator; T_B, T_I, and T_M – the temperatures of blood, the indicator, and mixture of them both, respectively.

1.3.1.2 Nuclear methods

1. Intraarterial injection of radioactive inert gas (^{133}Xe or ^{85}Kr)

To measure CBF based on intra-arterial injection of radioactive inert gas that emits γ-rays (photons) or β particles (electrons) is a prevalent intraoperative technique. Scintillation detectors (Høedt-Rasmussen et al., 1966), an Anger camera (Holman et al, 1972), or a Geiger–Müller tube (Hanson et al, 1975) detect the diffusible tracer's clearance curve in brain tissue regions. Radioactive isotopes, ^{133}Xe and ^{85}Kr, disintegrate by emitting γ-rays and β particles, respectively. γ-rays and β particles are detected to give clearance curves to regional radioisotopes. This method relies on the same concepts as the Kety–Schmidt method (Sec. 1.3.1.1), but it provides regional measurements of CBF. It measures the tracer's clearance curve continuously.

2. Single-photon emission computed tomography

Single-photon emission computed tomography (SPECT) method injects hexamethylpropyleneamine oxime or ethyl cysteinate molecule, labelled with the radioisotope technetium-99m (^{99m}Tc) (Walovitch et al., 1989). The compound is injected intravenously, passes the blood-brain barrier, and is metabolized and retained intracellularly (Ishizu et al, 1996). The SPECT system measures the spatial distribution of the radiotracer in the cerebral tissue and its temporal evolution. SPECT measurements yield brain perfusion indexes that reflect CBF as well as the radiotracer's kinetics rather than absolute CBF (Asenbaum et al, 1998).

3. Positron emission tomography

Positron emission tomography (PET) is used for cerebral blood flow imaging. This method gives a spatial resolution on the order of 1 cm^3. PET uses ^{15}O-labeled oxygen ($^{15}O_2$), carbon dioxide ($C^{15}O_2$), or water ($H_2{}^{15}O$) as a radioactive diffusible contrast agent. The local instant tissue radiotracer concentration is expressed in (7) with the autoradiographic method (Herscovitch et al, 1983) after intravenous injection of the contrast agent:

$$c_T^{(15O)}(t) = CBF \int_0^t c_a^{(15O)}(\tau) e^{-\frac{CBF}{\lambda}(t-\tau)} d\tau \quad (7)$$

where $c_a^{(15O)(t)}$ is the arterial concentration of the radiotracer (expressed in cps⁄ml) and λ is the tissue-blood equilibrium partition coefficient for the radiotracer.

1.3.1.3 Thermal Diffusion Flowmetry

Thermal diffusion flowmetry (TDF) method measures BF in the brain cortex or in the white matter. It is also considered as heat or thermal clearance technique. This technique provides continuous and invasive bedside monitoring of local CBF. TDF measures a spherical volume from 20 mm^3 to 30 mm^3 that surrounds the probe, which is placed within brain tissue (Le Roux, 2013). TDF is based on the idea of thermal transfer via the conductive characteristics of brain tissue and the convective effects of blood flow. A TDF probe consists of two thermistors: a neutral plate – a passive one that measures brain temperature and is kept at this temperature; and a heated plate – an active one that is held at a slightly higher temperature. A schematic diagram of thermal diffusion flowmetry is shown in Fig. 1.3.

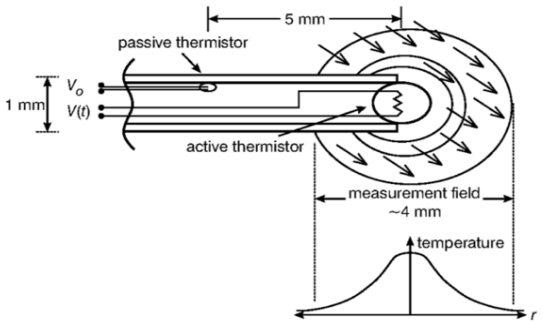

Fig. 1.3. A schematic diagram of thermal diffusion flowmetry. The thermal diffusion probe shows the active heated thermistor at the probe tip that produces a thermal measurement field in the surrounding tissue. The passive thermistor monitors the variations of tissue baseline temperature. Adapted from Martin and Browman, 2000.

1.3.2. Non-invasive methods

1.3.2.1. X-ray techniques

1. Xenon-enhanced computed tomography

The Xe-CT method uses steady xenon which is a diffusible contrast agent that easily crosses the blood-brain hurdle. The Xe-CT procedure begins with a baseline computed tomography (CT) scan. Then, sequential CT scans are performed during inhalation of ~30% xenon. Baseline values are subtracted from each voxel of the xenon-enhanced CT images to determine the concentration of xenon in the brain tissue. A curve is estimated to determine tracer accumulation over time within each voxel. Similarly to PET in Eq. 7, the tracer concentration can be measured directly in brain tissue which releases the Kety–Schmidt requirement of venous blood measurements. Hence, the equation for Xe concentration in tissue is as follows (Blokland et al, 2002):

$$C_T^{(Xe)}(t) = CBF \int_0^t C_a^{(Xe)}(\tau) e^{-\frac{CBF}{\lambda}(t-\tau)} d\tau \quad (8)$$

where λ is now the equilibrium tissue-blood partition coefficient for Xe; $C_a^{(Xe)}$ – arterial concentration of xenon.

2. Perfusion computed tomography

The bolus tracking methodology for cerebral perfusion computed tomography (PCT) uses the central volume principle, which relates the mean blood transit time through a region of interest – the CBV [ml_{blood}/g_{tissue}] and CBF. The central volume principle is expressed as:

$$CBF = \frac{CBV}{MTT_B} \quad (9)$$

here, MTT_B – mean blood transit time.

The PCT procedure begins with a baseline CT scan. Then, a non-diffusible contrast agent is injected intravenously. Time–concentration curves of the contrast agent are formed by performing rapid coherent scans (Turowski and Schramm, 2015).

1.3.2.2. Magnetic Resonance Imaging

1. Dynamic susceptibility contrast/perfusion-weighted MRI

MRI measurements of CBF with dynamic susceptibility contrast (DSC-MRI) are also referred to as perfusion-weighted imaging. This method requires the injection of a contrast agent (Gadolinium-based). The magnetic resonance contrast agents used for DSC-MRI do not diffuse via the blood–brain hurdle. Contrast agents remain in the vascular system. The source of contrast of DSC-MRI measurements is the magnetic

field gradient between the capillaries and the surrounding tissue (Villringer et al, 1988). Short transit time of the contrast bolus (~2 secs) is a fast technique of echo-planar imaging.

2. Arterial spin labeling

Arterial spin labeling (ASL) is based on the principle of labeling water magnetically in major arteries that perfuse the brain. Inversion of the blood magnetization together with a radiofrequency pulse and a field gradient toward BF is the reason for such labeling. Therefore, ASL uses a freely diffusible tracer in the form of magnetically labeled water. The basic concept for ASL is illustrated in Fig. 1.4, showing the labeling and imaging planes. The ASL technique uses a series of radiofrequency pulses to continuously saturate blood water spins. The expression of CBF used by continuous ASL is as follows (Detre et al, 1992):

$$BF = \frac{\lambda}{T_{1app}}\left(1 - \frac{M_T^{SS}}{M_T^0}\right) \tag{10}$$

where λ is the tissue–blood partition coefficient for water (ml_{blood}/g_{brain}) and T_{1app} is the time constant describing the decay of tissue magnetization from M_T^0 to M_T^{SS}.

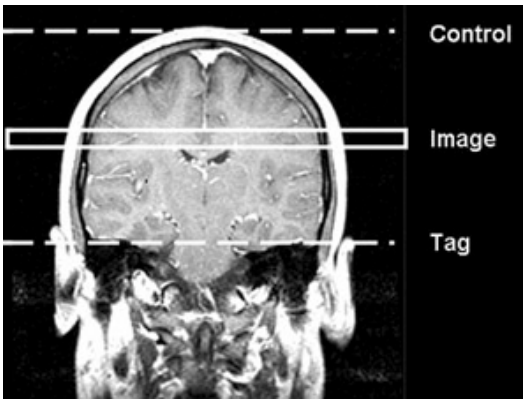

Fig. 1.4. A schematic presentation of the basic approach for blood flow measurement with arterial spin labeling MRI. Adapted from The Regents of the University of Michigan, 2017.

1.3.2.3. Optical techniques

1. Diffuse correlation spectroscopy

Diffuse correlation spectroscopy (DCS) measures relative changes in BF allowing for non-invasive measurements of the microvasculature of superficial brain cortical regions (Durduran and Yodh, 2014). It is a safe, non-invasive technique that can be used continuously at bedside.

A typical DCS system consists of a single-wavelength (utilizes one beam of light that passes through the sample), NIR, single-photon counting avalanche

photodiodes, continuous-wave light source (long coherence length ~10 m), single-mode optical fibres for light detection, multimode source fibres (diameters ~1 mm) and an autocorrelator. The DCS probe is placed on the subject's head and NIR light penetrates the brain. The light is scattered by static scatterers and by moving red blood cells. The light approaches the tissue surface and is measured by the optical detectors. The autocorrelator measures the intensity of the detected photons. A schematic image of a DCS system is shown in Fig. 1.5.

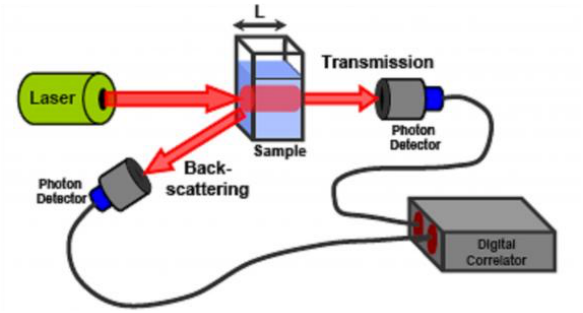

Fig. 1.5. A schematic diagram of DCS. Adapted from The University of Cambridge, 2017.

2. Near-infrared spectroscopy

Near-infrared spectroscopy (NIRS) is a non-invasive technique; optical probes are placed on the subject's scalp for measurements of the cerebral cortex. NIRS has been applied to functional brain studies (Scholkmann et al, 2014) as well as a variety of pilot clinical studies (Smith, 2011) aimed at brain monitoring during anesthesia (Casati et al, 2007), after brain injury (Leal-Noval et al, 2010); it is continuous bedside monitoring. The spatial resolution is of 1 cm order. The maximum tissue depth of investigation is 2–3 cm. The different absorption of NIR light of the oxygenated and deoxygenated heme is because of the concentrations of oxyhemoglobin [HbO_2] and deoxyhemoglobin [Hb]. The sum of [HbO_2] and [Hb] gives the total hemoglobin concentration [HbT]. The majority of oxygen in blood is bound to hemoglobin, so [HbT] is proportional to CBV. This balance is determined by several factors, including BF, blood volume, metabolic rate of oxygen, capillary density, and hematocrit. Although [HbD] (difference [HbO_2] – [Hb] expressed in mol/ml_{tissue},) and ScO_2 (oxygen saturation in the hemoglobin) provide a measure of intravascular oxygenation and are referred to CBF. The concentration difference [HbD] was found to correlate with CBF in piglets (Brady et al, 2007) and in critically ill patients (Wagner et al, 2011).

$$CBF = k\frac{\Delta[HbO_2]}{ctHb\int_0^{\Delta t}\Delta SaO_2(t)dt} \tag{11}$$

where Δ[HbO_2] is the oxyhemoglobin concentration change measured with NIRS [molHbO_2 /ml_{tissue}] over time Δt, ctHb is the blood concentration of hemoglobin [mol_{HbT} /ml_{blood}], ΔSaO_2 is the change in arterial saturation (molHbO_2 /mol_{HbT}),

measured non-invasively with a pulse oximeter placed on the finger, and k is a constant [ml_{tissue}/g_{tissue}] that considers the small-to-large vessel hematocrit ratio and the mass density of brain tissue.

1.3.2.4. Ultrasound Doppler technique

Transcranial Doppler ultrasound provides non-invasive measurements of the BF velocity (cm/s) in the basal brain arteries: middle cerebral artery (MCA), proximal anterior cerebral arteries and posterior cerebral arteries (Aaslid et al., 1982). The ultrasound transducer is placed in a subject-specific ultrasonic window for example in the temporal region. The principle is shown in Fig.1.6.

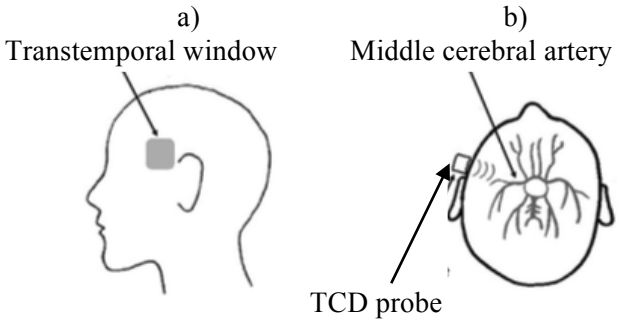

Fig. 1.6. a) The location of transtemporal window on the left side of subject. b) TCD probe placed on the left transtemporal window approaches the left MCA to measure blood flow velocity. Adapted from Lu et al., 2014.

The basic principle is that a Doppler frequency shift (Δf) occurs in an ultrasound wave emitted by ultrasonic transducer at frequency f when it is reflected by the red blood cells that are moving at speed v_B. The connection between v_B and Δf is as follows (Smith and Webb, 2011):

$$v_B = \frac{c_S}{2f\cos(\theta)}\,\Delta f \tag{12}$$

where c_S – ultrasonic speed in soft tissues.

This subchapter reviewed the conventional methods and techniques to measure CBF that are based on direct intravascular measurements, nuclear medicine, thermal diffusion, X-ray imaging, MRI, optical methods and ultrasound techniques. A comprehensive description of principles, methods, and clinical requirements of CBF measurements highlights the potentially important role that non-invasive methods can play in the assessment of cerebrovascular health.

1.4. Arterial blood pressure measurement methods

1.4.1. Invasive method – arterial line

The arterial line is an invasive "Gold standard" technique to measure ABP. The arterial line technique is implemented through an intra-arterial cannula to access an artery, usually the radial artery. To provide hydraulic coupling between blood in the cannula and the transducer, a fluid filled tube is used. A transducer, a processor, an amplifier and a display are used to convert the changes in blood pressure into electrical signals.

1.4.2. Non-invasive methods: photoplethysmography, sphygmomanometry, tonometry

1. Finger photoplethysmography

Finger photoplethysmography is a non-invasive method for continuous monitoring of ABP. This technique uses an inflatable finger cuff, a sensor built into the finger cuff and a pressure controller device. The plethysmography sensor detects the variations of light intensity because the arterioles expand at the cardiac rate when the finger cuff is not inflated. The temporal tendency that is applied to the cuff pressure equals the temporal tendency of ABP.

2. Sphygmomanometry

Sphygmomanometry is a non-invasive method allowing for discrete time point measurement of ABP. Mean, systolic and diastolic ABP can be detected, because it is not a beat-to-beat technique.

This is an auscultatory technique based on listening to the Korotkoff's sounds. Systolic blood pressure is considered to be the pressure at which the first Korotkoff sound is heard (when the cuff is deflated below the systolic pressure, the reducing pressure exerted on the artery allows blood to flow through it) and the diastolic blood pressure is the pressure at which the fourth Korotkoff sound is just barely audible (Peter et al, 2014). These sounds are detected by using a stethoscope placed over the brachial artery and below a blood pressure cuff.

Automatic sphygmomanometers are based on the detection of variations in the pressure applied to an arm cuff as the pressure is decreased below the systolic pressure. This technique uses a piezoelectric sensor, electronic components, and microprocessors to determine the sound. Mean ABP corresponds to the maximal oscillations during cuff deflation. However, systolic and diastolic ABP correspond to the appearing and disappearing oscillations of pressure cuff, respectively. Therefore, it is more difficult to detect it. Detection of systolic and diastolic ABP requires sophisticated algorithms for the analysis of temporal trends of the pressure cuff oscillations, with different manufacturers using different algorithms (Dieterle, 2012).

3. Tonometry

Tonometry of the radial artery provides a non-invasive assessment of the central pulse pressure waveform in the aorta. The procedure is performed by placing a hand-held tonometer on the radial artery and applying a mild pressure to induce an occlusion of the artery. The pressure from the radial artery is transmitted to the sensor and recorded digitally. An algorithm based on the reflection of the central pulse pressure waveform that comes from the smaller resistance vessels allows the estimation of central pressure indexes from a peripheral brachial artery blood pressure (Nelson et al, 2010).

1.4.3. Validation of methods and deriving issues regarding arterial blood pressure measurements

With regards to techniques based on an arm pneumatic cuff, several factors must be considered to receive an accurate reading of ABP. These factors include but are not limited to the cuff size and posture of the body, especially of the arm. Additionally, auscultatory methods depend on the operator. That is why electronic devices are used at home to measure blood pressure (Ogedegbe and Pickering, 2010). Finger photoplethysmography seems to be a reliable method to measure the beat-to-beat ABP, and several studies have validated this technique with the arterial line method (Imholz et al, 1998). Tonometry has also been validated against the invasive arterial line method and good agreement has been found except for its limited capacity to respond to fast variation in ABP (Sato et al 1993).

1.5. Methods and approaches of ICP monitoring

1.5.1. Invasive ICP measurement techniques

Several different invasive techniques of measuring ICP exist. ICP can be measured in different intracranial anatomical locations: intraventricular, intraparenchymal, epidural, subdural, and subarachnoidal.

1. External Ventricular Drainage

The “Gold standard” ICP monitoring is the invasive external ventricular drainage (EVD) technique. A catheter is introduced into one of the ventricles via a drilled hole into the skull.

Surgical placement of EVD is a minor surgical procedure, but it has a few risks, such as hemorrhagic and infectious complications. Conventionally, a coronal burr-hole is used for EVD placement to approach the Kocher’s point, EVD located in the 3rd ventricle. Alternative methods, such as the Frazier burr-hole (occipital-parietal), Keen’s point (posterior-parietal) and Dandy’s point (occipital) are used as secondary options. Nevertheless, there has been no consensus regarding EVD placement (Greenberg, 2010).

2. Microtransducer ICP Monitoring Devices

The group of invasive microtransducer ICP monitoring devices can be divided into: strain gauge devices, fiber optic devices and pneumatic sensors.

The Codman MicroSensor, the Raumedic Neurovent-P ICP sensor and the Pressio sensor belong to the group of piezoelectric strain gauge devices. ICP is estimated when the transducer is inclined due to the ICP and its resistance changes. Fiber optic devices, such as the Camino ICP Monitor, transmit light through a fiber optic cable towards a displaceable membrane. Variations in ICP will move the membrane and the differences in intensity of the reflected light are computed to an ICP value (Raboel et al, 2012). Pneumatic sensors, such as Spiegelberg, are based on a small balloon at the distal end of the catheter to record changes in ICP. This device permits quantitative measurement of intracranial compliance.

1.5.2. Non-invasive ICP measurement approaches

The earliest attempts to measure ICP non-invasively appeared 37 years ago. Since then, many teams of researchers have developed a wide variety of approaches to measure ICP non-invasively. Some of these approaches are complex, based on mathematical modelling. Other approaches rely on the idea that physiological parameters within a human's head correlate with ICP. The measurement of absolute ICP value linear relationship which would be stable in time is necessary. The general form of such relationship is as follows:

$$x(t) = aICP(t) + b \tag{13}$$

where $x(t)$ – physiological parameter; a – time invariant slope; b – time invariant bias.

The correlation between a physiological parameter and ICP is invariant to individual patient's specific slope a and bias b. In physiological reality, a and b are influenced by many patient's specific influential factors and are time-dependent. Therefore, a calibration procedure is necessary to identify $a_{(t_c)}$ and $b_{(t_c)}$, where t_c is the moment of calibration. Calibration is impossible regarding the impossibility to create a "Gold Standard" non-invasive ICP meter. Despite the diversity of non-invasive ICP measurement approaches, the exposure of principle techniques will be explained in detail below.

Table 1.4. The patents of non-invasive ICP measuring approaches sorted by type of approach

No	Type of Approach	Patent Information		Patent issued to
		Year	First Inventor	
1	Correlation Based	1980	John A. Allocca	Allocca, J. A. (US)
2		1986	John G. Rosenfeld et al.	Rosenfeld, J., et al. (US)
3		1989	Robert J. Marchbanks	Marchbanks, J. (US)
4		1990	Naoki Kageyama et al.	

5	1994	Naoki Kageyama et al.	Hitachi Construction Machinery Co., Ltd., Hiroji Kuchiwaki (JPN)
6	1994	Naoki Kageyama et al.	
7	1995	Arminas Ragauskas et al.	Uab Vittamed (LT)
8	1997	William T. Yost et al.	The United States Of America As Represented By The Administration Of The National Aeronautics And Space Administration (US)
9	1999	Keith Bridger et al.	Active Signal Technologies, Inc. (US)
10	2002	David Michaeli	Inta Medics, Ltd. (ISR)
11	2001	Royce Johnson et al.	Johnson, R., And Quirk, W.H. (US)
12	2002	William T. Yost et al.	The United States Of America As Represented By The Administration Of The National Aeronautics And Space Administration (US)
13	2004	William T. Yost et al.	
14	2010	Chung-Yuo Wu et al.	Micro-Star Int'l Co, Ltd. (TW)
15	2012	Martin M. Lenhardt et al.	Virginia Commonwealth University (US)
16	1991	Edwin C. Mick	Mick, E. C.
17	1992	Edwin C. Mick	Mick, E. C.
18	1993	Edwin C. Mick	Medys, Inc. (US)
19	2000	Dipen N. Sinha	The Regents Of The University Of California (US)
20	2004	William T. Yost et al.	The United States Of America As Represented By The Administration Of The National Aeronautics And Space Administration (US)
21	2011	Karla Mossi	Virginia Commonwealth University (US)
22	2013	Sérgio Mascarenhas Oliveira et al.	Oliveira, S.M.
23	2013	Guy Weinberg et al.	Headsense Medical Ltd. (ISR)
24	2000	Joseph R. Madsen et al.	Children's Medical Center Corporation (US)
25	2000	Klaus Paulat	Nicolet Biomedical Inc. (US)
26	2003	Joseph R. Madsen et al.	Children's Medical Center Corporation (US)
27	2005	Kevin E. Crutchfield et al.	New Health Sciences, Inc. (US)
28	2004	Klaus Paulat	Dwl Elektronische Systeme Gmbh. (DE)
29	2005	Pierre D. Mourad et al.	Aller Physionix Limited, University Of Washington (US)
30	2006	Kevin Crutchfield et al.	New Health Sciences, Inc. (US)
31	2009	Pierre D. Mourad et al.	Physiosonics, Inc. (US)
32	2010	Marek Swoboda et al.	Neurodx Development Llc. (US)

33		2006	Pierre D. Mourad et al.	Allez Physionix Limited et al. (US)
34		2000	Mark S. Borchert et al.	California Institute Of Technology (US)
35		2001	Kurt R. Denninghoff	The Uab Research Foundation (US)
36		2002	Kurt R. Denninghoff	
37		2006	Ernest Braxton	Braxton, E.
38		2006	Henry W. Querfurth	Caritas St. Elizabeth Medical Center Of Boston, Inc. (US)
39		2017	Terry A. Fuller et al.	Third Eye Diagnostics, Inc. (US)
40		2003	Scott C. Meyerson et al.	Rice Creek Medical, Llc. (US)
41		1999	Noam Alperin	Alperin, N.
42		2005	Noam Alperin	
43		2011	Anthony Bellezza et al.	Third Eye Diagnostics, Inc. (US)
44		2012	Ben Zion Poupko et al.	Orsan Medical Technologies Ltd. (ISR)
45		2013	Shlomi Ben-Ari et al.	Ben-Ari, S., Marcovitch, S., Kinrot, O.
46		2014	Shannon E. Campbell et al.	Covidien Lp. (US)
47	Mathematical Model Based	1997	Bernhard Schmidt	Schmidt, B., et al.
48		2012	Gregory Zlatko Grudic et al.	The Regents Of The University Of Colorado (US)
49		2013	Faisal Mahmood Kashif et al.	Massachusetts Institute Of Technology (US)
50		2013	Gregory Zlatko Grudic et al.	The Regents Of The University Of Colorado (US)
51		2014	Zhong Ji et al.	Chongqing University (CHN)
52		2014	Xiao Hu et al.	The Regents Of The University Of California (US)
53		2014	Faisal Mahmood Kashif et al.	Massachusetts Institute Of Technology (US)
54	Pressure Balance Based	1999	Arminas Ragauskas et al.	Uab Vittamed (LT)
55		2009	Arminas Ragauskas et al.	Uab Vittamed Technologijos (LT)
56		2015	Arminas Ragauskas et al.	Uab Vittamed (LT)
57		2013	Arminas Ragauskas et al.	
58		2004	Arminas Ragauskas	Ragauskas, A.
59		2006	Arminas Ragauskas	Uab Vittamed (LT)
60		2012	Osvaldas Pranevicius et al.	Pranevicius, O., et al. (US)

1.5.2.1. Correlation-based approaches

The absolute majority of approaches of non-invasive ICP estimation are based on the principle that any changes in the anatomical structure, whether in the human's head or in the intracranial and/or extracranial physiology, correlate with the ICP

changes. A limitation of these approaches is that they do not show the slope and bias of relationship between correlating elements. Calibration is the only procedure for identification of slope and bias of correlation-based association. This is the reason to reflect ICP changes only with limited accuracy expressed by systematic error and limited precision expressed by standard deviation of random error. Calibration is impossible because of absence of the "Gold Standard".

Most patented methods for non-invasive ICP monitoring rely on the idea that variations in ICP affect the physical dimensions and/or acoustic properties of the cranial vault or intracranial structures. Table 1.5 provides information on the focus of object or characteristic related to ICP according to the technique of measurement.

Table 1.5. Correlation-based approaches and non-invasively measured parameter (noted as X) to assess ICP

No.	Technique of measurement	Patent Information		
		Year	First Inventor	Non-invasively measured parameter
1	Blood flow measurement	1980	John A. Allocca	Blood flow in a jugular vein
2	Electroencephalography	1986	John G. Rosenfeld et al.	Electrical brain activity
3	Audiometric technique	1989	Robert J. Marchbanks	Characteristics of eardrum
4	Ultrasound	1990	Naoki Kageyama et al.	Thickness of dura matter
5		1994	Naoki Kageyama et al.	Thickness of dura matter
6		1994	Naoki Kageyama et al.	Thickness of dura matter
7		1995	Arminas Ragauskas et al.	Acoustic properties of brain parenchyma tissue
8		1997	William T. Yost et al.	Diameter of cranium
9		1999	Keith Bridger et al.	Acoustic impedance, resonance characteristics and US velocity in the cranium
10		2002	David Michaeli	Third cerebral ventricle
11		2001	Royce Johnson et al.	Cranial vault
12		2002	William T. Yost et al.	Diameter of cranium
13		2004	William T. Yost et al.	Cerebrospinal fluid components
14		2010	Chung-Yuo Wu et al.	Contrast agent
15		2012	Martin M Lenhardt et al.	Retinal artery pulsations
16	Acoustic Measure	1991	Edwin C. Mick	Sound attenuation in skull bones
17		1992	Edwin C. Mick	Sound attenuation in skull bones
18		1993	Edwin C. Mick	Sound attenuation in skull bones
19		2000	Dipen N. Sinha	Stress level of skull bones
20		2004	William T. Yost et al.	Diameter of cranium
21		2011	Karla Mossi	Damping of acoustic signals
22		2013	Sérgio Mascarenhas Oliveira et al.	Skull deformation
23		2013	Guy Weinberg et al.	Damping of acoustic signal

24	Transcranial Doppler ultrasonography	2000	Joseph R. Madsen et al.	Blood vessel wall geometry changes
25		2000	Klaus Paulat	Alterations in the brain pressure
26		2003	Joseph R. Madsen et al.	Blood vessel wall geometry changes
27		2005	Kevin E. Crutchfield et al.	Blood flow parameters
28		2004	Klaus Paulat	Alterations in the brain pressure
29		2005	Pierre D. Mourad et al.	Tissue displacement
30		2006	Kevin Crutchfield et al.	Blood flow parameters
31		2009	Pierre D. Mourad et al.	Flow velocity of middle cerebral artery
32		2010	Marek Swoboda et al.	Impedance mismatches
33		2006	Pierre D. Mourad et al.	Flow velocity of middle cerebral artery
34	Optical coherence tomography of retina	2000	Mark S. Borchert et al.	Parameters of an optic nerve of the eye
35	Ophtalmodynamometry	2001	Kurt R. Denninghoff	Eye vessels and intraocular pressure
36		2002	Kurt R. Denninghoff	Eye vessels and intraocular pressure
37		2006	Ernest Braxton	Retinal venous outflow pressure
38		2006	Henry W. Querfurth	Venous outflow pressure and central retinal arterial blood flow
39		2017	Terry A. Fuller et al.	Intraocular blood vessel
40	Otoacoustic emission	2003	Scott C. Meyerson et al.	Intensity or phase of OAE signal
41	Magnetic resonance imaging	1999	Noam Alperin	Arterial and venous blood flow and the cerebrospinal fluid flow
42		2005	Noam Alperin	Arterial and venous blood flow and the cerebrospinal fluid flow
43	Optic Nerve Sheath ultrasonography	2016	Anthony Bellezza et al.	Blood velocity metric
44	Plethysmography	2012	Ben Zion Poupko et al.	Cardiac respiration cycles
45		2013	Shlomi Ben-Ari et al.	Waveform of signal
46	Electromagnetism	2014	Shannon E. Campbell et al.	Venous pulsations

1. Blood flow measurement

The first attempt included in this thesis to measure ICP non-invasively was published in 1980 belongs to John A. Allocca. The approach is based on the occlusion of blood flow in a jugular vein (because it was found that pressure rise slope correlates with intracranial pressure) and the electromagnetic measurement of the change of blood flow within the jugular vein upstream of the occlusion. The correlation of pressure rise slope with ICP is poor. The described venous outflow model does not

consider the existence of parallel venous drainage systems – jugular veins (JV-12) and vertebral venous plexus (VVP-14).

2. Electroencephalography

John G. Rosenfeld (1986) diverts a flash of light towards the patient's eyes and measures the latency of a negative-going wave of the electrical brain activity. It is considered as an index of intracranial pressure. Nevertheless, the latency of visual evoked potential is not a specific indicator of ICP.

3. Audiometric technique

Another non-invasive ICP assessment technique that has been proposed involves observing the tympanic membrane of the ear. The tympanic membrane displacement technique, proposed nearly twenty years ago by Marchbanks (1989), exploits the relation of ICP to the reflex contraction of the stapedius and tensor tympani muscles in response to a sound. The muscles normally contract in response to vocalization, jawing and loud external sounds, which is accompanied by a small but measurable displacement of the eardrum from its initial position. The displacement can be measured with common computerized tympanometers with a fully automated measurement procedure used for impedance audiometry which are portable, relatively inexpensive and easy to use.

A method for measuring tympanic membrane displacement may provide an indirect index that is related to ICP (Reid et al., 1990; Moss, 1991; Madan Samuel, 1998). The accuracy of TMD estimates of ICP was found to be at the order of ±15mmHg (Shimbles, 2005), which is not sufficient for a reliable quantitative measurement of ICP in clinical practice.

4. Ultrasound

Naoki Kageyama et al. (Hitachi Construction Machinery Co., Ltd., Hiroji Kuchiwaki, 1990; Hitachi Construction Machinery Co., Ltd., Hiroji Kuchiwaki, 1994; Hitachi Construction Machinery Co., Ltd., Hiroji Kuchiwaki, 1994) claim that ICP can be inferred from the thickness of the dura mater that is estimated from interfering echoes of an ultrasonic wave. The technique was successfully completed on four healthy subjects and four patients with intracranial hypertension. However, larger validation studies have never been performed because the method did not attract interest of clinicians. This approach also needs calibration to individual patients.

Multivariate approaches have been proposed by Arminas Ragauskas et al. (Uab Vittamed, 1995) who derive ICP by combining the transit times with dispersion of the ultrasound wave on its way through the brain parenchyma. In addition, Bridger et al. (Active Signal Technologies, Inc., 1999) suggest a non-invasive device and method for measuring ICP based on the properties of acoustic signals which interact with the brain, for example velocity of sound, acoustic transmission impedance, resonance

characteristics and resonant frequency. Low-intensity acoustic signals of less than 100 kHz frequencies are used.

William T. Yost et al. and Royce Johnson et al. (The United States of America as Represented By The Administration Of The National Aeronautics And Space Administration, 1997) derive ICP from the diameter of the cranium which is measured with the pulsed phase-locked loop ultrasound technique.

David Michaeli (Inta Medics, Ltd., 2002) derives ICP from the size and shape of pulsations of the 3rd ventricle which are measured along the propagation axis of an ultrasound wave, synchronous with the cardiac cycle or respiration. This approach has not been independently validated. However, the discussion in the embodiment of the patent document suggests that the approach can evaluate among three ranges of ICP: mild (10–20 mmHg), moderate (20–40 mmHg) and severe (above 40 mmHg) ICP elevation but cannot provide an exact value of ICP within the range because of impossibility for calibration of ICP for each patient (Michaeli, 2002).

Yost et al. (The United States of America as represented by The Administration of The National Aeronautics and Space Administration, 2002; The United States of America as represented by The Administration of The National Aeronautics and Space Administration, 2004) devised an approach that extracts pulsatile changes in the ultrasound signal caused by beat-to-beat oscillations of ABP to provide a data signal with components wherein substantially all the components are related to intracranial pressure. The method is calibrated by comparing the amplitude of the extracted waveform with the absolute difference between the systolic and diastolic blood pressure.

Chung-You Wu et al. (Micro-Star Int'l Co, Ltd., 2010) present an approach according which ICP can be measured from the intracranial area filled with micro-bubbles formed by an injected contrast agent and by calculating the size of the micro-bubble according to the resonant frequency and a property of the contrast agent.

Martin M. Lenhardt et al. (Virginia Commonwealth University, 2012) propose an approach to measure increases in ICP with acoustic energy applied to the head. Acoustic eye patches are applied to a patient's eye or eyelid, and an ultrasonic sweep generator applies an acoustic signal across the patient's skull. The eye patches have piezoelectric film sensors for measuring the acoustic signal. In one version, the predetermined range is in the ultrasonic band and an analyser determines from the output of the sensors a resonant frequency and a damping of acoustic amplitude at said resonant frequency. A correlation between said damping and ICP is calculated.

Ultrasound "time-of-flight" methods for non-invasive ICP monitoring have not been extensively validated and currently many of them do not seem to be accurate enough for routine clinical use.

5. Acoustic measure

Approaches from this group attempt to derive ICP from the mechanical properties of skull bones. Changes in ICP result in a small but measurable skull expansion and modifies their mechanical properties. The transfer function is derived

by applying a wide-band, low frequency (<100 Hz) mechanical excitation at one location of the skull (via a piezo-transducer or an impact hammer) and comparing its spectrum with the received signal at another location on the upper half of skull. Edwin C. Mick (Mick, 1991; Mick, 1992; Medys, Inc., 1993) proposes that the measurement can calibrate itself by receiving the frequency response spectrum from a point of the skull of the subject, who is assumed not to be affected by ICP. Alternatively, pre-calibrate on subjects with normal ICP.

Other methods from this group vary this basic Mick's approach in different ways. In Sinha's approach (The Regents of the University Of California, 2000), resonant frequency of the skull bones is set first, then a sinusoidal stimulation at the resonant frequency is transferred via a piezo-transducer and ICP is calculated directly from the phase difference between the stimulated signal and the response detected with a second transducer. Yost and Cantrell, Jr. (The United States of America as represented by The Administration of the National Aeronautics and Space Administration, 2004) divided the process into two steps. Firstly, changes in the circumference of the cranium are estimated from the phase difference between a sinusoidal stimulated signal and the response which is obtained at a distance with another piezo-transducer. Then, changes in ICP are calculated as a product of variations in the cranium circumference and the elasticity constant of the skull that has been set earlier. Using a mathematical relation between ICP, Yost and colleagues (2004) put forward skull elasticity and pulse pressure derived by Ursino and colleagues (1988).

Karla Mossi (Virginia Commonwealth University, 2011) suggests an approach that consists of a frame that holds an acoustic sensor on the eyelid of a subject. The frame includes the means of adjusting and managing the magnitude of pressure. Changes in intracranial pressure, which result in changes of dampening of the acoustic signals transmitted through the cranium of the patient, are non-invasively detected by the acoustic sensor on the eyelid.

Sérgio Mascarenhas Oliveira et al. (2013) present an approach to digitally produce and communicate intracranial pressure data from the electric signals of skull deformation. The method includes: 1) receiving, from at least one sensor, the electric signals of detected skull deformation using electrical equipment configured to transform and process the skull deformation signals which are received; 2) transforming and processing the received electric signals of skull deformation to produce digital intracranial pressure data; 3) and outputting the digital intracranial pressure data via an output device to render the digital intracranial pressure data.

Guy Weinberg et al. (Headsense medical, Ltd., 2013) patented a device which contains a disposable headset, capable of performing accurate and continuous monitoring of various brain conditions, and a tablet-based monitor. The headset includes an ear-bud-like device which is placed on the patient's ears. A low frequency acoustic signal is generated by the headset for a few seconds. The signal propagates through the cranium and is picked up in a different ear by an acoustic sensor. The received acoustic data is then analysed using proprietary signal processing algorithms. The procedure can be repeated automatically for continuous monitoring.

None of the aforementioned methods have been properly validated in relevant clinical populations, and their accuracy is unknown.

6. Transcranial Doppler ultrasonography

Kevin E. Crutchfield et al. (New Health Sciences, Inc., 2005) use TCD to measure the velocity of blood flow through the major intracranial vessels by emitting a high frequency (>1,6 MHz) wave from an ultrasound probe and detecting a frequency shift between the incident and reflected wave which directly correlates with the speed of the blood. TCD has been used to provide a non-invasive, qualitative indication of ICP variations. The measurement is taken over the regions of the skull with thinner walls as the bones strongly attenuate the transmission of the ultrasound at these frequencies (New Health Sciences, Inc., 2006). TCD waveforms have been correlated with ICP. The estimates are, however, insufficiently accurate with the margin of error of ±10–15 mmHg (Stettin and Paulat, 2011).

Joseph R. Madsen et al. (Children's Medical Center Corporation, 2000; Children's Medical Center Corporation, 2003) proposes systems for non-invasive measurement of blood velocity based on the Doppler shift and the correlation of blood flow velocity before and after the manual application of an externally applied pressure to the eye.

Klaus Paulat (Nicolet Biomedical Inc., 2000; Dwl Elektronische Systeme Gmbh., 2004) calculates 1) the mean of the first amplitude value (an extreme value of the electrical signal, following a blood pressure maximum according to a systole with a substantially uniform delay); 2) the value of the second amplitude (at a point where the electrical signal reaches either a maximum or a turning point for the first time after the first amplitude value); 3) and a third amplitude value (which is obtained from the electrical signal after the second amplitude value) to determine the intracranial pressure. An interesting research investigating the assessment of ICP by measuring infrasonic emissions from the tympanic membrane was done by Eduard Stettin and Klaus Paulat in 2011. An increase in ICP was induced in 22 patients with implanted ICP sensors. ICP waveforms which were obtained invasively and continuously were compared with infrasonic emission waveforms. The assessment of infrasonic emissions, however, does not yet provide exact figures.

Pierre D. Mourad et al. (Aller Physionix Limited, University of Washington, 2005; Allez Physionix Limited et al., 2006) assess and track ICP changes from data relating to tissue displacement and related to biological changes that may be recorded by detecting acoustic properties of tissue using ultrasound interrogation pulses by Doppler. Pierre D. Mourad et al. (Physiosonics, Inc., 2009) used transcranial Doppler ultrasound to measure ICP indirectly by assessing the elasticity of the biological material in a particular part of the brain. Therefore, this approach would require calibration and expert positioning.

Marek Swoboda et al. (Neurodx Development Llc., 2010) suggest estimating ICP by non-invasively detecting impedance mismatches between carotid arteries and cerebral vessels through a reflection of the carotid pressure waveform. The ICP

estimate is determined by analysing the reflection and comparing the analysis with the known cerebral vasculature data obtained by TCD.

Unfortunately, TCD only provides a qualitative and not quantitative indication of variations in ICP. However, according to the investigations done by Czosnyka M. and Pickard J. (2004) there is not a linear relationship between ICP and TCD indices. Moreover, the accuracy of these TCD measurements is low, particularly in patients with raised ICP.

7. Optical coherence tomography of retina

The diameter of an optic nerve of the eye is determined along with the intraocular pressure of the eye. By using a tonometer, Mark S. Borchert et al. (California Institute of Technology, 2000) determined ICP from the intraocular pressure of the eye and the parameter of an optic nerve of the eye.

8. Ophthalmodynamometry

The ophthalmodynamometry method was described in 1925 by Baurmann and belongs to the public domain, but several modifications have been recently patented that combine the classic ODM with reflectance oximetry of the retina by Kurt R. Denninghoff (The Uab Research Foundation, 2001; The Uab Research Foundation, 2002), the ultrasound measurement of blood flow in the central retinal artery by Henry W. Querfurth (Caritas St. Elizabeth Medical Center Of Boston, Inc., 2006), or automate the method by adding a camera and an image processing software capable of recognizing venous pulsations from a sequence of images of the eye fundus by Ernest Braxton (2006). An evaluation in patients confirmed a strong linear relationship and clinically negligible differences (2–3 mmHg) between VOP and the invasively measured ICP. Neurolife Non-invasive Solutions Inc. developed technology based on Braxton's patent. The technology works as non-invasive ICP meter by observing the changes in the retinal blood flow.

Third Eye Diagnostics, Inc. is developing the Cerepress™ (Fig. 1.7.) – a non-invasive, hand-held intracranial pressure monitor which gathers information from the patient's dilated eye pupil with regards to Henry W. Querfurth, Terry A. Fuller et al. (Third Eye Diagnostics, Inc., 2017) and Anthony Bellezza et al. (Third Eye Diagnostics, Inc., 2011) patents. The Cerepress™ apparatus measures blood pressure in the central retinal vein (CRV) of the eye and blood velocity in the ophthalmic artery. Third Eye Diagnostics, Inc. has developed a device that simultaneously records images of the CRV and measures intraocular pressure while the pressure in the eye is increased to obtain CRV pressure. CRV pressure is considered to correlate to ICP. This method requires an individual patient-specific calibration as every other correlation-based method.

Ophthalmodynamometry requires a skilled physician or medic, dilated eye pupils and collaboration of the patient. It cannot be applied in cases of ocular trauma.

Fig. 1.7. Cerepress™ a non-invasive, hand-held intracranial pressure monitor. Adapted from Third Eye Diagnostics, Inc., 2017.

9. Otoacoustic emission

Otoacoustic emission, which is a sound generated by subtle oscillations of the endolymph and perilymph caused by contractions of the outer hairy cells of the inner ear in response to short ~1 ms acoustic impulse, seems to offer a possibility to assess ICP. In the patent issued to Scott C. Meyerson and colleagues (Rice Creek Medical, Llc., 2003), the use of both the transient evoked otoacoustic emission (TEOAE) and distortion product otoacoustic emission (DPOAE) for assessment of ICP are included. TEOAE is used first to set the optimum OAE response frequency, after which a pair of pure tones is located in a DPOAE paradigm. There is little data to this date about the clinical utility or accuracy of otoacoustic emission as a measure of ICP. A pilot study of Finnerty and colleagues (2000) that evaluated different modalities of OAE in 12 healthy volunteers and 5 patients with implanted ventricular catheters for direct ICP monitoring revealed that increased ICP was associated with notable decreases in the intensity of the evoked OAE. This method, as all other correlation-based approaches, cannot be used for absolute ICP value measurement because of impossibility of individual calibration.

10. Magnetic resonance imaging

Noam Alperin (1999; 2005) applies MRI to measure arterial inflow, venous outflow and cranial spinal fluid flow and calculates the intracranial volume change over a cardiac cycle. The approach also includes the steps for calculating a pressure gradient of spinal fluid flow over a cardiac cycle; and calculating a pressure change per unit volume change based upon the calculated intracranial volume change and cranial pressure gradient. A comparative study of invasive ICP measured with lumbar puncture versus MRI estimates presented in the patent document was excellent in a baboon and in four patients. The huge shortcoming of this approach it is not bedside assessment.

Xiaobin Xie et al. (2013) did a prospective observational comparative study which included 72 neurology patients who underwent lumbar cerebrospinal fluid (CSF) pressure measurement and 3.0-Tesla orbital magnetic resonance imaging. The width of the orbital subarachnoid space (OSASW) around the optic nerve was measured with MRI at 3, 9, and 15 mm behind the globe. Unfortunately, this will not replace invasive ICP monitoring.

11. Optic Nerve Sheath ultrasonography

The use of optic nerve sheath diameter for the assessment of ICP dates to 1987 when Cennamo and colleagues (1987) demonstrated a linear relationship between ICP and the sheath diameter measured with a trans-orbital ultrasound probe in an A-scan mode.

A study led by Aaron Strumwasser and colleagues (2011) was done with 10 trauma patients. The overall diagnostic sensitivity, specificity, and accuracy for estimating ICP with using ONSD measurements were 36%, 38%, and 37%, respectively.

A prospective clinical study (Ragauskas et al, 2014) of a non-invasive ICP estimation method based on ONSD correlation with ICP and an absolute ICP value measurement method based on a two-depth TCD technology has recruited 108 neurological patients. All non-invasive ICP measurements were compared with the "Gold Standard" invasive cerebrospinal fluid pressure measurements obtained by lumbar puncture. The diagnostic sensitivity, specificity, and the area under the ROC curve of the ONSD method for detecting elevated intracranial pressure (ICP > 14.7 mmHg) were calculated using a cut-off point of ONSD at 5.0 mm and found to be 37.0%, 58.5%, and 0.57, respectively.

12. Plethysmography

Ben Zion Poupko et al. (Orsan Medical Technologies Ltd., 2012) state an approach based on the measurement of electrical impedance plethysmography, which reflects transient cerebral volume alterations and blood flow in cerebral arteries as a function of the cardiac and respiratory cycles. The authors claim that the system is calibration free and allows continuous ICP monitoring.

Shlomi Ben-Ari et al. (2013) assert an approach by extracting waveforms from the impedance plethysmography signals and using it to estimate the intracranial hemodynamic parameters.

13. Electromagnetism

Shannon E. Campbell et al. (Covidien Lp., 2014) propose an approach to estimate ICP by emitting an electromagnetic wave into the forehead tissue of a patient and detecting the characteristics of the electromagnetic wave after it has been scattered by the tissue and received by a detector. The second part of the suggestion is based on analysing the variations of wave to identify venous pulsations, and determining

whether the patient's intracranial pressure is elevated based on a correlation between the venous pulsations and ICP level measured using an invasive ICP channel.

1.5.2.2. Mathematical modelling-based approaches

Mathematical modelling is a system based on mathematical concepts. Recently, several teams of researchers have also developed mathematical models in order to increase the possibility to measure ICP non-invasively. As computer technology advanced, these models became more popular; the earliest of them appeared in 1997. Some of these models are complex and comprehensive, some are designed with clinical application in mind, and others are conceptual or theoretical in nature. The following section synthesizes the information provided in Table 1.3, including one thesis, important findings, and the limitations of current models.

Bernhard Schmidt (Schmidt et al, 1997) developed a mathematical method which needs flow velocity (FV) and ABP signals measured non-invasively as input variables to compute a set of parameters, called TCD characteristics. The impulse response function is generated by using a specific procedure algorithm from TCD characteristics. It transforms the ABP signal into the target signal, the non-invasive ICP signal (Fig. 1.8.). This method is integrated into ICM+ software (Cambridge, UK) for non-invasive ICP estimation.

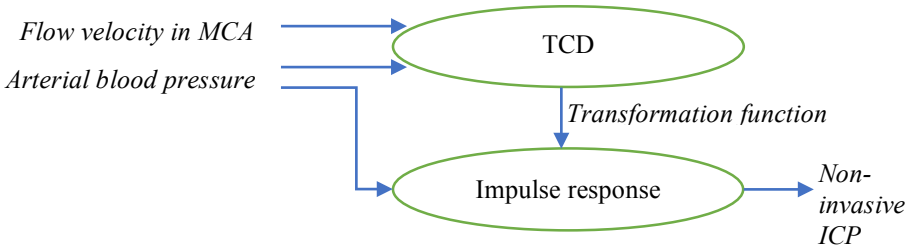

Fig. 1.8. A simplified block diagram of procedures used for non-invasive assessment of ICP. Adapted from Schmidt et al, 2003.

Xiao Hu et al. (The Regents of the University of California, 2014) describe a model which correlates the values of arterial blood pressure, cerebral blood flow velocity, and intracranial pressure. The intracranial pressure is set by creating an output data set indicative of the determined intracranial pressure (Xu et al, 2014).

Gregory Zlatko Grudic et al. (The Regents of the University of Colorado, 2012; The Regents of the University of Colorado, 2013) claim a computational method of predicting ICP. The model which collects parameter data in a computer system (a set of input data from one or more physiological sensors), determines the calculated parameters, applies the model of ICP, applies the Machine-Learning paradigm, extracts parameters for determining ICP, collects and/or determines parameters from patient, determines a patient's ICP, takes medical action if indicated and, finally, revises model. No clinical application data is provided.

Zhong Ji et al. (Chongqing University, 2014) offer an approach which is comprised of three steps: applying TCD to determine the middle cerebral artery velocity of the subject and estimating changes in the ICP, generating a flash visual evoked potential (FVEP) on the subject, processing a detected FVEP signal, obtaining an estimated ICP and combining the estimated ICP trend with the estimated ICP obtained by signal processing of the detected FVEP signal to periodically correct the trend and obtain a non-invasive measure of ICP.

Faisal Mahmood Kashif et al. (Massachusetts Institute of Technology, 2013; Massachusetts Institute of Technology, 2014) suggest a model-based approach on estimation and tracking of ICP continuously. It uses non-invasive (or minimally invasive) measurements of peripheral arterial blood pressure and blood FV in the MCA. The measured signals may be used to estimate the parameters and variables of a computational model that is representative of the physiological relationships among the cerebral flows and pressures (Kashif, 2011).

1.5.2.3. Pressure balance-based method

The accurate, precise and patient-specific calibration-free non-invasive absolute ICP value measurement method relies not on correlation or mathematical modelling but on the principle of direct ICP and extracranial pressure comparison (Uab Vittamed, 1999; Uab Vittamed, 2006) (see Table 1.3).

An innovative non-invasive method using two-depth TCD of intracranial pressure quantitative absolute value measurement relies on the same fundamental principle as the one used to measure blood pressure with a sphygmomanometer (Uab Vittamed Technologijos, 2009). The non-invasive measurement of ICP is performed by gradually increasing pressure in an air-filled chamber applied to the tissues surrounding the orbit, and by measuring blood flow velocities in the intracranial and extracranial segments of the ophthalmic artery (OA) with an ultrasonic two-depth transcranial Doppler (Uab Vittamed, 2013; Uab Vittamed, 2015). Blood flow velocity parameters derived from these dynamic velocity measurements are then compared with the intracranial and extracranial segments of the OA. The difference between these parameters is identified. When the pressure in the chamber causes the difference (between intracranial and extracranial segments) to approach a targeted minimum value of close to zero, that pressure value is determined as an indicator of non-invasively derived ICP value. (Ragauskas et al, 2005).

TCD is used instead of a stethoscope for the pressure balance indication to translate the pressure balance principle of blood pressure measurement with a sphygmomanometer to the measurement of ICP. Intracranial arteries are natural pressure sensors. The ophthalmic artery is a unique vessel with almost the same anatomy of intracranial and extracranial segments. This became the reason to use the OA as natural “scales” for absolute ICP measurement and TCD as a balance indicator of these “scales”. This is a “re-invention” of the non-invasive ABP measurement method applied to measure the absolute ICP value. (Bartusis et al, 2012). The mean value of blood flow velocity in OA, systolic and diastolic values, pulsatility and other

indexes are almost the same in both OA segments in the point of balance when ICP = Pe (Uab Vittamed, 2006). Individual influential factors (ABP, cerebrovascular autoregulation impairment, individual pathophysiological state of patient, individual diameter and anatomy of OA, hydrodynamic resistance of eyeball vessels, etc.) do not influence the balance ICP = Pe and, therefore, these natural "scales" do not need calibration (Zakelis, 2012).

Another interesting approach of direct manipulations on the tympanic membrane was proposed as one of the embodiments in a US patent by A. Ragauskas (2004). The inventor explains that firstly a measurement of the baseline position of the tympanic membrane must be measured while ICP is zero. The equalization of ICP to the atmospheric pressure can be obtained by the head-up tilt in a non-invasive manner, or the measurement can be taken during a neurosurgical operation (Ragauskas and Petkus, 2001). After that, ICP can be measured by exerting an external pressure to the tympanic membrane and applying the same pressure onto the oval window and inner ear simultaneously until the eardrum returns to the baseline position. This will occur when the exerted external pressure equals the ICP. There is no data regarding clinical applications of this technique.

Osvaldas Pranevicius et al. (2012) comprise the steps of registering cerebral hemodynamics, then changing the pressure surrounding the external tissues to affect cerebral venous outflow. The external pressure in a pressure cuff is estimated and jugular pressure value is set when a change in the cerebral hemodynamics occurs. Jugular vein pressure value at that point is displayed as an absolute value of ICP. No clinical data are provided to support the eligibility of the approach.

1.6. A summary of the chapter

1. The assessment of CA has formerly been performed using various methods which are based on the calculation of the correlation coefficient between ABP and ICP slow waves or ABP and CBF velocity slow waves; however, clinical tests of these methods have not imparted a real-time continuous CA index. The main limitation of the above-mentioned methods is invasiveness or local measurement.
2. The disadvantages of invasive technologies can be eliminated by means of non-invasive technologies which are the research object of this work. Such non-invasive technologies can monitor the state characteristics of the human brain in real time and do not require a catheter implantation or additional injury to the brain. While the world has a huge demand for non-invasive technologies to monitor the human physiological parameters, such technologies are still unavailable in clinical practice. However, several non-invasive methods have already been developed and patented in the world. These methods are based on monitoring the CBF and ABP, and brain cerebrovascular function monitoring technologies have been developed on their basis.
3. A detailed analysis of the parameters suitable to define the cerebral autoregulation state of a human brain and to solve its monitoring problems were

performed in the first chapter. The development of non-invasive technologies is aggravated by strictly individual anatomy variations of skull structures and brain as well as different brain injuries. The CA state constantly changes with regards to different brain conditions and it must be continuously monitored.

4. The implementation of non-invasive CA status assessment currently is possible by monitoring cerebral blood flow velocity fluctuations with transcranial Doppler technology and calculating Mx instead of ICP waves (Czosnyka et al, 1996; Reinhard et al, 2003). The CBF and non-invasive ABP slow wave monitoring technology has been proposed together with Mx calculation for the continuous monitoring of CA (Czosnyka et al, 1996; Panerai, 1998; Reinhard et al, 2003).
5. It is essential to assess non-invasive CA monitoring technologies to make sure that in all clinical cases the developed methods and equipment can be applied to monitor the physiological state of the brain as well as the condition of cerebral autoregulation. Table 1.6. presents the proposed new derivative input parameter combinations used to calculate the CA index as non-invasive $vPRx1$ and $vPRx2$ and invasive $PRx3$. More details about different calculation methods are presented in the next chapter.

Table 1.6. Different combinations of input parameters used to calculate the CA index

$\boldsymbol{vPRx1 = r\{IBV_{SW}(t \dots \Delta t); ABP_{SW}(t \dots \Delta t)\}}$
$\boldsymbol{vPRx2 = r\{IBV_{SW}(t \dots \Delta t); IBV_{PW}(t \dots \Delta t)\}}$
$\boldsymbol{PRx3 = r\{ICP_{SW}(t \dots \Delta t); ICP_{PW}(t \dots \Delta t)\}}$
$\boldsymbol{PRx = r\{ICP_{SW}(t \dots \Delta t); ABP_{SW}(t \dots \Delta t)\}}$
$\boldsymbol{Mx = r\{CBF_{SW}(t \dots \Delta t); ABP_{SW}(t \dots \Delta t)\}}$

SW - slow waves; **r** – Pearson correlation coefficient; **t** – time moment; $\Delta \boldsymbol{t}$ = 120…600 sec - time window for calculation of correlation coefficients PRx and Mx; $\Delta \boldsymbol{t}$ = 30…120 sec - time window for calculation of correlation coefficients vPRx1, vPRx2 and PRx3.

Considering all the statements declared above, the aim of this work is to determine the clinical applicability and diagnostic value of a non-invasive CA monitoring system by performing experimental research and analysing the experimentally collected new empirical data. To accomplish the aim of this thesis, the following tasks are formulated:

1. To investigate the innovative non-invasive CA monitoring technology proposed by A. Ragauskas and V. Petkus to understand cerebral autoregulation; to create a personal CA management system. To establish new mechanisms to expand the set of this priceless information and ensure that it benefits people with brain disorders.

2. Carry out a prospective comparative study of PRx vs vPRx1 and vPRx2 indexes derived from the non-invasively monitored IBV waves using the investigated CA monitoring system on traumatic brain injury patients. To produce a dynamic picture of the functioning cerebrovascular autoregulation mechanism by developing and applying the improved non-invasive cerebrovascular autoregulation monitoring

method for large-scale monitoring. To seize the challenge of recording parameters defining dynamic cerebral autoregulation, because there are promising opportunities both for improving the existing technology and for developing a "Gold Standard" by encompassing different facets of the cerebrovascular autoregulation mechanism.

3. To carry out a prospective outcomes study of traumatic brain injury patients and link TBI patients' outcomes with the performance of non-invasive cerebrovascular autoregulation monitoring technology. To enable an unexploited potential of non-invasive cerebral autoregulation monitoring for a wide use in clinical practice.

4. To carry out an observational study of patients undergoing cardiac surgery with cardiopulmonary bypass. To collect empirical data and assess the conditions causing CA impairment and deterioration of mental abilities for patients undergoing surgery with cardiopulmonary bypass.

5. To integrate new scientific-technological and conceptual approaches produced in tasks 1–4 to explain why and how dynamic cerebrovascular autoregulation works.

2. RESEARCH OF FULLY NON-INVASIVE CEREBROVASCULAR AUTOREGULATION MONITORING TECHNOLOGY

2.1. An electronic system for cerebrovascular autoregulation monitoring

The possibility to estimate the CA status non-invasively is implemented by using a new ultrasonic "time-of-flight" (TOF) technique (Ragauskas et al., 2011; Ragauskas et al., 2008) which enables to continuously non-invasively monitor slow and pulse intracranial waves. The non-invasive ultrasonic "time-of-flight" method dedicated for intracranial blood volume monitoring is based on the transmission of short ultrasonic pulses from one side of the skull to the other and on dynamic measurements of the TOF of ultrasonic pulses (Ragauskas et al, 2011). The TOF depends on the acoustic properties of intracranial blood, brain tissue and cerebrospinal fluid. A change in the volume of any of these components will change the TOF.

A fully non-invasive ultrasonic CA monitor has been created at the Health Telematics Science Institute of Kaunas University of Technology, Lithuania (Fig. 2.1).

a) b)

Fig. 2.1. a) A fully non-invasive CA monitor; b) head frame of CA monitoring system. The authorship of the device belongs to Vittamed, Inc. Adapted from Vittamed, Inc.

A light and a convenient head frame (Fig. 2.1. b) is mounted on the subject's head to fix the ultrasonic transducers in a proper position for transmitting the ultrasonic pulses through the brain parenchyma (Fig. 2.2.).

As US waves travel through tissues, they are partly transmitted to the deeper structures, partly reflected, partly scattered, and partly transformed to heat. The amount of echo signal after hitting a tissue interface is determined by acoustic impedance. This is an intrinsic physical property of a medium defined as the density of the medium. Air-containing organs have the lowest acoustic impedance, while dense organs, such as bones, have very high-acoustic impedance (Table 2.1.).

Table 2.1. Acoustic impedances of different parts of the head (Hynynen and Sun, 1999).

Brain tissue	Acoustic impedance dB/cmMHz^n	US waves velocity, m/s	Attenuation degree, n
Skull bone	11.089	2652	1.890
CSF	0.002	1533	1.994
Tissue	0.869	1563	1.078
Blood	0.212	1583	1.266

Intraventricular or supraventricular location of the brain parenchyma is within the acoustic pathway that is being used to monitor intracranial fluctuations (Fig. 2.2.). The parenchyma acoustic pathway contains the parenchyma, blood vessels (arteries, arterioles, veins, venules, and capillaries) and cerebrospinal fluid. The arterioles and capillaries within the parenchyma are responsible for cerebrovascular autoregulation. US velocity throughout the parenchyma depends on the blood volume within the acoustic path. US attenuation depends on the parenchyma tissue volume throughout the acoustic path.

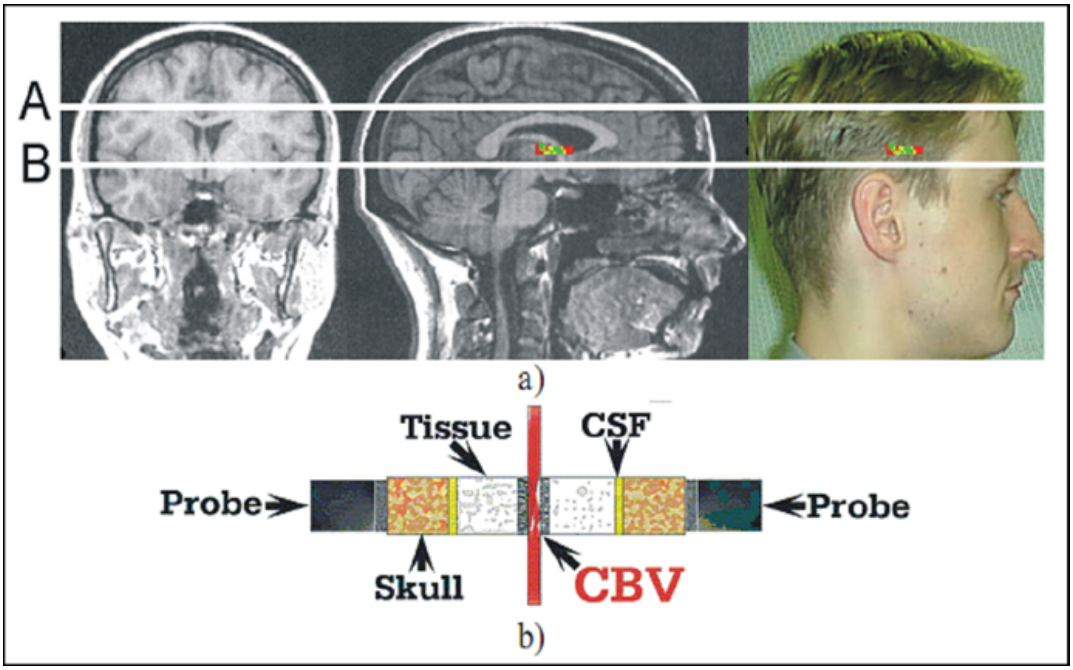

Fig. 2.2. a) A schematic representation of US acoustic paths: A – intraventricular; B – microvascular. The acoustic path consists of outer tissues, skull bones and the trans-intracranial parenchyma acoustic path which consists of blood, the parenchyma (or brain) tissue and the cerebrospinal fluid; b) A schematic representation of intracranial compartments. Adapted from Ragauskas et al. 2000.

As the ultrasound waves penetrate brain tissues of different acoustic impedances along the path of transmission, some are reflected to the transducer (echo signals) and some continue to penetrate deeper. To calculate the velocity difference throughout the parenchyma acoustic path, a broadband US signal was transmitted and the propagation time was measured. Sequential pulses are processed and combined to obtain an IBV signal and, consequently, CA state. (Fig. 2.3.)

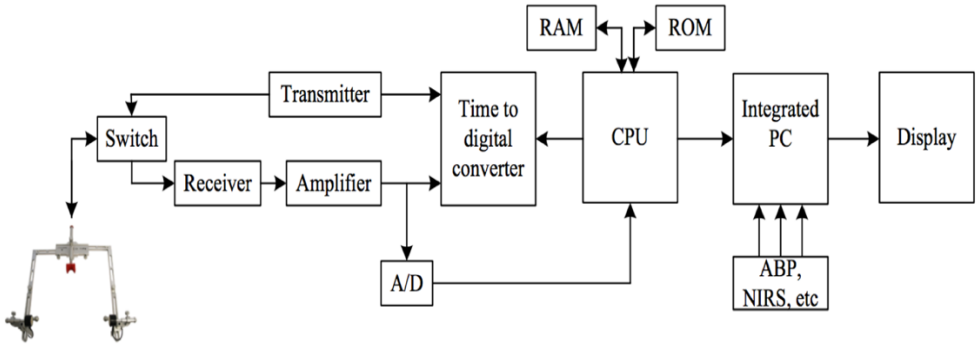

Fig. 2.3. A block scheme of the electronic system for non-invasive CA monitoring

2.2. The implementation of novel cerebrovascular autoregulation state calculation method – vPRx1

It is shown experimentally (Ragauskas et al, 2003) that the slow and pulse ICP waves are the consequences of intracranial blood volume variations. The speed of ultrasound in blood is higher than in other intracranial components (Ragauskas et al, 2011) (Table 2.1.), therefore the increase of blood volume during each heartbeat cycle will result in the increase of average relative ultrasound speed $\Delta C(t)/C_0$ (C_0 – US speed at initial time $t = t_0$) which is inversely proportional to TOF, i.e., $\Delta C(t) \sim 1/TOF(t)$.

Hereby, IBV waves can be monitored continuously, non-invasively and in real-time by using the TOF technique (Petkus et al, 2014). By using this technique, the invasive ICP slow and pulse wave monitor can be replaced by the non-invasive monitoring of the relative speed $\Delta C/C_0$ of the ultrasound passing through the volume of the brain parenchyma, which also reflects the variations of intracranial blood volume.

The IBV slow and pulse waves are the consequence of the physiological fluctuations in ABP signal (reference signal) in the corresponding frequencies of these waves. The latencies of IBV slow and pulse waves regarding these waves in the reference ABP signal are different and, can reflect the information on the CA status.

In the case of intact CA status, the IBV slow wave (informative) and ABP slow wave (reference) have an almost opposite phase due to the existing latency of slow waves at low frequency (0.008 Hz–0.033 Hz). In this case, the phase shift between these waves is about 180 degrees due to the autoregulatory properties of cerebral vasculature. In the case of a degrading CA, the phase shift between these waves

decreases and is close to zero when CA is totally impaired. For the higher frequency pulse waves (0.5 Hz–2 Hz) comparing with slow waves (0.008 Hz–0.033 Hz), the latency between IBV and ABP waves is small because healthy human time constant τ of cerebral blood flow autoregulation is normally 3–7 s, i.e. a few times higher than a typical period of the pulse wave. Hence, the latency between IBV and ABP pulse waves is negligibly small and not affected by the CA status.

2.3. Non-invasive real-time cerebrovascular blood flow autoregulation calculation without the arterial blood pressure line – vPRx2

The pulse waves are not the informative waves for the CA status assessment. However, they can be used to extract the reference signal which exists in the envelope without latency. The envelope of intracranial pulse wave is modulated with the slow wave which can be extracted by applying a specially created amplitude demodulation algorithms. It can be used as a reference signal instead of ABP waves for the calculation of PRx index used to assess the CA status. Therefore, it is no longer necessary to use the invasive or non-invasive extracranial ABP wave sensors to get the reference signal for CA status evaluation (see Fig. 2.4.).

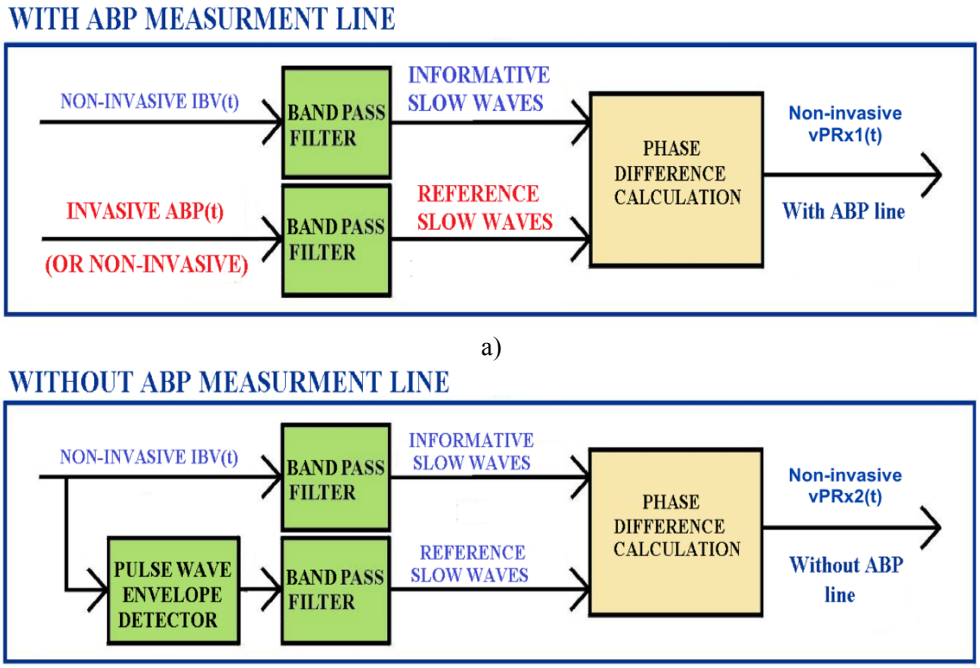

Fig. 2.4. Structural diagrams of non-invasive CA status monitoring a) using two b) or one channel

Hence, another approach to derive the CA state defining index is possible by calculating the Pearson's correlation coefficient r between the informative slow waves

of IBV signal (iSW) and the reference slow waves signal extracted from the envelope of IBV pulse waves (rSWE):

$$vPRx2(t) = r[rSWE(t);\ iSW(t)] \tag{14}$$

or

$$vPRx2(t) = -\cos(\pi - PS(rSWE(t); iSW(t))) \tag{15}$$

here, PS is the phase shift between informative slow waves $iSW(t)$ and reference slow waves $rSWE(t)$.

Therefore, it is no longer necessary to use the invasive or non-invasive extracranial ABP wave sensor to get the reference signals for the CA status estimation (Panerai, 1998). In this case, all ABP monitoring errors and artefacts are removed from the CA status estimation results.

The estimation of CA status is performed using linear calculation of the phase shift between the reference slow waves extracted from the pulse waves and the informative slow waves. Non-invasive vPRx2 index is calculated using monitoring data of the corresponding phase shifts. The algorithm of CA status measurement is shown in Fig. 2.5. The "time-of-flight" measurement unit is used to measure TOF(t) data with the resolution of about 60 ps. The envelope demodulator is used to demodulate the envelope of pulse waves PWE. The PWE data are filtered by using the band-pass filters to extract reference slow waves rSWE.

Informative slow iSWE waves are additionally processed with the pulse wave filter to compensate phase delay caused by the filtering reference waves. The phase shift difference between slow waves is used to calculate the non-invasive index which assesses the cerebrovascular autoregulation status vPRx2(t).

2.4. Mathematical processing of data received by the non-invasive cerebrovascular autoregulation status monitoring system

The US TOF(t) signal received from a media was transferred to a data processing device – CPU (see Fig. 2.3) to estimate the total flow volume. Data processing is divided into six steps (Fig. 2.6) as follows:

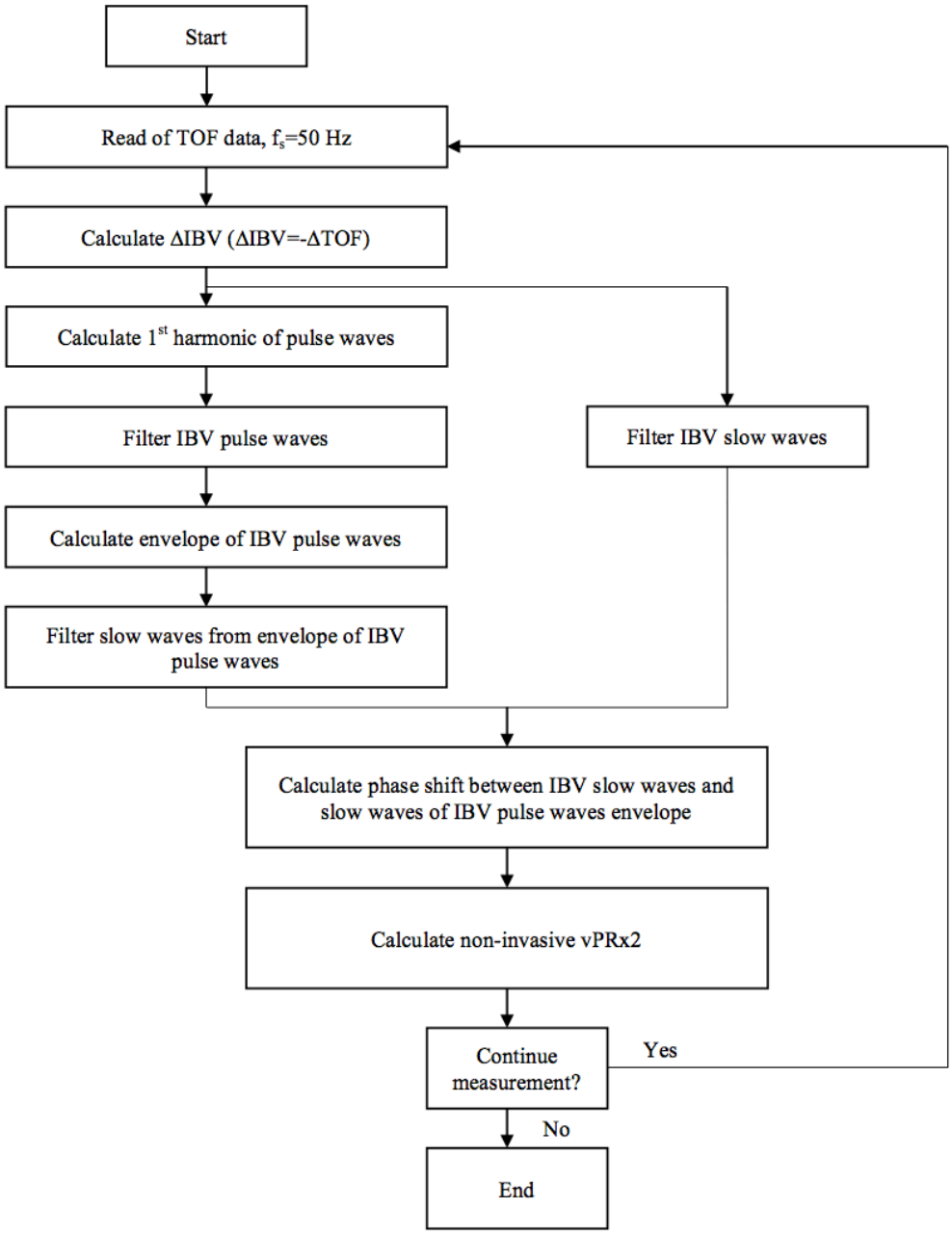

Fig. 2.5. The algorithm for non-invasive CA status measurement

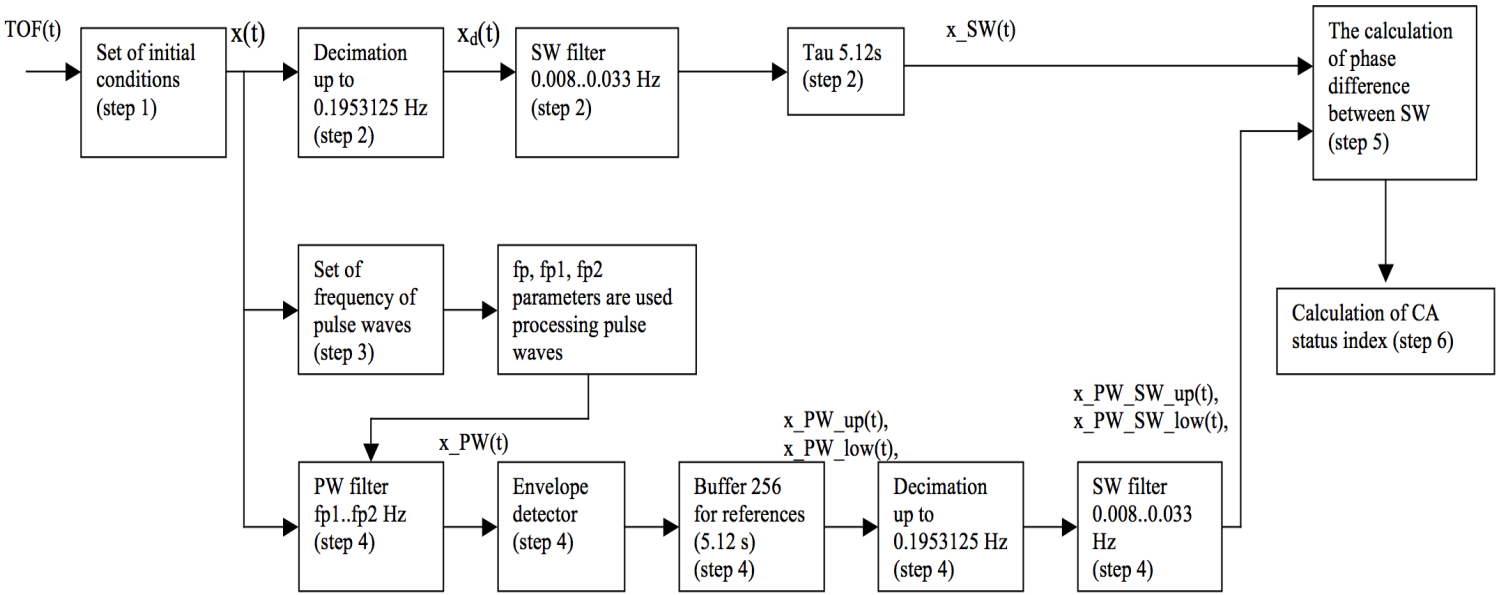

Fig. 2.6. A structural scheme of mathematical data processing

1. Set of initial conditions

- Initial signal processing:

$$X(t_i) = -\frac{(TOF(t_i) - TOF(t_0)}{TOF(t_0)} \quad (16)$$

$X(t_i)$ – relative US velocity, sampling frequency $f_S = 50\ Hz$; $TOF(t_i)$ – sample at time moment t_i; $TOF(t_0)$ – initial sample at time moment t_0.

- The elimination of initial baseline:

$$X(t) = X(t) - X(t_0) \quad (17)$$

$t = t_0, t_1, t_2 \ldots t_i$ - time moments.

- The formation of half of Hanning window (512 points) to reduce an amplitude of transient oscillations in the filters is used only on the initial data:

$$\omega(n) = 0.5\left(1 - \cos\left(2\pi\frac{n}{N}\right)\right), when\ 0 \le n \le N \quad (18)$$

n – the whole number, N – the width of the Hanning window.

2. Slow wave processing

Raw IBV signal data is provided in Fig. 2.7. The essential features of these waves are: 1. long period (from 30 s to 120 s); 2. volatility.

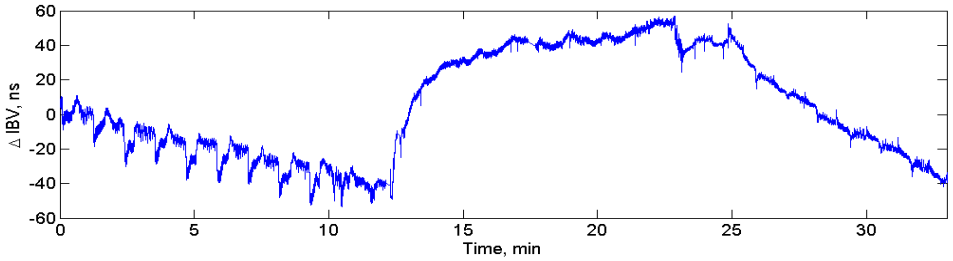

a)

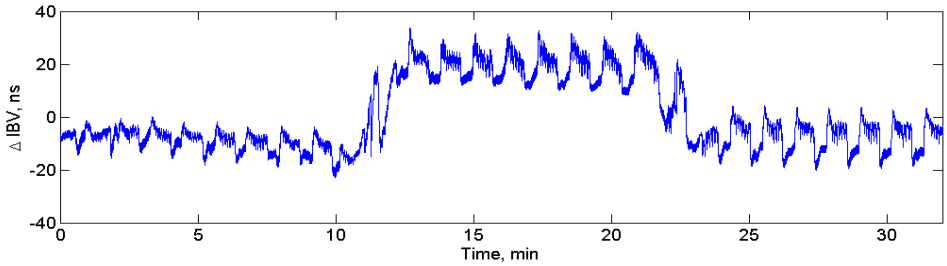

b)

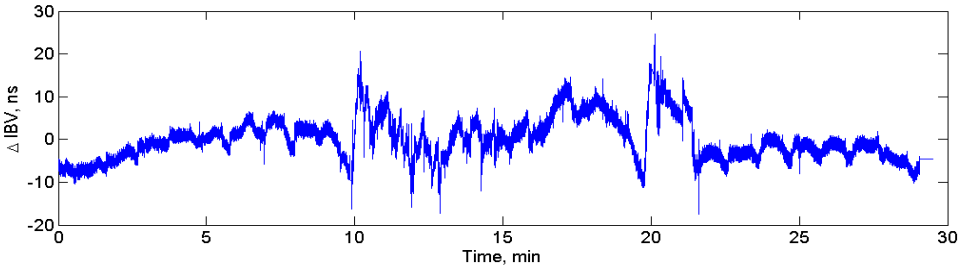

c)

Fig. 2.7. a), b), c) Non-invasively measured raw IBV data of healthy volunteers

- $X(t)$ signal is decimated up to 0.1953125 Hz;
- $X(t)$ signal is filtered with lowpass Butterworth filter (N = 8); N – filter row;

$$X(t) \rightarrow X_D(t)$$

- The decimated signal $X_D(t)$ is filtered with a bandpass Butterworth filter (N = 9), the filter range is from 0.008 Hz to 0.033 Hz; N – filter row;

$$X_D(t) \rightarrow X_{SW}(t)$$

- $X_{SW}(t)$ signal is delayed per one sampling period to compensate for the delay of processing the envelope of pulse waves by using the interpolation method.

3. A set of pulse wave frequency

- Temporal realization:

$$X_{t_0:t_{1023}} \times 0.5\left(1 - \cos\left(2\pi\frac{n}{N}\right)\right), when\ 0 \le n \le N \qquad (19)$$

here, $X_{t_0:t_{1023}}$ – input signal temporal realization (from 0 to 1023 points), n – whole number, N – Hanning window width – 1024 points.

- Fourier transformation:

$$X(k) = \left|\sum_{j=1}^{N} x(j)\omega_N^{(j-1)(k-1)}\right| \qquad (20)$$

$$x(j) = \frac{1}{N}\sum_{j=1}^{N} X(k)\omega_N^{-(j-1)(k-1)}$$

here, $\omega_N = e^{\frac{(-2\pi i)}{N}}$ – root of N unit, $X(k)$ – spectrum of $X_{t_0:t_{1024}}$signal (further sp).

- The estimation of pulse wave frequency:

$$f_p = index \times \frac{50}{1024} \quad (21)$$

here, f_p – pulse waves frequency, $index$ – spectrum maximum.

- f_{p1} and f_{p2} – initial cut-off frequencies of bandpass pulse wave filter are 0.5 Hz and 2 Hz, respectively. The verification of f_p satisfies the condition $f_{p2} > f_p > f_{p1}$:
  - If the condition is satisfied, the parameters are the same f_p, f_{p2}, f_{p1};
  - If condition is not satisfied, the parameters f_p, f_{p2}, f_{p1} are recalculated according to formulas19–21.

4. Pulse wave processing

- $X(t)$ signal is filtered with a lowpass Butterworth filter, $f_s = 50$ Hz;

$$\mathrm{X}(t) \rightarrow X(t)_{PW}.$$

The coefficients of pulse wave filter are calculated according to the following instructions:

- bandpass Butterworth filter (N = 4), N – filter row;
- pulse wave frequencies f_{p1} and f_{p2} are calculated according to step 3.

- Setting the upper $X(t)_{PW\_up}$ and lower $X(t)_{PW_{low}}$ envelope of pulse waves, $f_s = 50$ Hz:

$$X(t)_{PW\_up} = PW_{envelope}\left(X(t)_{PW}, f_{p2}, f_s\right); \quad (22)$$

$$X(t)_{PW\_low} = PW_{envelope}\left(X(t)_{PW}, f_{p1}, f_s\right); \quad (23)$$

here, $X(t)_{PW\_up}$ – upper envelope of pulse waves; $X(t)_{PW\_low}$ – lower envelope of pulse waves; $PW_{envelope}$ – the function of pulse wave envelope; f_{p2} – upper frequency of pulse waves and f_{p1} – lower frequency of pulse waves (set in step 3); f_s – sampling step of 50 Hz.

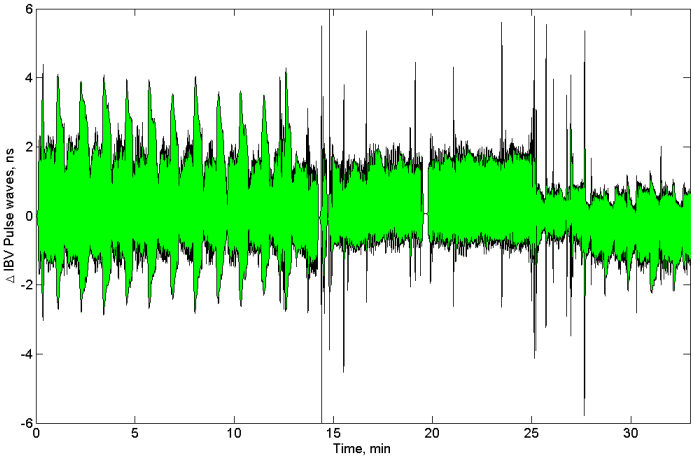

a)

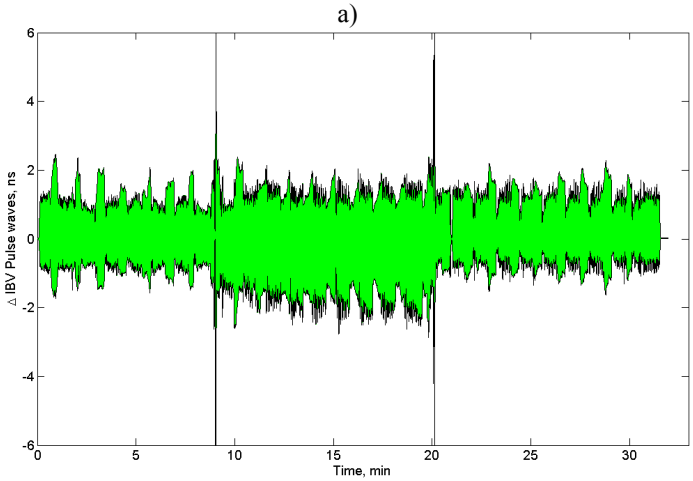

b)

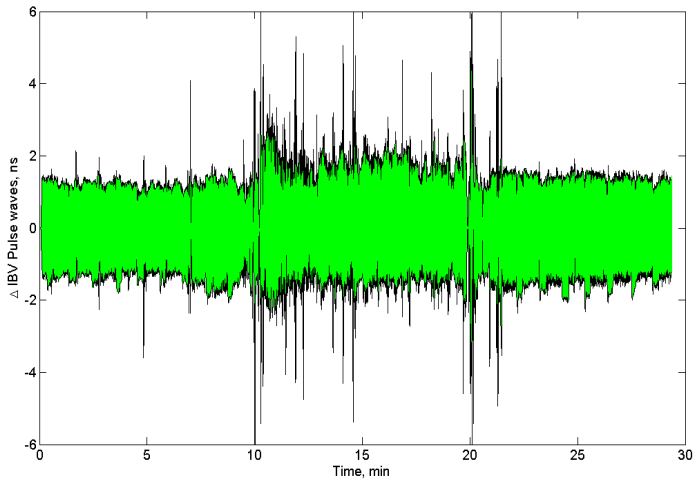

c)

Fig. 2.8. a), b), c) Pulse waves and envelope of IBV signal used for replacing the reference ABP signal.

- Slow waves are filtered from the envelopes of pulse waves $X(t)_{PW\_up}$ and $X(t)_{PW_{low}}$. Firstly, envelope signals are decimated up to sampling frequency f_{sSW}. Secondly, the decimated signals are filtered with a slow wave filter. After filtration, the slow waves of envelope are as follow:
  - $X(t)_{PW\_SW\_up}$ – after filtration of slow waves from $X(t)_{PW\_up}$;
  - $X(t)_{PW\_SW\_low}$ – after filtration of slow waves from $X(t)_{PW\_low}$.

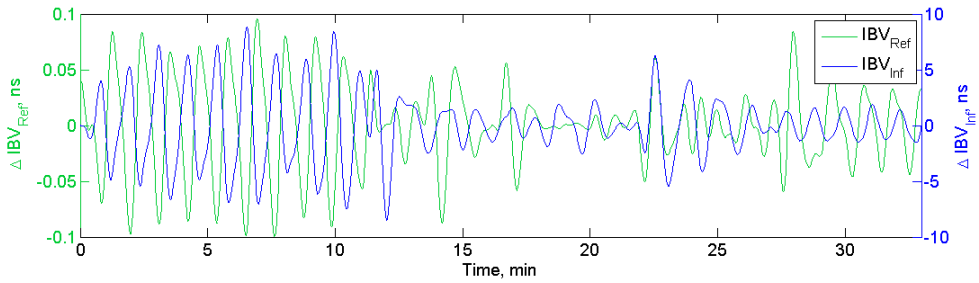

a)

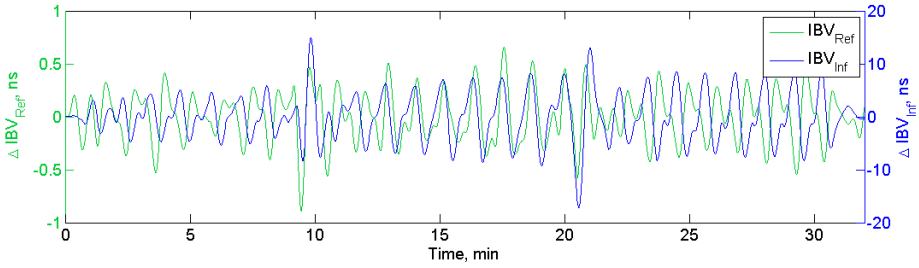

b)

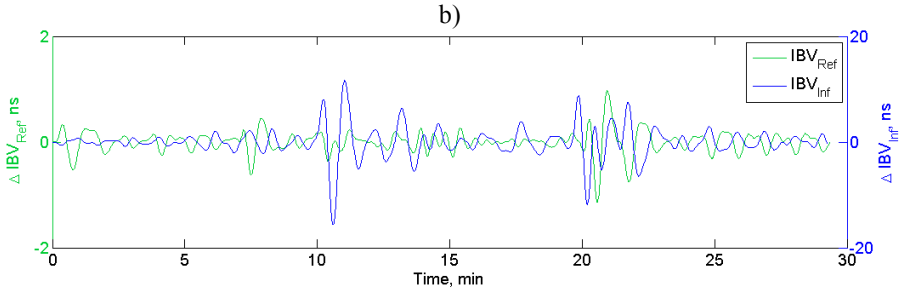

c)

Fig. 2.9. a), b), c) The slow waves filtered from the informative IBV signal and reference IBV signal

5. The calculation of phase difference between slow waves:

- Phase difference between the informative $(\mathrm{X(t)_{SW}})$ and reference $(\mathrm{X(t)_{PW\_SW\_up}})$ slow waves from the upper envelope of pulse waves:

$$\Delta\varphi(t)_{SW1} = \varphi(t)_{X(t)_{SW}} - \varphi(t)_{X(t)_{PW\_SW\_up}} \quad (24)$$

here, $\Delta\varphi(t)_{SW1}$ – phase difference; $X(t)_{SW}$ – slow waves; $X(t)_{PW\_SW\_up}$ – slow waves of upper envelope of pulse waves.

- Correlation coefficient between the informative $(\mathrm{X(t)_{SW}})$ and reference $(\mathrm{X(t)_{PW\_SW\_low}})$ slow waves from the lower envelope of pulse waves:

$$\Delta\varphi(t)_{SW2} = \varphi(t)_{X(t)_{SW}} - \varphi(t)_{X(t)_{PW\_SW\_low}} \quad (25)$$

here, $\Delta\varphi(t)_{SW2}$ – phase difference; $X(t)_{SW}$ – slow waves; $X(t)_{PW\_SW\_low}$ – slow waves of lower envelope of pulse waves.

- Correlation coefficient between the informative $(\mathrm{X(t)_{SW}})$ and reference $(\mathrm{X(t)_{PW\_SW\_up}})$ slow waves from the upper envelope of pulse waves:

$$r(t)_{SW1} = \frac{mean[(X(t)_{SW} - \mu(t)_{SW})(X(t)_{PW\_SW\_up} - \mu(t)_{PW\_SW\_up})]}{\sigma(t)_{SW}\,\sigma(t)_{PW\_SW\_up}} \quad (26)$$

here, $X(t)_{SW}$ – slow waves; $X(t)_{PW\_SW\_up}$ – slow waves of the upper envelope of pulse waves; $\mu(t)_{X_{SW}}$ and $\mu(t)_{X(t)_{PW\_SW\_up}}$ – the means of slow waves phases; $\sigma(t)_{X_{SW}}$ and $\sigma(t)_{X_{PW\_SW\_up}}$ – standard deviation of slow waves.

- Correlation coefficient between the informative $(\mathrm{X(t)_{SW}})$ and reference $(\mathrm{X(t)_{PW\_SW\_low}})$ slow waves from the lower envelope of pulse waves:

$$r(t)_{SW2} = \frac{mean[(X(t)_{SW} - \mu(t)_{SW})(X(t)_{PW\_SW\_low} - \mu(t)_{PW\_SW\_low})]}{\sigma(t)_{SW}\,\sigma(t)_{PW\_SW\_low}} \quad (27)$$

here, $X(t)_{SW}$ – slow waves; $X(t)_{PW\_SW\_low}$ – slow waves of the lower envelope of pulse waves; $\mu(t)_{SW}$ and $\mu(t)_{X(t)_{PW\_SW\_low}}$ – the means of slow waves phases; $\sigma(t)_{SW}$ and $\sigma(t)_{X_{PW\_SW\_low}}$ – standard deviation of slow waves.

- The calculation of phase-linearized CA index:

$$PRx(t)_{SW1} = 1 - 2\,arccos\{\cos(\pi - \Delta\varphi(t)_{SW1})\}/\pi = 1 - 2\,arccos\{r(t)_{SW1}\}/\pi \quad (28)$$

$$PRx(t)_{SW2} = 1 - 2\,arccos\{\cos(\pi - \Delta\varphi(t)_{SW2})\}/\pi = 1 - 2\,arccos\{r(t)_{SW2}\}/\pi \quad (29)$$

$$PRx(t) = (\alpha_1 PRx(t)_{SW1} + \alpha_2 PRx(t)_{SW2})/(\alpha_1 + \alpha_2) \quad (30)$$

This subchapter has defined the realisation of vPRx2. Seeking to compare both calculation methods – vPRx1 (with ABP signal) and vPRx2 (without ABP signal), Fig. 2.10. shows vPRx2 together with vPRx1.

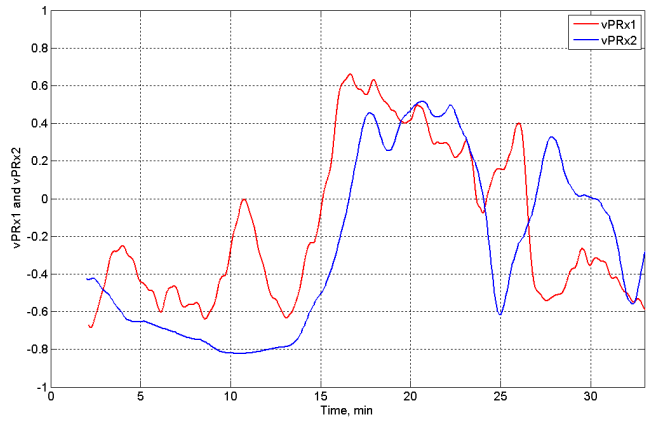

a)

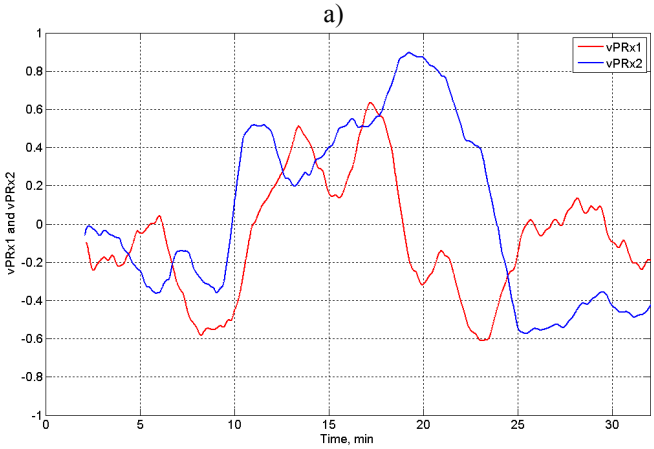

b)

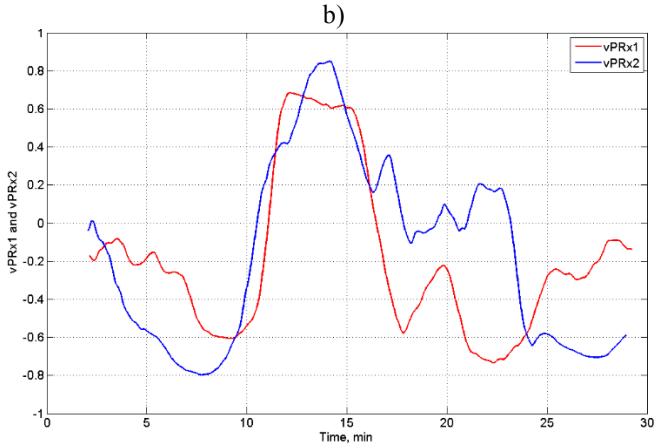

c)

Fig. 2.10. a), b), c) Non-invasively measured CA status defining indexes: index vPRx1 calculated from IBV and ABP signals (red curve), index vPRx2 calculated from IBV signal only (without ABP line) (blue curve).

2.5. Testing the ultrasonic "time-of-flight" prototype on healthy subjects

Preliminary testing of the "time-of-flight" prototype has been performed on consenting healthy volunteers by demonstrating the changes of TOF pulse waveform depending on the body position. Body position has been changed by using body tilting equipment which allowed to tilt a volunteer's body from the vertical position to head-down -30 degrees. The example illustrating the changes observed on 20 healthy volunteers by using the TOF monitoring prototype is shown in Fig. 2.11. This figure presents similar changes and the shift of pulse wave from left–to-right when ICP is increased by changing the body position from vertical to head-down. The ICP value increases during the head-down tilt test due to an increased hydrostatic pressure of cerebrospinal fluid in the human brain causing a worsening brain compliance condition. The pulse waveform becomes more rounded, the value of the second peak increases and even exceeds the first peak when the volunteer is tilted down (Fig. 2.11).

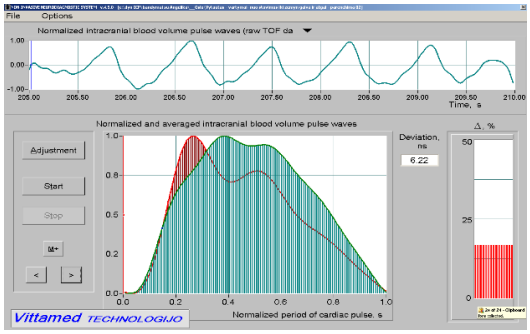

Fig. 2.11. The diagnostic study of TOF pulse wave shape during a body tilt test on healthy volunteers: red curve – vertical position, green – head down position (-30°).

The test of increasing ICP was also performed by doing the Valsalva test which causes a deterioration of venous blood outflow and influences a similar shift of TOF pulse wave from the left to the right side (Fig. 2.12.).

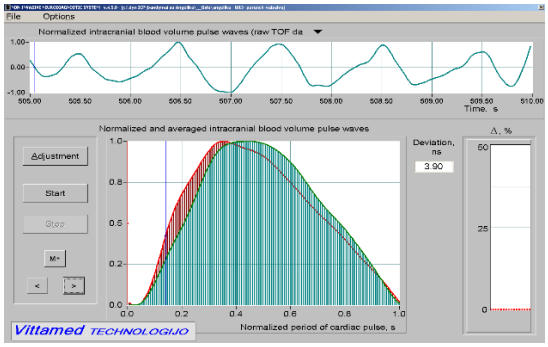

Fig. 2.12. The diagnostic study of TOF pulse wave shape during the Valsalva test on healthy volunteers: red curve – sitting position, green – Valsalva test at sitting position.

The opposite test of decreasing ICP was implemented by performing a hyperventilation test. Hyperventilation improves brain compliance and induces the appearance of the second peak in a pulse wave form (Fig. 2.13.).

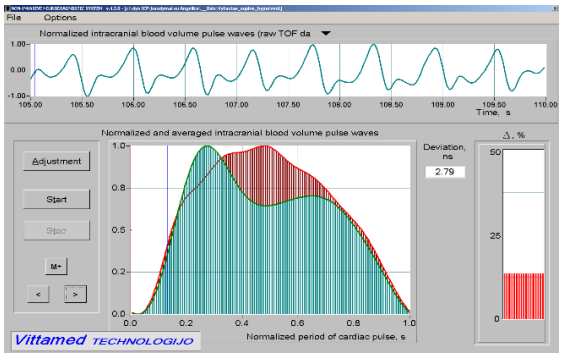

Fig. 2.13. The diagnostic study of TOF pulse wave shape during the hyperventilation test on healthy volunteers in supine position: red curve – normal breathing, green – hyperventilation.

2.6. A summary of the chapter

This chapter has investigated and described an innovative non-invasive CA monitoring technology to assess cerebral autoregulation state. However, the non-invasive CA monitoring method based on the application of slow waves has several limitations.

Firstly, a limitation of slow waves monitoring is the intermittent nature of these waves. Low amplitude slow waves or their absence cause a misleading estimation of the CA status, thus leading the shift of vPRx1 index close to zero value (which means no correlation between IBV and ABP). Discrete clinical tests, e.g., the cuff leg test has been introduced to raise temporal changes of ICP and ABP values allowing to assess the CA status (Panerai, 1998). However, this did not provide the continuous monitoring data needed for continuous real-time CA status estimation and optimal treatment.

The second limitation of the slow wave-based CA status monitoring method is the necessity to use an invasive or non-invasive ABP sensor. Although the non-invasive ABP measurement technique (Finapres plethysmograph) might be used to assess the CA status (Kasprowicz et al, 2010), invasive ABP sensors are more often used in clinical practice. The disadvantages of using the invasive ABP sensor are:

- implantation of the ABP sensor in the artery is a complex and risky procedure;
- it is necessary to replace the ABP sensor periodically to avoid mortification of the body parts;
- artefacts caused by body movements often distort the results of ABP measurements and give a misleading evaluation of the CA status.

It was found that the reference slow waves might be extracted after demodulation of the non-invasively measured IBV pulse waves and used instead of the reference ABP waves. It means that ABP waves might be rejected from PRx

calculation and only one channel of the non-invasively measured intracranial waves, i.e. slow and pulse waves might be used to estimate the CA status.

The existing CA status monitoring method should be assessed. The following chapters are going to present the findings of three clinical studies in two extremes of brain state: a healthy brain, when patients undergo cardiac surgery vs an injured brain (Fig. 1.2.). The studies were conducted by using a fully non-invasive electronic cerebrovascular autoregulation status monitoring system described in this chapter.

3. A COMPARATIVE CLINICAL STUDY OF CONVENTIONAL PRx vs vPRx1 AND vPRx2 ON TRAUMATIC BRAIN INJURY SUBJECTS

3.1. Materials and methods

A total of 39 severe traumatic brain injury patients (the author participated in half of data collection sessions) in different pathophysiological states (Annex 1) were monitored simultaneously by using an ICP monitor (Codman) (see Annex 1 for the details of ICP catheter placement) together with an ABP monitor (Datex), implanted in the radial artery, and a non-invasive CA status monitoring system (Vittamed 505) at the Republican Vilnius University Hospital (Lithuania). An ethical approval No.158200-06-498-145, 2012-06-12 was granted for the clinical study in the intensive care unit of the Republican Vilnius University Hospital (Lithuania). A total of 50 hours of monitoring has been performed including all 39 patients from 2012 to 2017. The data from the ICP and ABP monitors were transferred and processed by using the ICM+ software (Cambridge, UK). This software was used for online real-time calculation of the invasive PRx index. All data were used to perform the post hoc analysis to extract information – to find a link between the invasive and non-invasive methods; to assess the correlation coefficient between data and difference SD; and to optimize monitoring and real-time algorithms.

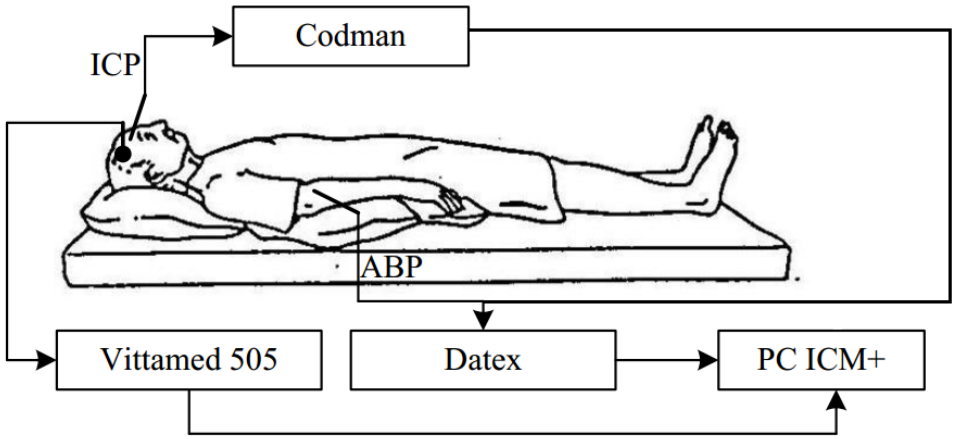

Fig. 3.1. A schematic depiction of CA data collection

3.2. Results

PRx was calculated as a moving linear correlation coefficient between the ABP and ICP spontaneous slow waves within a 10-min time window. The real-time artefacts were rejected from the ABP and ICP signal and only the artefact-free data were used for PRx calculation. Below are the examples of 1-hour simultaneous invasive PRx and non-invasive vPRx2 (without ABP line) and vPRx1 (with ABP line) monitoring on TBI patients in a coma.

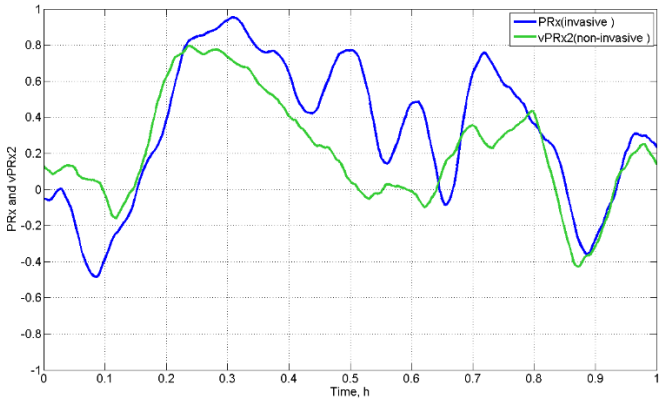

a)

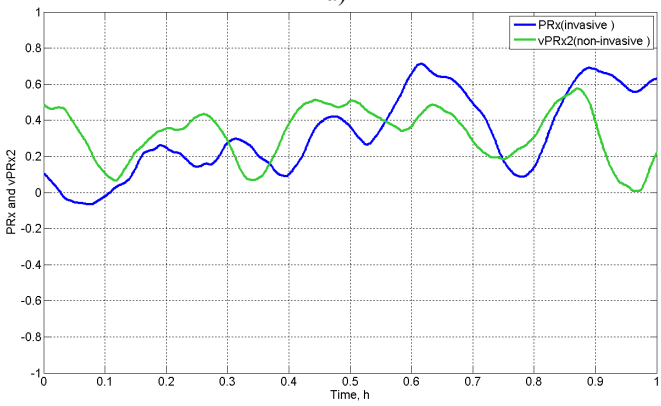

b)

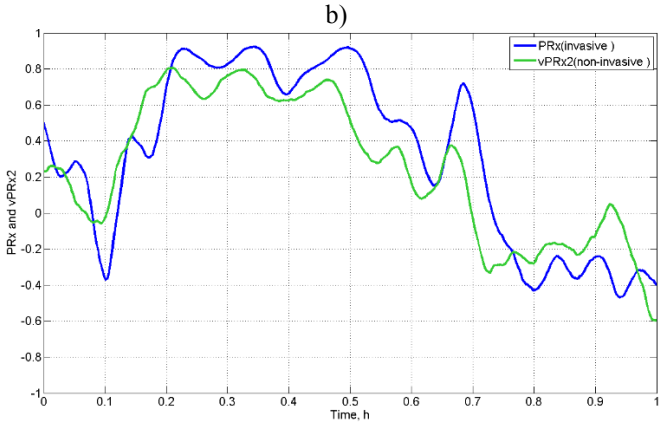

c)

Fig. 3.2. a), b), c) PRx and vPRx2 curves obtained in cases of impaired CA (PRx>0). Co-authorship of the clinical study and joint publications: Aidanas Preiksaitis, MD, Saulius Rocka, MD, Prof.

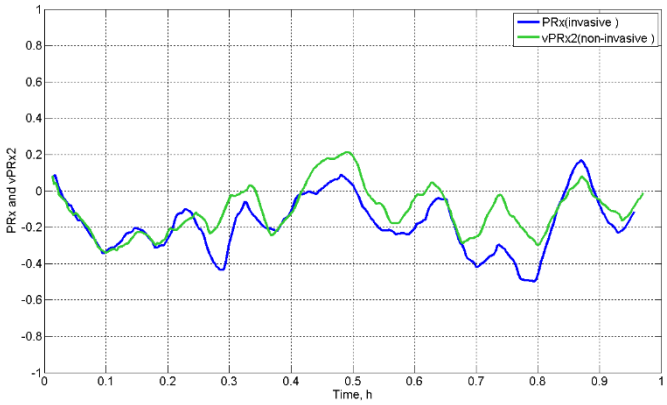

a)

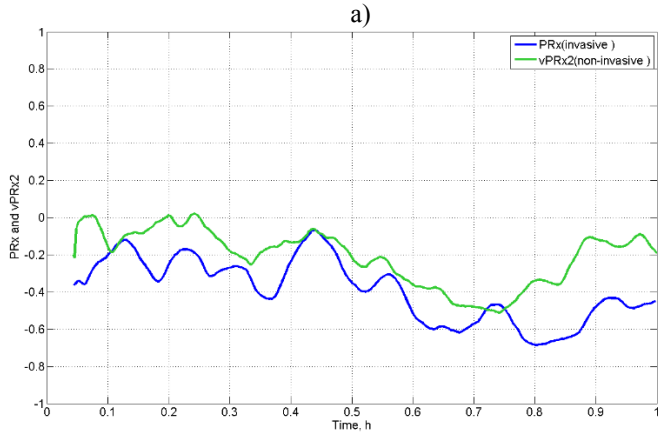

b)

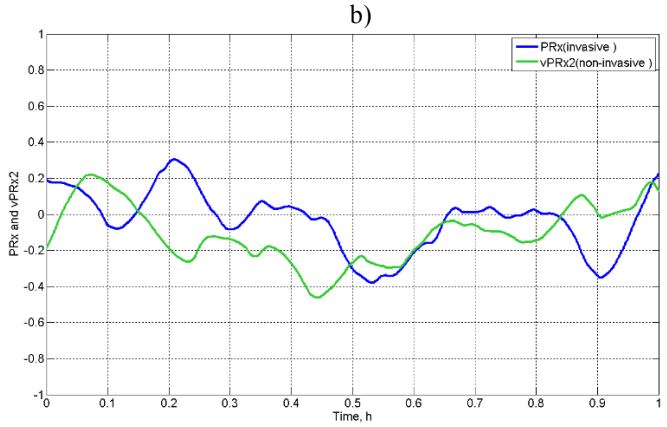

c)

Fig. 3.3. PRx and vPRx2 curves obtained in cases of a), b) intact and c) mildly impaired CA. Co-authorship of the clinical study and joint publications: Aidanas Preiksaitis, MD, Saulius Rocka, MD, Prof.

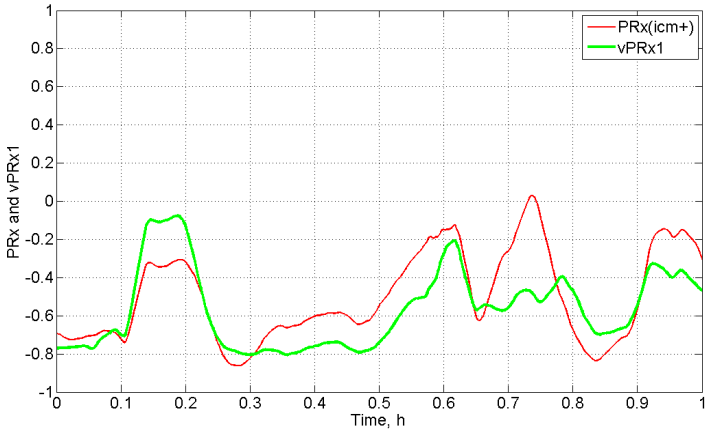
PRx(icm+)
vPRx1
PRx and vPRx1
Time, h

a)

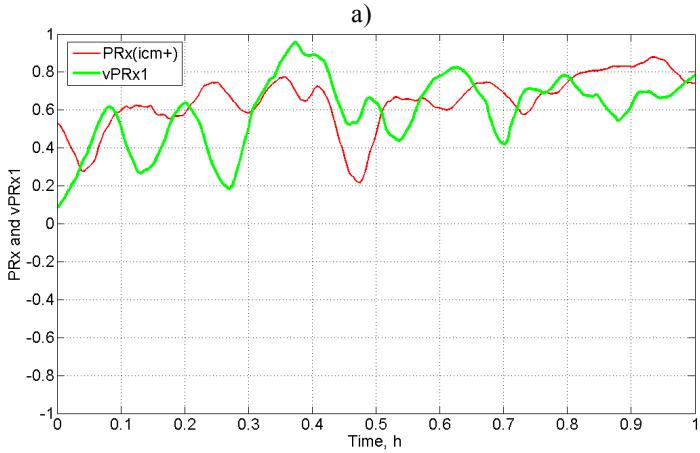
PRx(icm+)
vPRx1
PRx and vPRx1
Time, h

b)

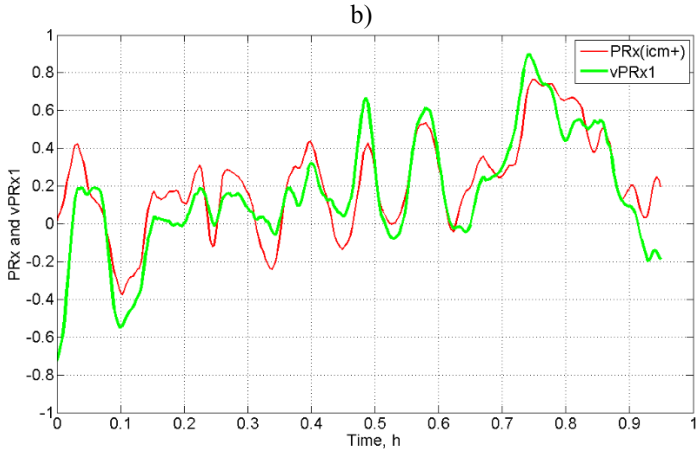
PRx(icm+)
vPRx1
PRx and vPRx1
Time, h

c)

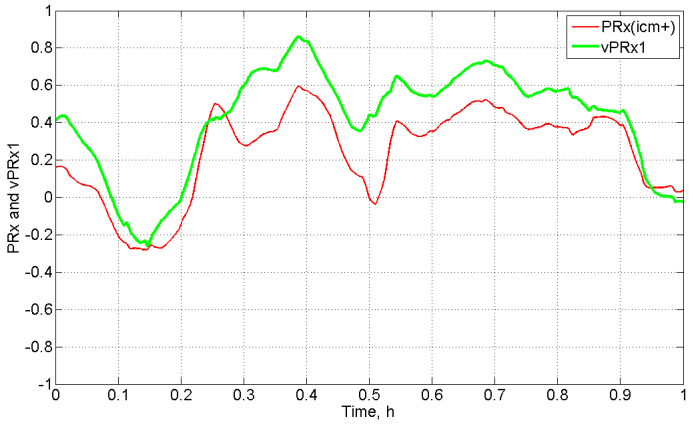

d)

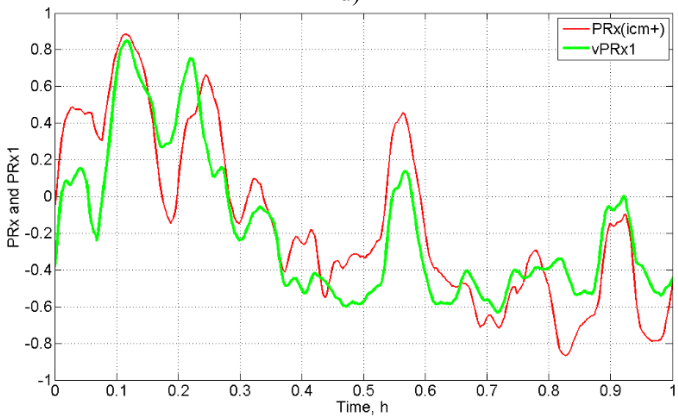

e)

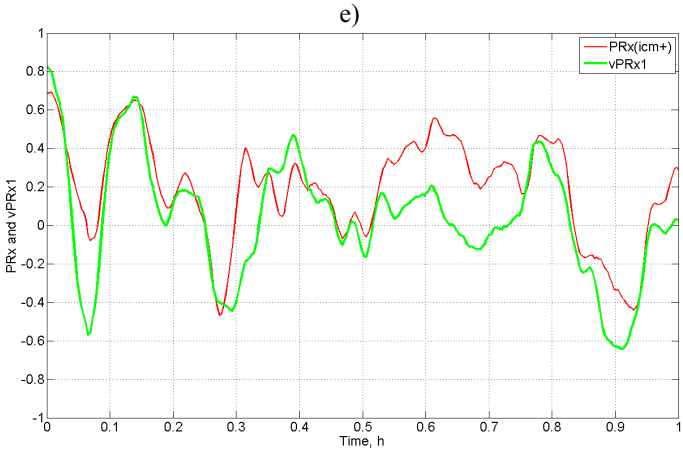

f)

Fig. 3.4. PRx and vPRx1 curves obtained in cases of a) intact CA; b) totally impaired CA; c), d), e), f) intact/impaired CA. Co-authorship of the clinical study and joint publications: Aidanas Preiksaitis, MD, Saulius Rocka, MD, Prof.

Scattered plots of PRx vs vPRx2 and PRx vs vPRx1 indices which assess the CA status are presented in Fig. 3.5. for comparison. The correlation coefficient between PRx and vPRx2 was r = 0.673 including all 39 patients and the total of 50 hours of monitoring. The correlation coefficient between PRx and vPRx1 was r = 0.707 including all 39 patients and the total of 50 hours of monitoring.

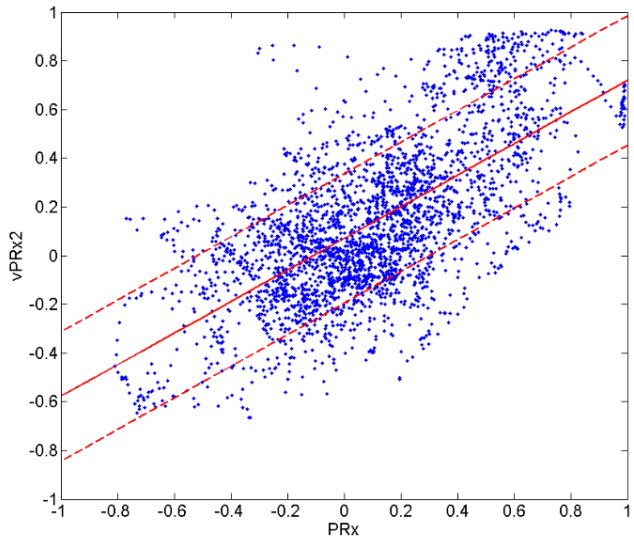

a)

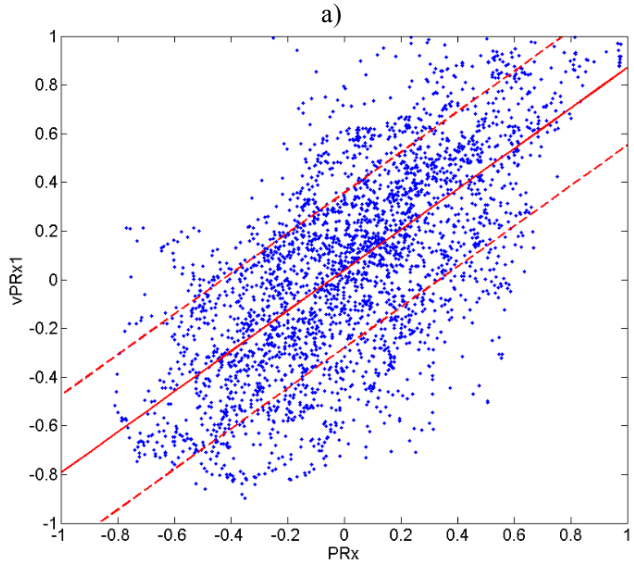

b)

Fig. 3.5. The assessment of CA status by comparing a) PRx vs vPRx2 (without ABP line) and b) PRx vs vPRx1 (with ABP line). Co-authorship of the clinical study and joint publications: Aidanas Preiksaitis, MD, Saulius Rocka, MD, Prof.

3.3. The development possibilities of the electronic cerebrovascular autoregulation status monitoring system – PRx3

The development of the presented methodology for non-invasive cerebrovascular autoregulation status estimation without the ABP line can be extended by exploring different methodologies of the CA status estimation. Firstly, the CA status might be estimated by using invasively measured ICP waves only. This way, the CA status might be evaluated by calculating the phase shifts between the reference slow or (and) respiratory waves extracted from the invasive ICP pulse waves and the informative slow or (and) respiratory ICP waves (Petkus et al, 2013). Such an approach assumes that the ABP pulse waves are modulated with the reference respiratory (and/or slow) waves which might be extracted from the envelope of the ICP pulse waves with a negligible delay. To test the possibility of evaluating the CA status by only using the ICP data, the presented method was compared to the conventional method based on the PRx index calculation from the ICP and ABP slow waves. The data were collected at the Republican Vilnius University Hospital (Lithuania) and ethical approval No.158200-06-498-145, 2012-06-12 was granted for the clinical study in the intensive care unit of the Republican Vilnius University Hospital (Lithuania). A total 350 hours of monitoring have been performed including 16 patients from 2012 to 2015. The analysis of simultaneously recorded ICP and ABP data from 16 traumatic brain injury patients (the author participated in 10 data collection sessions) showed that both methods provide similar information. The correlation coefficient between PRx (calculated from the ICP and ABP waves) and PRx3 (calculated from ICP waves only) including all patients was r = 0.724 (the total time of monitoring all patients was 350 hrs). The examples which illustrate the similarity between these two methods during long-term monitoring of traumatic brain injury patients under different CA conditions are shown in Fig. 3.6 and Fig. 3.7.

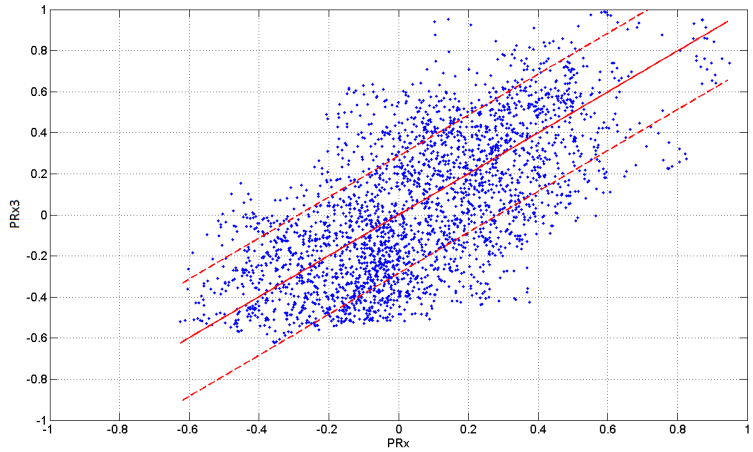

Fig. 3.6. A comparison of PRx vs PRx3 indexes. Correlation coefficient r = 0.724. The SD of difference between PRx and PRx3 is 0.286 (dashed red line). Co-authorship of the clinical study and joint publications: Aidanas Preiksaitis, MD, Saulius Rocka, MD, Prof.

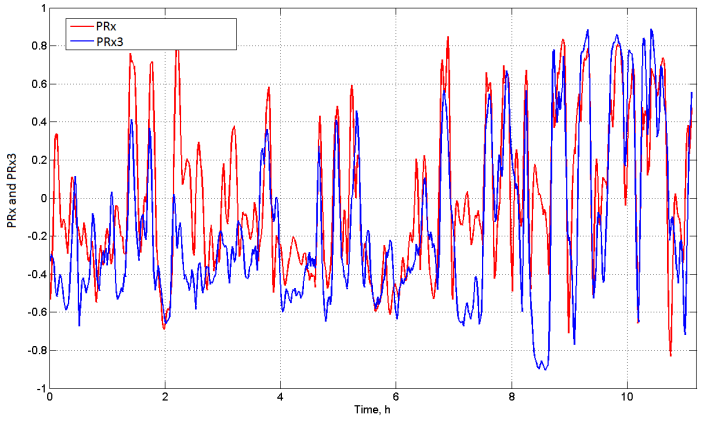
PRx
PRx3
PRx and PRx3
Time, h

a)

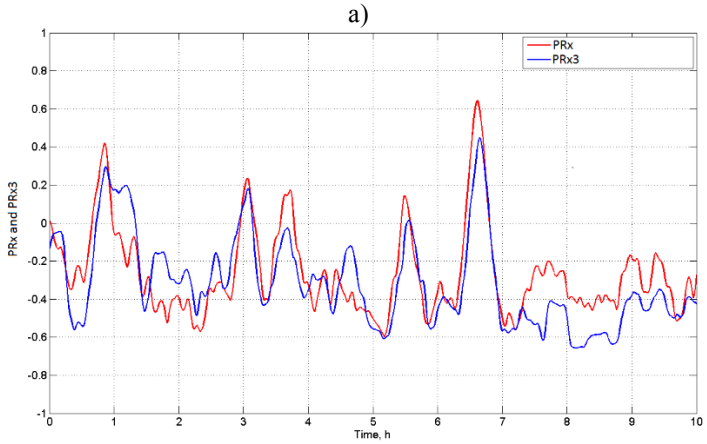
PRx
PRx3
PRx and PRx3
Time, h

b)

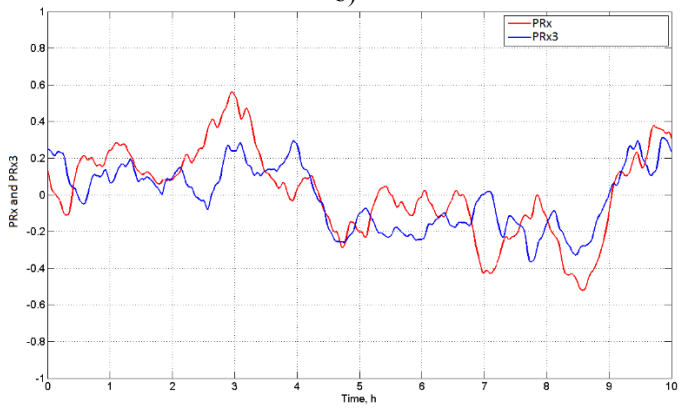
PRx
PRx3
PRx and PRx3
Time, h

c)

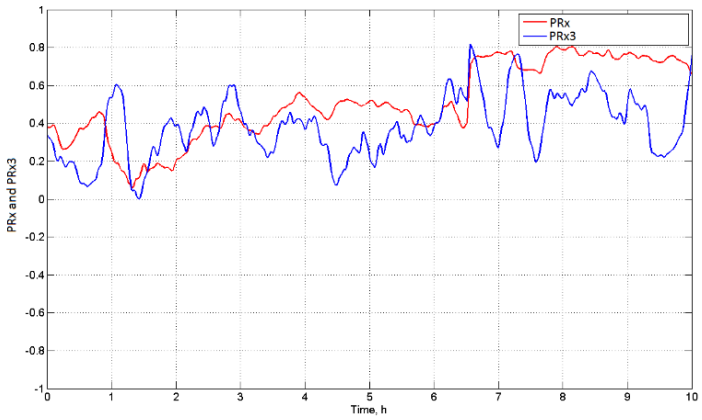

d)

Fig. 3.7. Examples of 10-hour simultaneous PRx3 and PRx monitoring sessions: a), b), c) – CA changes between impaired and intact; d) – CA is impaired. Co-authorship of the clinical study and joint publications: Aidanas Preiksaitis, MD, Saulius Rocka, MD, Prof.

3.4. A summary of the chapter

This chapter has demonstrated the results of a fully non-invasive CA status assessment tool vPRx2 and vPRx1 (with ABP reference signal) in comparison with the invasive PRx. The results of both non-invasive technologies –vPRx2 and vPRx1 – have significant correlation with the invasive PRx. A better correlation was obtained between vPRx1 (with ABP line) and PRx ($r = 0.707$) as compared to vPRx2 vs PRx ($r = 0.673$).

A limitation of this study is that some patients' data had artefacts, especially in ABP measurement. These artefacts were corrected or excluded from the measurements during retrospective data analysis. However, they might cause errors when evaluating the durations of CA impairment episodes.

It must be noted that a short artefact, lasting a few seconds in the ABP channel can distort the PRx value for ~5–10 min (depending on the length of time window used for the calculation of moving correlation coefficient).

An extension of the present method is the possibility to implement the fully non-invasive CA status monitoring by introducing other non-invasive methods of intracranial wave monitoring, such as TCD (Czosnyka et al, 1996; Eames et al, 2002) or the near-infrared-based (Zweifel et al, 2010) monitoring methodology.

This thesis presents a possible extension to use only the ICP(t) signal. It was found that the reference slow waves might be extracted after demodulation of the non-invasively or invasively measured ICP pulse waves and used instead of the reference ABP waves. It means that ABP waves might be rejected from the PRx calculation and only one channel might be used for estimating the CA status.

4. AN OUTCOMES STUDY OF SEVERE TRAUMATIC BRAIN INJURY SUBJECTS

4.1. Background of the study

Although the outcome of patients with traumatic brain injury is highly associated with the severity of brain injury and many other factors (Gerber et al, 2013; Firsching et al, 2001), it might be improved by optimizing treatment strategies (Schmidt et al, 2014; Lang et al, 2005; Czosnyka et al, 2009; Balestreri et al, 2006). The main factors influencing the possibility to treat the patient leading to a better outcome are cerebral perfusion pressure, cerebrovascular autoregulation, age and the severity of the brain injury. The initial state of a TBI patient is estimated according to the Glasgow coma scale (GCS), which, together with other factors such as, age, computed tomography scans, etc., might provide a prognosis of the outcome (Crach Trial MRC, 2008). Moreover, such prediction of a patient's outcome based on the initial GCS does not contain the patient's treatment protocol. The impairment of CA has a strong impact on the outcome of the traumatic brain injury patients. Therefore, it is essential to monitor the real-time status of CA (Sviri and Newell, 2010). A consensus has already been reached that the cerebral blood flow autoregulatory state of TBI patients must be monitored and an individualized treatment strategy should be re-evaluated regularly over the course of CBF autoregulation status (Brain Trauma Foundation, 2007).

In this study, continuous CA state monitoring was implemented by calculating a pressure-reactivity index PRx as a moving linear correlation coefficient between the reference arterial blood pressure and the invasively measured intracranial pressure slow waves, as described in the methodology (Chapter 2) (Czosnyka et al, 1997; Kasprowicz et al, 2010; Petkus et al, 2014; Ragauskas et al, 2003). It is proven that an increased PRx above the critical thresholds is associated with brain vascular deterioration leading to the fatal outcome (Sorrentino et al, 2012). Different PRx thresholds are associated with the survival (when the averaged PRx is below 0.2–0.25) and for a favourable outcome (when the averaged PRx is below 0.05) were reported in recent studies (Lavinio et al, 2008; Sorrentino et al, 2012). Moreover, PRx can be used as a variable for setting an individual target for the optimal CPP management (Menon, 2003). Continuous PRx monitoring might help to identify the optimal CPP under the condition of the longest cerebrovascular autoregulation impairment (LCAI). The optimal CPP is determined by plotting PRx against CPP in individual cases (by the moving time window of 3 h or even up to 6 h) and by finding the CPP value or CPP range at which PRx is minimal (Steiner et al, 2002). Minimal PRx reflects the condition of intact CA. The patients with greater deviation between their averaged CPP and post hoc assessed optimal CPP have worse outcomes after a head trauma (Rasulo et al, 2012; Depreitere et al, 2014). However, there are a few limitations of practical usage of PRx and optimal CPP-based treatment strategies:

- Statistically determined PRx thresholds for survival are rough due to the use of averaged PRx values for the threshold calculation. In most cases, the real-

time monitored PRx values vary considerably above and below the determined PRx thresholds. Therefore, it complicates a patient's specific treatment decision making.

- The determination of the optimal CPP requires more time for more accurate and precise estimation (3–6 h). Therefore, a delay in making a patient's treatment decision might be critical. The real-time monitored CPP value always varies with the delay respectively to the optimal CPP and the differences between the real-time monitored CPP and the optimal CPP are not investigated enough.
- Additional important factors, such as age and brain injury rate, influence the patient's outcome and should be considered in choosing patient-specific treatment strategies (Bigler, 2001).

The hypothesis formulated in this chapter is: the outcomes in TBI patients are negatively correlated with the longest duration in an episode of CA impairment, rather than with the averaged time of all episodes of CA impairment.

The aim of this study was to explore the relation of duration of CA impairment episodes on the outcomes of severe TBI patients by including the patient's age as an additional influential factor in the analysis. The identification of critical durations of relatively long CA impairments in association with severe TBI patient outcomes was also included in the aim of the prospective clinical study.

4.2. Materials and methods

A total of the same 39 severe traumatic brain injury patients in different pathophysiological states (used in the comparative study described in Chapter 3) were monitored simultaneously by using an ICP monitor (Codman) and an ABP monitor (Datex) at the Republican Vilnius University Hospital (Lithuania). Ethical approval No.158200-06-498-14. More about study materials on p. 67 and patients' description can be seen in Annex 1. The data from the ICP and ABP monitors were collected and processed by using ICM+ software (Cambridge, UK). This software was used for online real-time calculation of the PRx index as well as to determine the optimal CPP values.

The following parameters of the monitored data were calculated:

- PRx was calculated as a moving linear correlation coefficient between the ABP and ICP spontaneous slow waves within a 10-min time window. The real-time artefacts were rejected from the ABP and ICP signals and only the artefact-free data were used to calculate the PRx.
- CPP was calculated as the difference between the mean ABP and ICP values within a 10-min time window. The optimal CPP values were calculated by plotting the PRx values vs CPP values and fitting the U-shaped curve over the plotted points taken from a 6-hour monitoring window. The minimum point of the U shape was kept as an optimal CPP value.
- The difference between the real-time CPP and the optimal CPP was calculated as $\Delta CPPopt = CPP - CPPopt$.

- The longest CA impairment episodes, when PRx(t) continuously exceeded the high positive values of 0.5, 0.6, 0.7, and 0.8, were estimated for each patient.
- The total time in percentage of CA impairment when the PRx value exceeded the threshold associated with mortality (when the average PRx is above 0.2–0.25) was calculated for each patient.

The Glasgow outcome scale score (Table 4.1.) was determined after hospital discharge (GOS_{HD}) and 6 months (GOS_{6M}).

Table 4.1. The patients' outcome according to the GOS score

GOS score	State
1	Death
2	Constant vegetative state
3	Severe disability
4	Moderate disability
5	Low disability

The outcome was considered good if the GOS score was 3, 4 or 5, and unfavourable, if the GOS score was 1 or 2.

It is known that the exact location of brain lesions is statistically significantly related to the mortality and outcome of the survivors (Firsching et al, 2001). Although MRI and CT scans give useful information for patient treatment and prognosis, not all patients could be transferred to the MRI unit due to their critical state.

4.2.1. Statistical Analysis

The Pearson chi-squared test (χ^2) was used to determine the critical thresholds of the analysed factors associated with an (un)favourable outcome. A series of 2x2 tables were created by grouping the patients according to:

- Criteria of outcome: patient group with favourable [GOS score of 3, 4, and 5] vs unfavourable outcome [GOS score of 1 and 2];
- Influential factors: patient group with factor values greater or smaller than the coherent thresholds: for the survival when the averaged PRx is below 0.2–0.25 and for a favourable outcome when the averaged PRx is below 0.05.

The tables were reconstructed by changing the influential factors within their range, and the Pearson chi-square criteria was calculated for each table. For each outcome measure, the respective threshold of all analysed factors (PRx, ΔCPPopt, age) returning the highest χ^2 score was assumed to have the best discriminative value (Sorrentino et al, 2012). The additional plots of GOS association with PRx, LCAI, ΔCPPopt, and age were accompanied by fitting linear regression and calculating the Pearson correlation coefficient r. Multiple correlation coefficients were also calculated for the relationships between GOS indexes and multiple input factors (ΔCPPopt, age) by using the Matlab software and Surface fitting tool. The significance was set at $P < 0.05$.

4.3. Association of severe TBI patients' outcome with the duration of CA impairment events, age and ΔCPPopt

The patients' age ranged from 18 to 66 years; the mean age was 37.5 years. There were 32 male and 7 female patients. Detailed characteristics of the patients' demographic, their outcomes (Table 4.2.) and the registered values of LCAI, the averaged PRx and declination of CPP from optCPP values are listed in Annex 1.

Table 4.2. The patients' outcomes after the hospital discharge and after 6 months of brain injury were as follows

GOS score	Number of patients' after hospital discharge	Number of patients' after 6 months
1	4	7
2	6	1
3	12	7
4	4	10
5	0	3

Box plots of the outcome indexes GOS_{6M} were plotted in comparison with the mean values of PRx indexes, time of CA impairments and ΔCPPopt showing an association between these factors with GOS_{6M} are presented in Fig. 4.1.–4.3. The correlation coefficient between PRx and GOS was 0.444 (P = 0.001) after 6 months.

ΔCPPopt correlated significantly with the GOS score after 6 months (r = 0.387, P = 0.003). The calculated PRx critical threshold value for mortality outcome was 0.24 (χ^2 = 5.527, P = 0.0188) after 6 months. The threshold PRx value of > 0.24 was used to define the conditions of CA impairment and to calculate the total time of CA impairment under these conditions. There was a significant correlation between the GOS score and the total time of CA impairment after 6 months (r = -0.532, P = or < 0.001). The calculated duration of the longest CA impairment when PRx > 0.7 for mortality outcome was 40 min (χ^2 = 5.991, P = 0.014) after 6 months (Fig. 4.4).

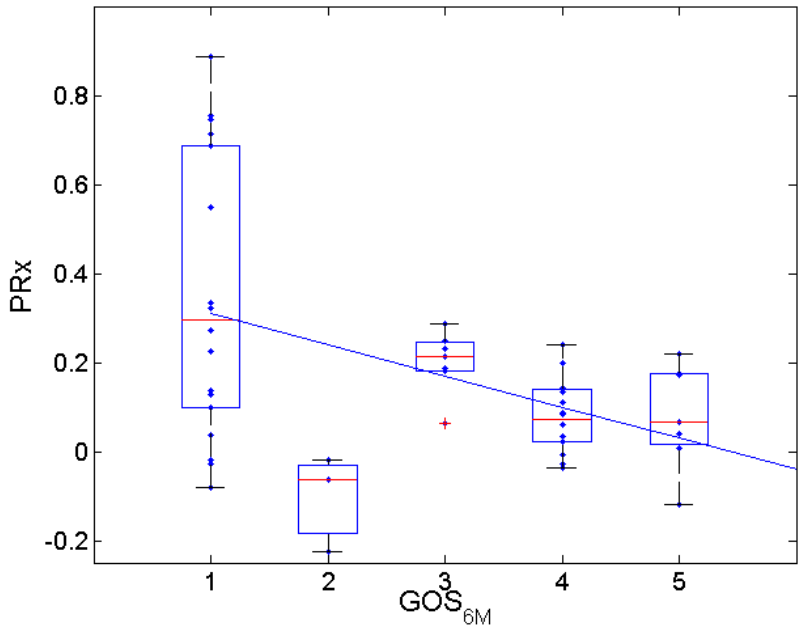

Fig. 4.1. A box plot of association between GOS and PRx. GOS after 6 months correlates negatively with PRx (r = -0.444, P = 0.001). Co-authorship of the clinical study and joint publications: Aidanas Preiksaitis, MD, Saulius Rocka, MD, Prof.

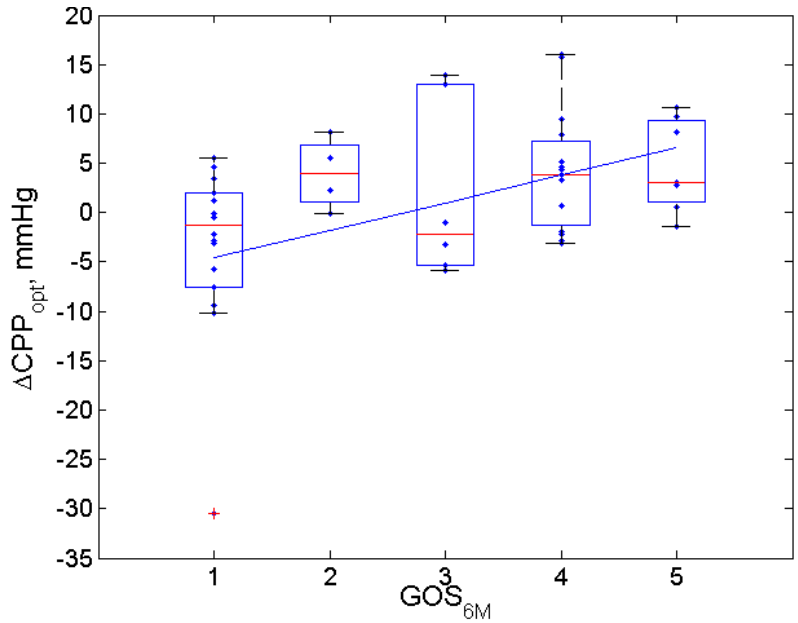

Fig. 4.2. A box plot of association between GOS and ΔCPPopt. The correlation coefficient between the GOS after 6 months and ΔCPPopt is r = 0.387 (P = 0.003). Co-authorship of the clinical study and joint publications: Aidanas Preiksaitis, MD, Saulius Rocka, MD, Prof.

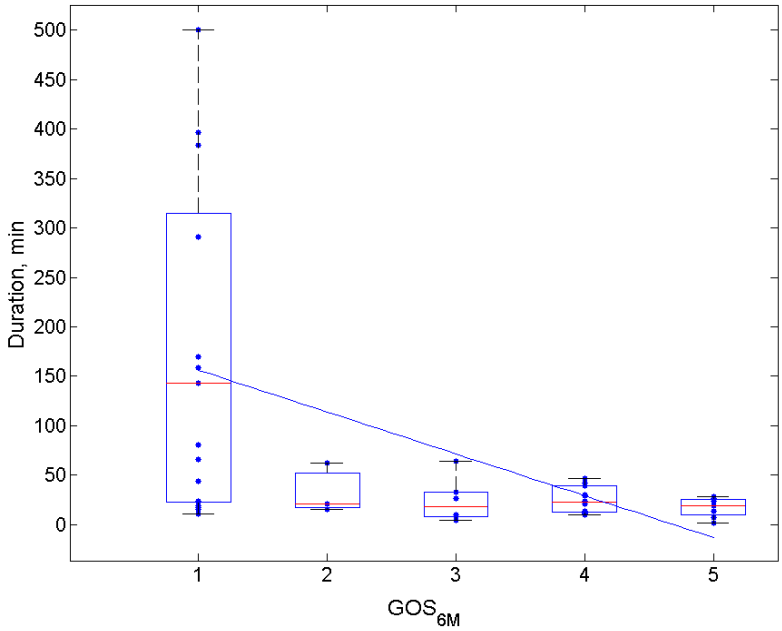

Fig. 4.3. A box plot showing the association between GOS after 6 months and the duration of the longest CA impairment event under conditions when PRx > 0.7 (r = -0.532, P = or < 0.001). CA impairment duration > 30 min (χ^2 = 7.405, P = 0.007) when PRx > 0.7 is associated with mortality. Co-authorship of the clinical study and joint publications: Aidanas Preiksaitis, MD, Saulius Rocka, MD, Prof.

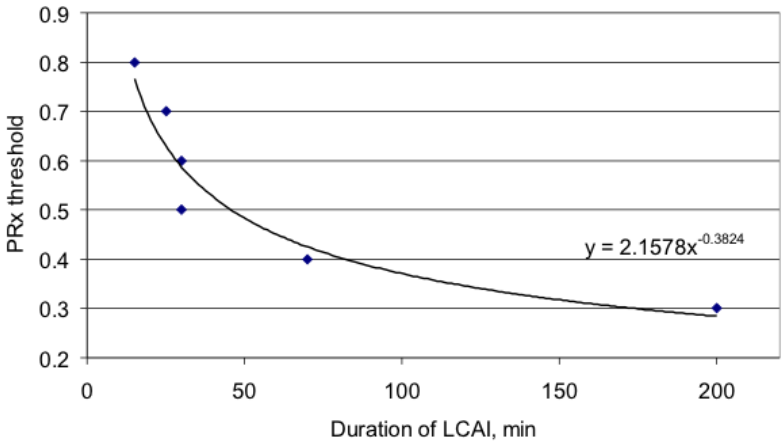

Fig. 4.4. Non-linear dependence between the longest critical duration of CA impairment event and the critical PRx thresholds associated with mortality. The correlation coefficient r = 0.964. Co-authorship of the clinical study and joint publications: Aidanas Preiksaitis, MD, Saulius Rocka, MD, Prof.

A 3-dimensional (3-D) association was used to show the age influence on the ΔCPPopt. The contour plots of 3-D surfaces show that the red area (Table 4.3. – good

outcome, GOS = 5) is in certain parts of the 3-D surface, defining the conditions for predicting and managing TBI patients' outcomes.

Table 4.3. GOS scale is represented by colours in 3D figures (Fig. 4.5. and Fig. 4.7).

GOS score	Colour
5	Red
4	Orange
3	Green
2	Light blue
1	Dark blue

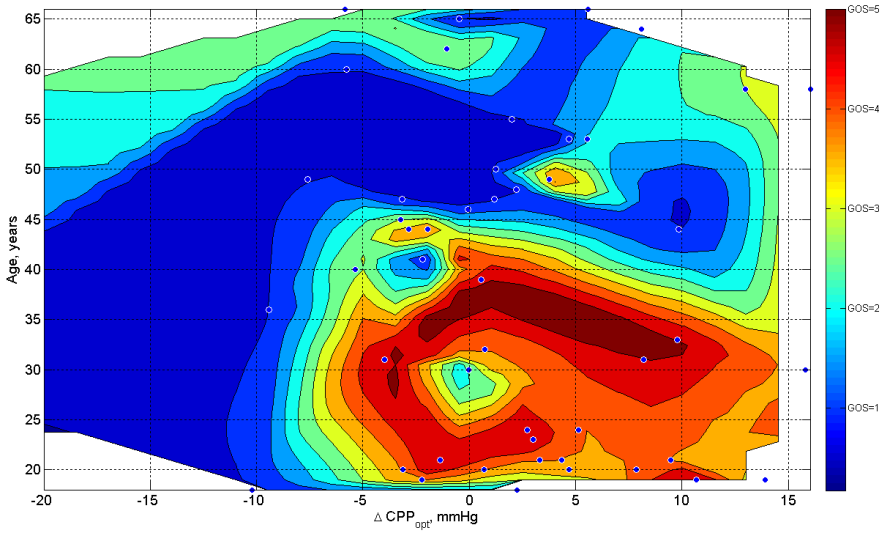

Fig. 4.5. Contour plots of GOS dependencies on the declination of CPP from the optimal CPP and age. Better outcome is associated with younger patients and for those whose CPP was kept within the range from optimal CPP to optimal CPP +10 mmHg. The multiple correlation coefficient between GOS and ΔCPPopt together with age was r = -0.615 (P < 0.001). Co-authorship of the clinical study and joint publications: Aidanas Preiksaitis, MD, Saulius Rocka, MD, Prof.

The PRx thresholds of good outcomes (GOS score: 4 or 5) were not determined. The statistically significant differences among the vegetative, severe disabilities and good outcomes were not found. The calculated ΔCPPopt threshold for the mortality outcome was 6 mmHg (χ^2 = 6.171, P = 0.012) after 6 months (Fig. 4.5.).

Additionally, the influence of age and brain injury rate on the patients' outcome was checked. The correlation coefficient between the age and GOS_{6M} was r = -0.480 (P < 0.001) and the age threshold separating poorer outcomes (GOS = 1 or 2) was 47 years (χ^2 = 8.397, P = 0.004) (Fig. 4.6).

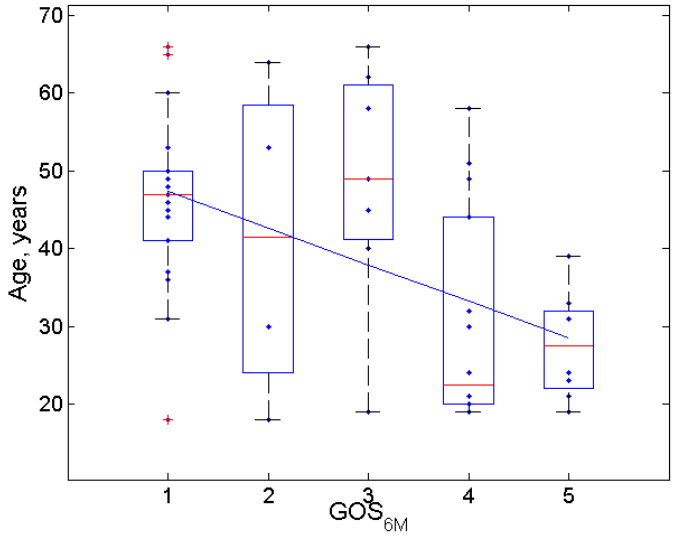

Fig. 4.6. A box plot showing the association between GOS after 6 months and age (r = -0.480, P < 0.001). The age of > 47 years ($\chi 2 = 5.71$, P = 0.017) is associated with a poor outcome (GOS 1–3). Co-authorship of the clinical study and joint publications: Aidanas Preiksaitis, MD, Saulius Rocka, MD, Prof.

To explore the influence of additional age factor on the duration of the LCAI more deeply, the outcomes of TBI patients were expressed as complex multidimensional functions influenced by the duration of LCAI at a critical threshold PRx(t) > 0.7 and age.

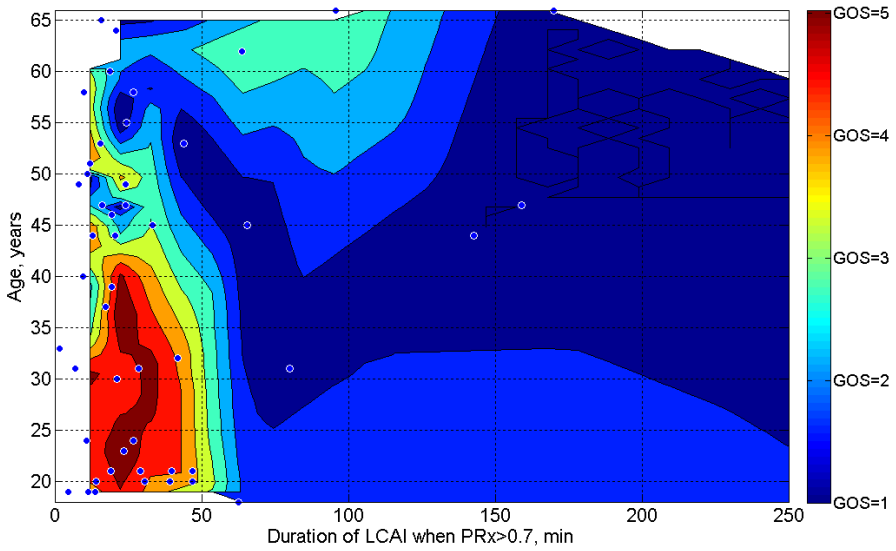

Fig. 4.7. Contour plots of GOS dependencies on the duration of CA impairment at PRx level above 0.7, and age. Co-authorship of the clinical study and joint publications: Aidanas Preiksaitis, MD, Saulius Rocka, MD, Prof.

The multiple correlation coefficient between GOS and the duration of LCAI and age was r = 0.679 (P < 0.001). Better outcomes are associated with younger patients and for those who did not have prolonged duration of CA impairment.

LCAI duration threshold when PRx = 0.7 was chasen because of its better association with patients' outcomes. The calculated thresholds of the LCAI duration for mortality outcome (after 6 months) were also calculated for different PRx levels, from 0.5 to 0.8:

- for PRx(t) > 0.5, the threshold of duration associated with mortality was 100 minutes ($\chi^2 = 5.183$, P = 0.023);
- for PRx(t) > 0.6, the threshold of duration associated with mortality was 80 minutes ($\chi^2 = 5.183$, P = 0.023);
- for PRx(t) > 0.7, the threshold of duration associated with mortality was 40 minutes ($\chi^2 = 5.991$, P = 0.014);
- for PRx(t) > 0.8, the threshold of duration associated with mortality was 25 minutes ($\chi^2 = 4.591$, P = 0.033).

4.3.1. Limitations

The present study was carried out on a limited number of 39 TBI patients. However, it was found that the critical PRx threshold associated with the patients' mortality (PRx > 0.24) calculated during this study was very close to the values obtained at other clinical centres: PRx > 0.25 (Sorrentino et al, 2012), PRx > 0.2 (Lavinio et al, 2008).

Another limitation is also related to the inaccuracy of calculation of the optimal CPP value. A longer time (up to 6 h) is needed to obtain the U-shaped approximation of PRx data as well as to calculate the optimal CPP. However, a longer processing of the time-series data for estimations of the optimal CPP is associated with the delay of making patient's treatment decisions and with the inaccuracy of CPP management.

In the population of this study, the duration of the LCAI events and age were assumed as the main independent variables influencing the long-term outcome, whereas other factors, such as Glasgow coma scale, CPP management, brain injury rate, and other treatment conditions, were not included.

The proposed critical parameter, LCAI, and its quantitative estimation also encountered some limitations. First, the CA status and the durations of the CA impairment events of the patient before hospitalization and monitoring are not known. The period before hospitalization might be critical for the patient, therefore, a CT scan should be done to evaluate the initial level of brain damage. This period, together with Rotterdam CT scores, should be included in the analysis of outcome prediction and their influences in upcoming studies.

The group of comatose patients with severe TBI in this study was not sufficiently large. The findings are applied to a more general population that includes TBI patients with a wide range of age. However, to investigate the specific influences of CA-related parameters to greater extent and validate the raised hypothesis of the influence of LCAI duration on TBI patient outcomes, a larger number of patients in

each patient group (grouping them into separate groups according to age, sex, brain injury scores, etc.) is necessary. This is a subject of an upcoming study, which will include the optimization of patient treatment strategies for each specific patient group.

4.4. Discussion

In this prospective study, GOS association with the CA estimation index PRx(t), age, ΔCPPopt and the duration of LCAI at specific PRx(t) value threshold was analyzed. All these factors were associated with GOS, but LCAI showed the most significant association with patient outcomes, compared with the average values of PRx(t). The correlation coefficient between the analysed CA status assessment indices and GOS varied from 0.4 to 0.5, showing an indirect influence of these indices on patients' outcomes. Moreover, such 1-dimensional GOS associations allow us to distinguish only the mortality outcome condition (GOS = 1); they did not show statistically significant differences between other outcome grades.

However, the contour plots of the association of GOS with the duration of LCAI and age clearly show that a better outcome is expected for younger patients and for those whose CA impairment was shorter than 40 minutes (Fig. 4.7.). The multiple correlation coefficient between GOS, duration of LCAI, and age is higher than single 1-dimensional associations between CA state estimation indexes and GOS, confirming that LCAI and age have a predominant impact on patients' outcomes. Moreover, the LCAI might be a clinically useful alert indicator for a prompt decision to treat specific patients urgently.

The use of averaged PRx threshold values is not practical for treatment purposes. The averaged values do not reflect the dynamics of the variation of CA status and might hide some critical events. The results presented in Fig. 4.1. and Fig. 4.2. show that unfavourable outcomes of TBI patients are more significantly associated with the complex influences of duration of the single LCAI episode and age, but not with the time average of all CA impairments, including relatively short secondary strokes. This finding contradicts the present integrative approach of association between CA impairments and unfavourable outcomes of patients with severe TBI. Pharmaceutical management (adrenomimetic, nitrite, thiopental, hypertonic saline, etc.), respiratory gas adjustment, or decompressive craniectomy are available tools for maintaining CPP close to optCPP.

Important and practical clinical factors might be the variability of CBF and the dynamics of CA status. Brain has a high metabolic demand, thus any process that increases prolonged perfusion variability has the potential to destabilize tissue metabolism and cause organ dysfunction. This means, that in addition to variability in blood pressure, the integrity of flow-stabilizing mechanisms as CA may in part underlie the relationship between elevated blood pressure variability and end-organ disease, particularly in the context of secondary brain injury (Hukkelhoven et al, 2003).

Contrary, short time pulsatility of CBF enhancement might be interpreted as a mechanism for protecting the blood supply to the cerebral tissues with decreasing

perfusion pressure. Less energy may be required to maintain forward flow, if the flow is pulsatile vs non-pulsatile because higher mean flow rate can be generated for equal mean arterial blood pressure.

However, prolonged CA impairment due to CBF instability might be dangerous, especially in the cases of secondary damage. The published extensive experimental results support the importance of protecting the cerebral vasculature to prevent the expansion of the ischemic/hypoperfusion zones. Post-ischemic reperfusion can impair the CA mechanisms and exacerbate non-reversible ischemic injury. It is not surprising that a relationship exists between the duration of CA dysfunction, the expansion of the ischemic/hypoperfusion area, and worse clinical outcomes. Only the use of high-resolution imaging modalities could quantify and track the development of secondary injury, guiding practitioners to better treatment decision-making for targeted approaches toward TBI treatment. However, literature does not reveal any analysis of the relationship between the duration of the longest and the most dangerous brain secondary insult caused by CA impairment and patient outcome.

4.4. A summary of the chapter

Patient-specific CPP management and better outcomes were obtained for patients whose CPP was kept within the range from the optimal CPP to the optimal CPP +10 mmHg for younger patients. The impairment of CA status and declination of CPP below the optimal CPP value were associated with a poor outcome. The determined critical thresholds associated with mortality of TBI patients were PRx > 0.24 and ΔCPPopt < 6 mmHg. The age limit associated with poorer outcomes was above 47 years.

An analysis of associations of severe TBI patients' outcomes with CA impairment conditions showed that the duration of the LCAI event and age are more significant factors impacting the patient's outcome than the average PRx(t) values or the average time of all episodes of CA impairment. The duration of LCAI when PRx > 0.7 for more than 40 min is associated with mortality (Fig. 4.3.).

A multidimensional representation of outcome plots showed that a better outcome was observed for younger patients and for those who did not experience prolonged episodes of CA impairment at high PRx(t) levels.

5. A PROSPECTIVE STUDY OF PATIENTS UNDERGOING CARDIAC SURGERY WITH CARDIOPULMONARY BYPASS

5.1. Background

Post-operative cognitive dysfunction (POCD) is a common complication after cardiac surgery with cardiopulmonary bypass. It occurs during the first post-operative week in approximately 33–83% of cases; and in 20–60% of cases, it may persist for several months after surgery (Gao et al, 2005; Rundshagen, 2014; Bruggemans, 2013). Most researcher groups agree that POCD does not increase post-operative mortality, but it deteriorates the patient's quality of life and impedes their rehabilitation, recovery, and return to normal daily activities. The spectrum of abilities referred to as cognition is diverse; they include learning and memory, verbal abilities, perception, attention, executive functions, and abstract thinking (Deiner and Silverstein, 2009). POCD is characterized by the impairment of those functions, which leads to a decline of concentration and orientation as well as deterioration of language comprehension and social integration. Increased expectations of patients make the post-operative quality of life and the return to normal daily life the main determinants of successful cardiac surgery. Thus, success is defined not only by the physical abilities but by psycho-emotional factors as well. The causes and predisposing factors of POCD are currently unclear. Inadequate cerebral perfusion due to impaired cerebrovascular autoregulation is one of the possible triggers.

The control of mean arterial pressure is typically meant to ensure a continuous adequate cerebral perfusion pressure and to prevent CA impairments (Murphy et al, 2009). Many cardiac centres maintain a MAP of 50–60 mmHg during cardiopulmonary bypass (CPB) (Murphy et al, 2009). This range is based on earlier findings that a MAP of 50 mmHg is the statistical mean value of the lower limit of CA (Lassen, 1959). However, the lower limit of CA is patient-specific and can vary in anesthetized patients during CPB (Murphy et al, 2009). Some studies recommend maintaining the MAP at 70 mmHg or higher for elderly and high-risk population patients (i.e., patients with hypertension, pre-existing cerebral vascular disease, or diabetes) (Olsen et al, 1995). Maintaining higher MAP also enhances collateral blood flow when emboli impair tissue perfusion. On the contrary, maintaining a lower MAP during CPB has some advantages, including less trauma to blood elements, reduced non-coronary collateral flow to the heart, which permits the use of smaller venous and arterial cannulas. Despite the procedures applied for maintaining the MAP within the specified limits during CPB, there are always episodes of drastic drops in MAP and CA impairments, consequently.

It was hypothesized that patients undergoing CPB experience episodes of CA impairment. This impairment is related to the deterioration of cognition (DC) and POCD.

Goals of this study were to describe CA impairment episodes, to investigate the relationship between CA impairments and cognitive functions, and to discover the impact of MAP in patients undergoing cardiac surgery with CPB.

5.2. Material and methods

This prospective observational study was conducted in Kaunas Clinics, the Hospital of Lithuanian University of Health Sciences (LUHS) from 2014 to 2016. The study was approved by the Kaunas Regional Ethics Committee of LUHS and written informed consent was obtained from all patients. The study included 65 patients without pre-operative neurological disorders, who underwent elective coronary artery bypass graft (CABG) surgery with CPB. All patients received a standardized anesthetic and CPB management. The CPB machine was primed with 1.5 L of crystalloid solution containing 10,000 units of heparin. A roller-pump with a membrane oxygenator (Dideco D703, Mirandola, Italy) and a venous reservoir were used. The non-pulsatile pump flow rates were maintained 2.4–2.6 L/min. MAP targets, transfusion of packed red blood cells, and rate of re-warming were based on a standard clinical practice during CPB.

5.2.1. Neurological and neuropsychological assessment

All patients underwent a set of neuropsychological tests the day before and 10 days after surgery that contained:

a) Mini Mental State Evaluation (MMSE) test;
b) Rey Auditory Verbal Learning test;
c) two subtests of the Whechsler Adult Intelligence Scale (Digit Span and Digit Symbol Substitution tests);
d) Shulte table.

The results were analysed according to the recommendations of the ISPOCD (an international multicentre study on long-term post-operative cognitive dysfunction) study (Rasmussen et al, 2001).

Relative changes between pre-operative and post-operative test scores were calculated and expressed as Z scores. The change in Z score relative to its associated error was used to estimate the deterioration of mental abilities and to detect POCD. A Z score exceeding 1.645 was considered a reliable indicator of deteriorated cognition (Frerichs and Tuokko, 2005). POCD was diagnosed when the sum of all Z scores was > 2 or at least 2; Z scores for separate tests were > 2 (Frerichs and Tuokko, 2005).

Post-operatively, patients were divided into 2 groups according to the changes in their cognitive functions: group I had no deterioration in cognition, group II had DC and POCD.

5.2.2. Monitoring the CA status

The CA status was monitored using a novel diagnostic tool “Vittamed 505” (Vittamed, Inc., USA), which can provide real-time information on intracranial blood volume fluctuations in the small parenchymal vessels and arterioles which are responsible for cerebral blood flow autoregulation. During normal CA, these vessels regulate their own diameter by maintaining a relatively stable cerebral

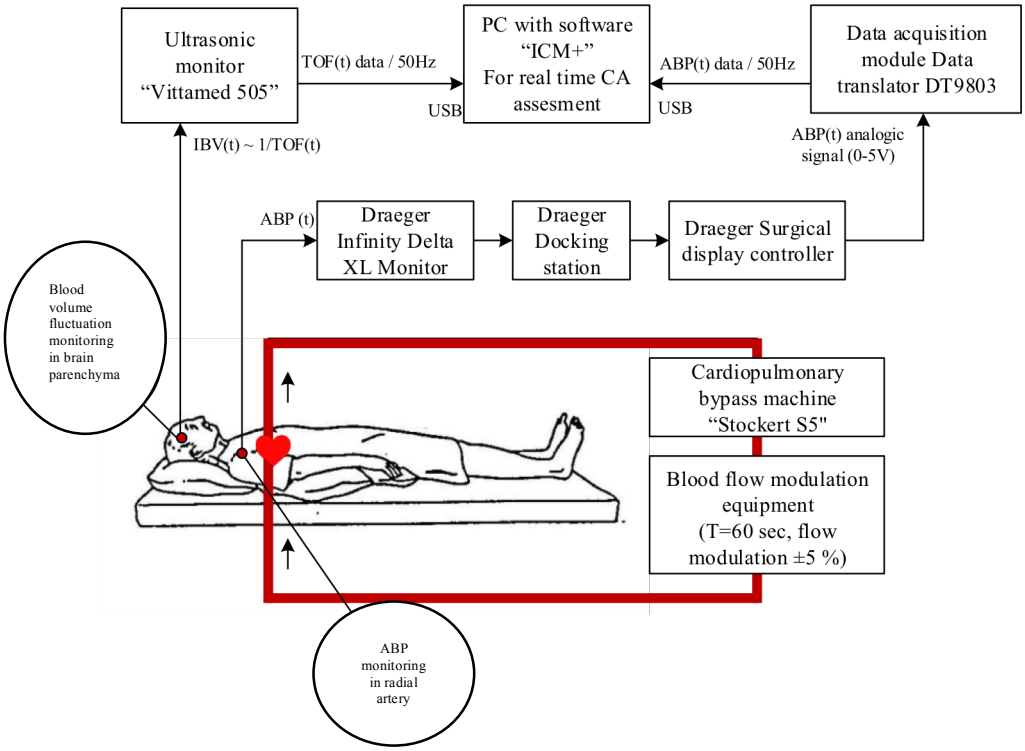

Fig. 5.1. A structural diagram of non-invasive CA status monitoring and invasive ABP monitoring during cardiac surgery with cardiopulmonary bypass.

blood flow and provide a continuous blood supply to brain cells within the physiological limits of arterial blood pressure. CA status was estimated continuously during surgery by calculating the time (t) dependence of non-invasively monitored Pressure Reactivity Index (vPRx1(t)) as a moving correlation coefficient between the slow waves of IBV(t) and MAP(t) within 2 min time averaging window. Slow MAP waves with a stable period of T = 60 s were generated by changing the blood flow rate in the CPB machine using specialized blood flow modulation equipment. Negative Pressure Reactivity Index values (vPRx1(t) < 0) correspond to intact CA status and positive values (vPRx1(t) > 0) indicate CA impairment as presented in the paper by Czosnyka et al (2009).

The episodes of CA impairment were detected and the duration of the longest CA impairment was estimated for each patient to find the relationship between CA impairment episodes and deterioration of cognitive functions. An algorithm of CA status assessment and detection of CA impairment episodes is shown in Fig. 5.2. Mathematical data processing is comprehensively described in Chapter 2.

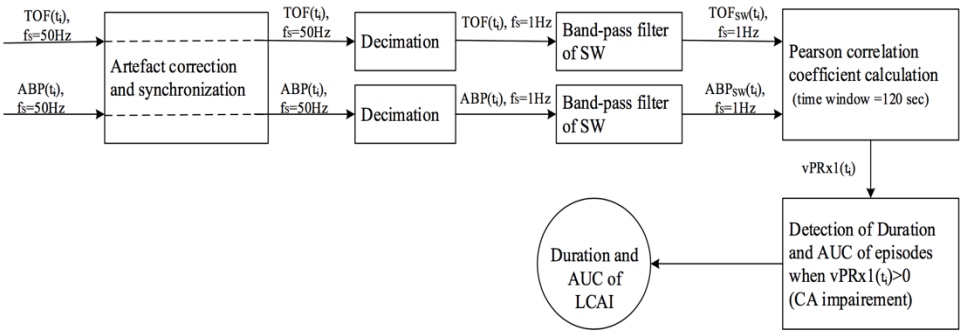

Fig. 5.2. A structural diagram of non-invasive CA status assessment and detection of CA impairment episodes

Statistical analysis

Normally distributed variables the Student's t test was used to compare the differences between 2 independent groups. The difference was considered statistically significant when $p < 0.05$; otherwise, not significant (ns). The Pearson chi-squared test (χ^2) was used to determine the critical threshold of the analysed factors (duration of LCAI and AUC) between groups.

5.3. The assessment of post-operative deterioration of cognitive functions

CA monitoring data were collected from 65 patients (the author participated in 30 data collection sessions). Six patients refused to participate in the follow-up and were excluded from the study. A statistical analysis was performed using the data from the remaining 59 patients. The oldest and youngest patients were 83 and 51 years of age, respectively. The mean age was 66.7 years. There were 34 men and 25 women involved in the final statistical analysis (59% and 41%, respectively). The men were younger than the women (64 (SD = 8.4) vs 71 (SD = 7.4) years, $p = 0.002$). The average education level was 11.9 years. Fifteen patients (25%) had diabetes mellitus.

The mean duration of CPB was 87 min. and the mean aortic cross-clamping time was 44 min. During surgery, all patients had episodes of impaired CA (when vPRx1 > 0). The longest episode of CA impairment was 12.4 min.; the shortest episode lasted 1 min.

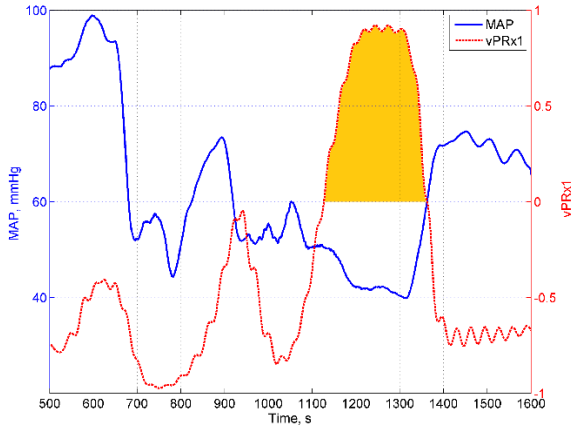
MAP
vPRx1
MAP, mmHg
vPRx1
Time, s

a)

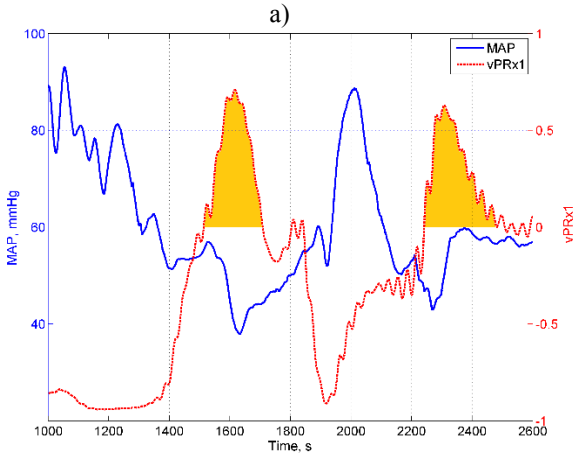
MAP
vPRx1
MAP, mmHg
vPRx1
Time, s

b)

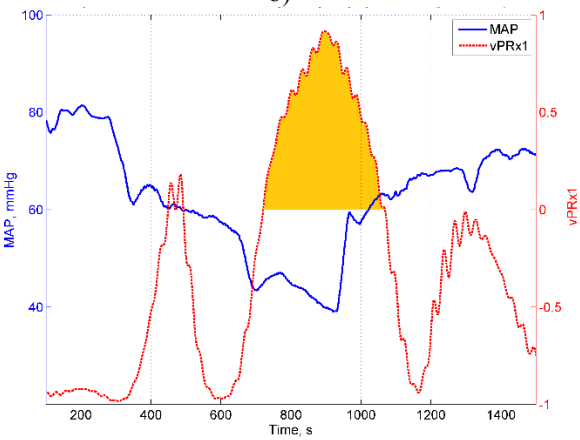
MAP
vPRx1
MAP, mmHg
vPRx1
Time, s

c)

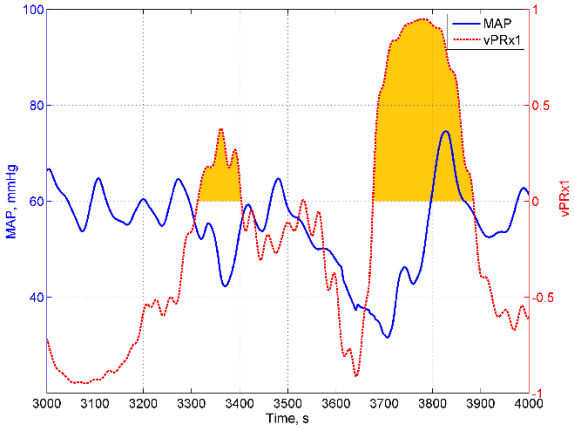

d)

Fig. 5.3. Examples of simultaneously monitored MAP and vPRx1 during surgery with CPB when CA was impaired a) patient No. 17, b) patient No. 42, c) patient No. 34, d) patient No 65. Co-authorship of the clinical study and joint publication: Birute Kumpaitiene, MD, Milda Svagzdiene, MD, Edmundas Sirvinskas, MD, Prof., Virginija Adomaitiene, MD, Rimantas Benetis, MD, Prof.

After surgery, 22 patients (37%) showed DC and experienced POCD (group II). The other 37 patients (63%) did not display any evidence of cognitive deterioration (group I). No one in the study experienced major neurological complications (stroke, coma, stupor, etc.).

The area under the curve (AUC) for each LCAI episode (when vPRx1 > 0) was also calculated as a parameter to characterize the "CA impairment dose" of such episodes (Fig. 5.3. yellow plots).

There were no significant differences between the patient groups in terms of age, sex, educational level, average MAP during surgery, duration of CPB, and time of aortic cross-clamping (Table 5.1.).

Comparing groups by using the characteristics of the LCAI episodes (duration when vPRx1 > 0, and AUC when vPRx1 > 0), significant differences between group I (without CD) and group II (with CD and POCD) were found (Fig. 5.4. and Fig. 5.5.).

Table 5.1. Demographic and operative data of the patients

Characteristic	**Group I without cognitive deterioration (n = 37)**	**Group II with cognitive deterioration and POCD (n = 22)**	**p**
Mean (SD) age, years	65 (8.7)	69.9 (8.8)	ns
Sex, Male/Female	20/17	14/8	ns
Averaged MAP, mmHg	62.9 (5.06)	63.9 (4.48)	ns
Averaged vPRx1	-0.24 (0.17)	-0.34 (0.18)	ns

Data in the table are presented as means (SD). Sex is presented as male/female ratio. ns – not significant ($p > 0.05$).

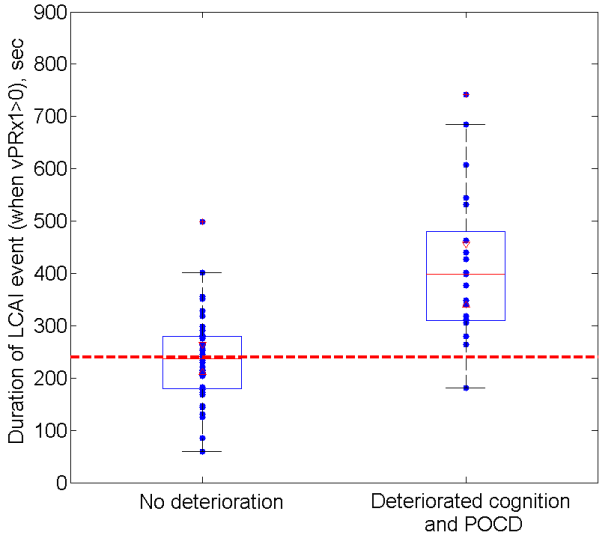

Fig. 5.4. The relationship between the longest episode of cerebrovascular autoregulation impairment when vPRx1(t) > 0 and post-operative cognitive function (POCD). The duration of the longest cerebral autoregulation impairment (LCAI) event above critical 240 sec threshold (red dashed line) when vPRx1 > 0 is associated with deteriorated mental abilities and post-operative cognitive dysfunction ($\chi^2 = 4.11$, $p = 0.042$). Two-sample t-test (a comparison of two groups with no deterioration and with deterioration) shows statistically different means of group I and group II ($p < 0.001$). Co-authorship of the clinical study and joint publication: Birute Kumpaitiene, MD, Milda Svagzdiene, MD, Edmundas Sirvinskas, MD, Prof., Virginija Adomaitiene, MD, Rimantas Benetis, MD, Prof.

Two-sample t-tests showed that the observed mean duration and AUC of these events were significantly higher ($p < 0.05$) for group II compared to group I (Table 5.2). The calculated critical duration threshold of the LCAI event, when vPRx > 0, which was related to deteriorated cognition, was 240 s ($\chi^2 = 4.11$, $p = 0.04$) (Fig. 5.4.).

Table 5.2. The distribution of characteristics of cerebrovascular autoregulation impairment episodes between patient groups

Characteristic	Group I without cognitive deterioration (n = 37)	Group II with cognitive deterioration and POCD (n = 22)	p (t test)
Duration of longest episode when vPRx1 > 0, s	243 (88)	413 (66)	p = 4e-7 < 0.001
AUC of the longest episode when vPRx1 > 0, s	98 (50)	188 (87)	p = 7e-6 < 0.001

Total duration vPRx > 0, s	1013 (512)	1571 (600)	p = 2e-4 < 0.001
Total AUC of all episodes when vPRx1 > 0, s	325 (222)	560 (235)	p = 4e-4 < 0.001

Data in the table are presented as means (SD). CA – cerebrovascular autoregulation.

5.4. Discussion

Historically, heart and lung bypass machines were enhanced by using both a blood pump and an oxygenator. Current protocols for cardiac bypass surgery were developed over 30 years ago. More recently, monitoring techniques of physiological parameters (e.g., invasive monitoring of central hemodynamic parameters, pulse oximetry, NIRS-based cerebral and tissue oxygenation, EEG, and somatosensory evoked potentials) have been used to maintain the perfusion of critical organ vascular beds including brain and kidney.

A better method for protecting the brain during cardiac surgery with bypass is real-time diagnosis of cerebral perfusion pressure by non-invasive monitoring of the CA status. CA protects the brain against inappropriate fluctuations in CBF when CPP changes. Temporal CA impairments are related to worse outcomes in various neurological diseases.

Physiologically, CA aims to maintain an adequate and stable CBF despite a wide range of ABP changes. Cerebral arterioles dilate or contract and maintain a stable and continuous blood supply to brain cells within the physiological limits of arterial blood pressure (Cipolla et al, 2009). But the lower and upper limits of CA are variable and can be influenced by various factors (hematocrit and hemoglobin concentrations, $PaCO_2$, PaO_2, blood pH, brain temperature, cardiac output, and concomitant diseases that affect blood vessels).

There has been interest in the effects of anaesthetic drugs on CA, since any impairment will potentially make the brain more vulnerable to changes in ABP during surgery (Payne, 2016). One study in humans showed that morphine-nitrous oxide anaesthesia does not significantly affect CA in normal subjects (Jobes et al, 1975). It has also been shown that CA is impaired in normal adult subjects during nicardipine-induced hypotension (Endoh et al, 2000). CA is unaffected under in the influence of either nitroglycerin or prostaglandin E1 (Endoh et al, 2001).

Etiology of POCD and deterioration of mental abilities is multifactorial and remains obscure. The studies examining patients who underwent off-pump cardiac surgery (Bruggemans, 2013) or non-cardiac surgery (Deiner and Silverstein, 2009) show a high rate of POCD and exclude CPB as a risk factor. In other studies, no relationship between POCD and air embolization was found; however, in this study, for patients undergoing heart valve surgery such possibility was not excluded.

There are studies indicating that senior age, a lower level of education, or some operative factor (such as the duration of CPB and aortic cross-clamping time) may be predisposing factors of POCD. In this study, no differences were found in these parameters among the groups.

The results of this study are consistent with Ono et al. (2012) and show no differences in the MAP between patients with and without POCD (Ono et al, 2014). However, individual analysis of the patients presented a correlation between MAP drop and CA impairment (Fig. 5.3.).

In this study, the non-invasive, ultrasonic "time-of-flight" technology "Vittamed 505" (Vittamed, Inc., US) was used to assess CA. Other technologies to non-invasively assess CA, such as transcranial Doppler sonography and NIRS have started to be recently used during cardiac surgery (Hori et al, 2015; Brady et al, 2010). CA assessment using TCD technology is based on blood flow velocity monitoring in the middle cerebral artery and the calculation of the mean velocity index (Mx) as a moving correlation coefficient between the slow fluctuation of blood flow velocity and MAP (Chapter 1). Another non-invasive technology, NIRS, is based on cerebral oxygenation (rSO_2). To obtain this monitoring, sensors are placed on the patient's forehead and the cerebral oximetry index (COx) is calculated as a moving correlation coefficient between the slow fluctuation of cerebral oxygenation and MAP (Chapter 1). Comparative studies of NIRS and TCD technologies in 60 adult patients undergoing cardiac surgery with CPB showed that these indexes can detect the status of CA impairment. The thresholds associated with CA impairment are: $Mx > 0.45$ and $COx > 0.38$, respectively. They also supply similar diagnostic information (correlation $r = 0.55$ between Mx and COx) (Brady et al, 2010).

However, both technologies have certain limitations. The main limitation of TCD is the need for frequent transducer repositioning and the inability to obtain a transcranial "window" in some patients (Brady et al, 2010). The NIRS technology has a spatial resolution of 1 cm and oxygenation measurements are limited to a maximum of 2–3 cm of tissue depth (Fantini et al, 2016). This means that deeper parts of brain parenchyma which contain the parenchymal arterioles are not accessed. Studies using NIRS and TCD applications in cardiac surgery mainly addressed finding a lower limit of MAP at which CA remains unaffected (Brady et al, 2010). This threshold can vary with a wide range of MAP (i.e., 45–80 mmHg). This means that the conditions which result in CA impairment vary, and the lower limit of autoregulation can be detected at low as well as at high MAP values. Therefore, in this study investigated the associations among the characteristics of CA impairment episodes and patients' neurological outcome.

This study detected CA impairment episodes in all patients throughout the entire surgery. To find the differences between the groups, the following characteristics of CA impairment episodes were analysed: the duration of the LCAI event at level $vPRx1(t) > 0$, and the AUC of the LCAI episodes. These characteristics were chosen based on earlier findings showing that a single longest CA impairment episode has a higher impact on the patient's outcome than the averaged CA status value (Preiksaitis et al, 2016). The assessment of vPRx1 level allows to better quantify the CA status during the impairment episode. Level $vPRx1(t) > 0$ represents the mathematical definition of CA impairment (Czosnyka et al, 1997).

To quantify the characteristics of CA impairment, some authors suggested calculating the AUC for all CA impairment episodes when $PRx > 0$ as the total "dose"

impacting the outcome in TBI patients (Schuhmann et al, 2016). AUC was also analysed in this study but it was calculated only for the single longest CA impairment episode.

It was found that the characteristics of an LCAI event (duration and AUC) significantly differed between the group without cognitive deterioration (group I) and the group with cognitive deterioration and POCD (group II). The highest significance was found by analysing the duration of the LCAI event when PRx > 0 ($p<0.001$ of t-tests comparing group I (without CD) and II (with CD and POCD) (Table 5.2.)). Much lower significance was obtained for the total duration of all CA impairment events or total AUC ("doses") of these events. Such findings complement the earlier described hypothesis suggesting a higher impact of a single LCAI event on the patient's outcome (Preiksaitis et al, 2016).

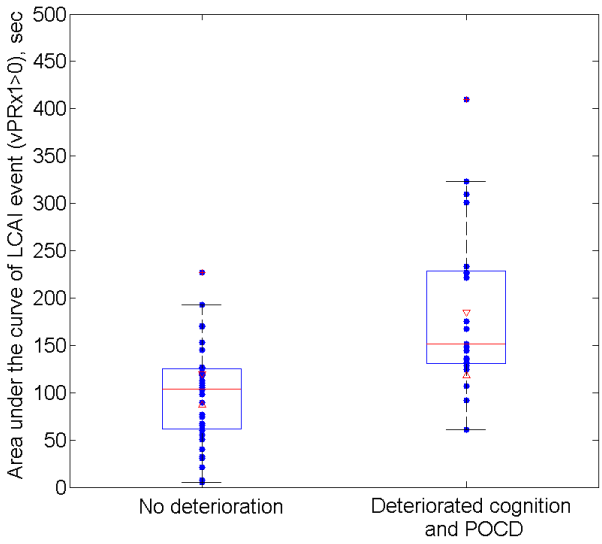

Fig. 5.5. The relationship between the area under the curve (AUC) of vPRx1 during the longest cerebrovascular autoregulation impairment event and post-operative cognitive function (POCD). The two-sample t-test (a comparison of two groups with no deterioration and with deterioration) shows a statistically significant difference of AUC means between two groups ($p < 0.001$). Co-authorship of the clinical study and joint publication: Birute Kumpaitiene, MD, Milda Svagzdiene, MD, Edmundas Sirvinskas, MD, Prof., Virginija Adomaitiene, MD, Rimantas Benetis, MD, Prof.

There are several controversial explanations regarding the lower limit of autoregulation in the anaesthetized patients. A normal autonomic response to hypotension includes some vasoconstriction of the large extracranial and intracranial vessels, which shifts the autoregulation curve rightwards. However, anesthetics prevent that autonomic response by blocking the autonomic nervous system, leading to a leftward shift of the autoregulation curve (Drummond, 2013). Additionally, patients can tolerate a MAP below the LLA because of a substantial central nervous

system blood flow reserve. CBF can decrease by approximately 40% of the baseline value before symptoms of ischemia begin to occur (Drummond, 2013).

5.5. A summary of the chapter

This observational clinical study of non-invasive CA status monitoring in anesthetized patients during cardiac surgery with cardiopulmonary bypass showed that temporary cerebrovascular autoregulation impairment occurs in all patients during surgery. This impairment can cause a deterioration of mental abilities.

The hypothesis on post-operative association between deteriorated mental abilities and post-operative cognitive dysfunction of cardiac bypass surgery patients and duration of the longest cerebral autoregulation impairment event is supported by the results of an observational clinical trial of 59 cardiac bypass surgery patients (37 patients without post-operative deterioration, 22 patients with deteriorated cognition and post-operative cognitive dysfunction).

Results of the trial show that one of the main causes of post-operative deterioration of mental abilities and cognitive dysfunction is patient-specific cerebrovascular autoregulation impairment event the duration of which is above the critical threshold of 240 sec., when $vPRx1(t) > 0$.

One possible cause of impaired CA is cerebral perfusion pressure lower than the patient's lower CA limit. Non-invasive real-time monitoring of CA status and individualization of the cerebral perfusion pressure may be beneficial for preventing POCD. However, additional studies with larger sample sizes and assessment of possible risk factors are needed to find the causes of CA impairment.

CONCLUSIONS

1. A detailed analysis of the parameters suitable to define a human brain cerebral autoregulation state and its measurement problems were performed. The existing literature regarding cerebral blood flow, intracranial pressure, arterial blood pressure was analysed in detail defining every possible measurement technology of CA status indexes PRx and Mx. The disadvantages of invasive technologies (remain restricted to a small proportion of patients, cannot be used for routine procedures, reliability, et al.) may be eliminated by means of non-invasive technologies which was the research object of this work. However, a non-invasive "Gold Standard" CA monitor does not exist and the errors involved in using each device are poorly understood. A fundamental understanding for convergence of analysis methods of cerebrovascular autoregulation status assessment was produced to prove clinical benefit thus laying the grounds for the relevance of this thesis.

2. An innovative non-invasive CA status monitoring technology was researched to assess cerebral autoregulation. Measures of CBF remain confined to a single vessel due to the need to be able to insonate the vessel. This major limitation to assessing CA, since it provides no spatial information and is of limited value in clinical contexts, was solved by the proposed CA status assessment method that is not local. However, for the implementation of the non-invasive CA status monitoring method based on the slow waves application there are a few limitations. First, the slow wave moving correlation monitoring method is non-continuous monitoring because of the intermittent nature of slow waves. The second limitation of the slow wave-based CA status monitoring method is the necessity to apply the invasive or non-invasive ABP(t) reference signal monitoring sensor.

3. A comparative invasive and non-invasive CA status monitoring study performed on TBI patients showed that non-invasive CA status monitoring technology provides similar diagnostic information to the invasive technology. The obtained correlation coefficient between the invasive and non-invasive CA monitoring technologies ($r = 0.707$ when reference ABP(t) signal was used for CA status calculation (39 patients, 50 hours of monitoring)) show high coincidence between both methods. A limitation here is the fact that invasive technology is not a "Gold Standard" technology, because "Gold Standard" does not exist in this case. Less correlation was obtained when CA status was assessed non-invasively without using reference ABP(t) signal ($r = 0.673$). A limitation of this study is also that some patients' data had artefacts, especially in the ABP channel. These artefacts were corrected or excluded from the monitoring data during retrospective data analysis. However, they might cause errors when evaluating the durations of CA impairment episodes. A methodological limitation is caused by the use of averaged values of CA-related parameters which do not reflect the

dynamics of variation of cerebrovascular autoregulation status and might hide some critical events.

4. The analysis of CA monitoring study of severe TBI patients showed that the duration of CA impairment events is highly associated with the outcomes of TBI patients. Continuous CA status assessment in TBI patients may help to choose the optimal and patient-specific management to avoid prolonged events of CA impairments and to, potentially, improve patients' outcomes. A limitation of this study is that the presented analysis was carried out on a limited number of 39 TBI patients. The proposed critical parameter for targeting a patient's LCAI treatment duration and its quantitative estimation shows that a clinically assessed electronic system potentially adds value to clinical practice. Additional studies are needed in order to minimize the dynamic errors of LCAI identification and to prove that LCAI management below the patient-specific critical threshold can be the target for brain protection from unfavourable patients' outcomes.

5. The study of non-invasive CA status monitoring technology applicability for CA assessment in patients undergoing cardiac surgery with CPB showed that the duration of a single longest CA impairment event during these events are reliably associated with post-operative cognitive deterioration when the critical duration of the longest CA impairment event was 240 s ($\chi^2 = 4.11$, $p = 0.04$). One cause of impaired CA is the drop of mean arterial blood pressure below the individual lower limit of CA. However, future assessments of possible risk factors are needed to find the causes of long CA impairments.

The most important finding of the doctoral dissertation is a comprehensive explanation of cerebrovascular autoregulation mechanism that emerges from a synergistic application of the new technology and conceptual structures developed under this thesis. It has been shown that patient's outcome is related to the longest cerebrovascular autoregulation impairment episode, and the technological approach proposed in the thesis solves the problem of the lack of "Gold Standard".

REFERENCES

1. AASLID R., T. M. Markwalder, and H. Nornes. Noninvasive transcranial Doppler ultrasound recording of flow velocity in basal cerebral arteries. J. Neurosurg. 1982, 57, 769–774.
2. AASLID R., Lindegaard KF, Sorteberg W, Nornes H. Cerebral autoregulation dynamics in humans. Stroke. 1989, 20, 45–52.
3. AASLID R., Blaha M, Sviri G, Douville CM, Newell DW. Asymmetric dynamic cerebral autoregulatory response to cyclic stimuli. Stroke. 2007, 38, 1465–9.
4. ACTIVE SIGNAL TECHNOLOGIES, INC. (US). Apparatus and method for measurement of intracranial pressure with lower frequencies of acoustic signal. Inventors: Keith BRIDGER, Arthur V. COOKE, Frank J. CROWNE, Philip M. KUHN, et al. IPC: A61B8/08. US Patent US5919144 A. 1999-07-06. United States Patent and Trademark Office [2014-10-13]. Link: https://www.google.com/patents/US5919144
5. ANDREWS PJ, Citerio G, Longhi L, Polderman K, Sahuquillo J, Vajkoczy P. NICEM consensus on neurological monitoring in acute neurological disease. Intensive Care Med. 2008, 34, 1362-1370.
6. AKOPIAN G, D. J. Gaspard, and M. Alexander. Outcomes of blunt head trauma without intracranial pressure monitoring. American Surgeon, 2007, 73, 447–450.
7. ALLOCCA, J. A. (US). Method and apparatus for noninvasive monitoring of intracranial pressure. Inventor: John A. ALLOCCA. IPC: A61B5/05. US patent US4204547. 1980-05-27. United States Patent and Trademark Office [2014-10-13]. Link: https://www.google.com/patents/US4204547.
8. ALPERIN, N. Method of measuring intracranial pressure. Inventor: Noam ALPERIN. IPC: A61B5/03. US patent US5993398. 1999-11-30. United States Patent and Trademark Office [2014-10-13]. Link: https://www.google.com/patents/US5993398.
9. ALPERIN, N. Improved method of measuring intracranial pressure. Inventor: Noam ALPERIN. IPC: A61B5/03. US patent US6245027. 2005-11-16. United States Patent and Trademark Office [2014-10-13]. Link: https://www.google.com/patents/EP1223865B1.
10. ALLER PHYSIONIX LIMITED, UNIVERSITY OF WASHINGTON (US). Systems and methods for making noninvasive physiological assessments. Inventors: Pierre D. MOURAD, Michel KLIOT, Ali MESIWALA, Rex PATTERSON, et al. IPC: A61B5/03. US patent US6875176 B2. 2005-04-05. United States Patent and Trademark Office [2014-11-20]. Link: https://www.google.com/patents/US6875176.
11. ALLEZ PHYSIONIX LIMITED ET AL. (US). Systems and methods for determining intracranial pressure non-invasively and acoustic transducer assemblies for use in such systems. Inventors: Pierre D. MOURAD, Brandt MOHR, Michel LIOT, Robert C.A. FREDERICKSON. IPC: A61B5/03. European patent EP1633234 A2. 2006-03-15. European Patent Office [2014-11-21]. Link: https://www.google.com/patents/EP1633234A2.

12. ARIES M.J., Czosnyka M., Budohoski K.P., et al. Continuous determination of optimal cerebral perfusion pressure in traumatic brain injury. Crit Care Med. 2012, 40(8), 2456-2463.
13. ASENBAUM S., et al. Imaging of cerebral blood flow with technetium- 99m-HMPAO and technetium-99m-ECD: a comparison. J. Nucl. Med. 1998, 39(4), 613–618.
14. BALESTRERI M., Czosnyka M., Hutchinson P., Steiner L.A., Hiler M., Smielewski P., et al. Impact of intracranial pressure and cerebral perfusion pressure on severe disability and mortality after head injury. Neurocrit Care. 2006, 4(1), 8–13.
15. BRUGGEMANS E.F. Cognitive dysfunction after cardiac surgery: Pathophysiological mechanisms and preventive strategies. Neth Heart J. 2013, 21(2), 70-73.
16. BARTUSIS L., R. Zakelis, G. Daubaris, A. Ragauskas. Ophthalmic Artery as a Sensor for Non-invasive Intracranial Pressure Measurement Electronic System. Electronics and Electrical Engineering. 2012, 122(6), 45-48. DOI: http://dx.doi.org/10.5755/j01.eee.122.6.1194
17. BEEK Arenda HEA, Jurgen AHR Claassen, Marcel GM Olde Rikkert and Rene WMM Jansen. Cerebral autoregulation: an overview of current concepts and methodology with special focus on the elderly. Journal of Cerebral Blood Flow & Metabolism. 2008, 28, 1071–1085.
18. BEN-ARI, S., MARCOVITCH, S., KINROT, O. Devices and methods for monitoring intracranial pressure and additional intracranial hemodynamic parameters. Inventors: Shlomi BEN-ARI, Shmuel MARCOVITCH, Opher KINROT. IPC: A61B5/0402. US patent US20130041271. 2013-02-14. United States Patent and Trademark Office [2014-10-14]. Link: https://www.google.com/patents/US20130041271.
19. BIGLER, E.D. The lesion(s) in traumatic brain injury: implications for clinical neuropsychology. Arch Clin Neuropsych. 2001, 16(2), 95–131. doi: 10.1016/ S0887-6177(00)00095-0.
20. BIRCH, A.A., M.J. Dirnhuber, R. Hartley-Davies, F. Iannotti, G. Neil-Dwyer. Assessment of autoregulation by means of periodic changes in blood pressure. Stroke. 1995, 26, 834–7.
21. BIRCH, A.A., G. Neil-Dwyer, A.J. Murrills. The repeat- ability of cerebral autoregulation assessment using sinusoidal lower body negative pressure. Physiol Meas. 2002, 23, 73–83.
22. BLOKLAND, J., et al. Positron emission tomography: a technical introduction for clinicians. Eur. J. Radiol. 2002, 44(1), 70–75.
23. BRADY, K., B. Joshi, C. Zweifel, et al. Real-time continuous monitoring of cerebral blood flow autoregulation using near-infrared spectroscopy in patients undergoing cardiopulmonary bypass. Stroke. 2010, 41(9), 1951-1956.

24. BRADY, K.M, J. K. Lee, K.K. Kibler, P. Smielewski, M. Czosnyka, R.B. Easley, et al. Continuous Time-Domain Analysis of Cerebrovascular Autoregulation Using Near-Infrared Spectroscopy. Stroke. 2007, 38(10), 2818–2825.
25. BRAIN FACTS. A PRIMER ON THE BRAIN AND NERVOUS SYSTEM. Society of Neuroscience. Link: http://www.brainfacts.org/~/media/Brainfacts/Article%20Multimedia/About%20Neuroscience/Brain%20Facts%20book.ashx.
26. BRAIN TRAUMA FOUNDATION. American association of neurological Surgeons, Congress of neurological Surgeons, Joint Section on Neurotrauma and critical care, AANS/CNS. Guidelines for the management of severe traumatic brain injury. IX. Cerebral perfusion thresholds. J Neurotrauma. 2007, 24(suppl 1), S59-S64.
27. BRATTON, S.L., R. M. Chesnut, J. Ghajar et al. Guidelines for the management of severe traumatic brain injury. IX. Cerebral perfusion thresholds. Journal of Neurotrauma. 2007, 24, S59–S64.
28. BRAXTON, E. Apparatus and method for non-invasive measurement of intracranial pressure. Inventor: Ernest BRAXTON. IPC: A61B5/00. US patent US20060206037. 2006-09-14. United States Patent and Trademark Office [2014-10-14]. Link: https://www.google.com/patents/US20060206037.
29. CALIFORNIA INSTITUTE OF TECHNOLOGY (US). Non-invasive method of measuring cerebral spinal fluid pressure. Inventors: Mark BORCHERT, James L. LAMBERT. IPC: A01B5/00. US patent US6129682. 2000-10-10. United States Patent and Trademark Office [2014-10-14]. Link: https://www.google.com/patents/US6129682.
30. CARITAS ST. ELIZABETH MEDICAL CENTER OF BOSTON, INC. (US). Methods of and systems and devices for assessing intracranial pressure non-invasively. Inventor: Henry W. QUERFURTH. IPC: A61B5/02. US patent US7122007 B2. 2006-10-17. United States Patent and Trademark Office [2014-12-02]. Link: https://www.google.com/patents/US7122007.
31. COVIDIEN LP (US). Method and system for monitoring intracranial pressure. Inventors: Shannon E. CAMPBELL, Clark R. BAKER, Jr. IPC: A61B5/00. US patent US8696593 B2. 2014-04-15. United States Patent and Trademark Office [2014-10-13]. Link: https://www.google.com/patents/US8696593.
32. CASATI, A., et al. Continuous monitoring of cerebral oxygen saturation in elderly patients undergoing major abdominal surgery minimizes brain exposure to potential hypoxia. Anesth. Analg. 2007, 101, 740–747.
33. CENNAMO, G., et al. The correlation between endocranial pressure and optic nerve diameter: an ultrasonographic study. Ophthalmic Echography. Documenta Ophthalmologica Proceedings. 1987, 48, 603–606. doi:10.1007/978-94-009-3315-6_99.
34. CIPOLLA, M.J. The Cerebral Circulation. San Rafael (CA): Morgan & Claypool Life Sciences. 2012.
35. CIPOLLA, M.J., J. Smith, M.M. Kohlmeyer, et al. SKCa and IKCa Channels, myogenic tone, and vasodilator responses in middle cerebral arteries and

parenchymal arterioles: effect of ischemia and reperfusion. Stroke. 2009, 40(4), 1451-1457.
36. CRACH TRIAL MRC, COLLABORATORS. Predicting outcome after traumatic brain injury: practical prognostic models based on large cohort of international patients. Br Med J. 2008, 336:425. doi: http://dx.doi.org/10.1136/bmj.39461.643438.25.
37. CHILDREN'S MEDICAL CENTER CORPORATION (US). Non-invasive in vivo pressure measurement. Inventors: Joseph R. MADSEN, George A. TAYLOR. IPC: A61B8/04. US patent US6086533 A. 2000-07-11. United States Patent and Trademark Office [2014-11-16]. Link: https://www.google.com/patents/US6086533.
38. CHILDREN'S MEDICAL CENTER CORPORATION (US). Non-invasive in vivo pressure measurement. Inventors: Joseph R. MADSEN, George A. TAYLOR. IPC: A61B8/04. US patent US6547734 B2. 2003-08-15. United States Patent and Trademark Office [2014-11-16]. Link: https://www.google.com/patents/US6547734.
39. CHILLON, J.M., G.L. Baumbach. Autoregulation: arterial and intracranial pressure. In: Cerebral blood flow and metabolism. Lippincott Williams & Wilkins. 2002, 395–412.
40. CHONGQING UNIVERSITY (CHN). Method and system for non-invasive intracranial pressure monitoring. Inventors: Zhong JI, Li YANG, Shuang YANG, Mingxi ZHAO. IPC: A61B8/00. US patent US8647278 B2. 2014-02-11. United States Patent and Trademark Office [2014-11-22]. Link: https://www.google.com/patents/US8647278.
41. CUSHING, H. (1926). The Third Circulation in Studies in Intracranial Physiology and Surgery. Oxford University Press, London, UK.
42. CZOSNYKA, M., P. Smielewski, A. Lavinio, Z. Czosnyka, J.D. Pickard. A synopsis of brain pressures: which? when? Are they all useful? Neurol Res. 2007, 29(7), 672-679.
43. CZOSNYKA, M., P. Smielewski, P. Kirkpatrick, D.K. Menon, J.D. Pickard. Monitoring of cerebral autoregulation in head-injured patients. Stroke. 1996, 27, 1829–34. doi http://dx.doi.org/10.1161/01.STR.27.10.1829.
44. CZOSNYKA, M., J.K. Richards, M. Reinhard, L.A. Steiner, K. Budohoski, P. Smielewski, J.D. Pickard, and M. Kasprowicz. Cerebrovascular time constant: dependence on cerebral perfusion pressure and end-tidal carbon dioxide concentration. Neurol Res. 2012, 34,17-24. doi: http://dx.doi.org/10.1179/1743132811Y.0000000040.
45. CZOSNYKA, M., P. Smielewski, P. Kirkpatrick, R.J. Laing, D. Menon, and J.D. Pickard. Continuous assessment of the cerebral vasomotor reactivity in head injury. Neurosurgery. 1997, 41, 11–17.
46. CZOSNYKA, M., J. Picard. Monitoring and interpretation of intracranial pressure. Journal of neurology, neurosurgery & psychiatry. 2004, 75(6), 813–821. doi: http://dx.doi.org/10.1136/jnnp.2003.033126.

47. CZOSNYKA, M., K. Brady, M. Reinhard, P. Smielewski, L.A. Steiner. Monitoring of cerebrovascular autoregulation: facts, myths, and missing links. Neurocrit Care. 2009, 10, 373–86.
48. DEINER, S., J.H. Silverstein. Postoperative delirium and cognitive dysfunction. Br J Anaesth. 2009, 103 Suppl 1, i41-46.
49. DEPREITERE, B., F. Güiza, G. Van den Berghe, M.U. Schuhmann, G. Maier, I. Piper, et al. Pressure autoregulation monitoring and cerebral perfusion pressure target recommendation in patients with severe traumatic brain injury based on minute-by-minute monitoring data. J Neurosurg. 2014, 120(6), 1451–7. Doi: http://dx.doi.org/10.3171/2014.3.JNS131500.
50. DETRE, J.A., et al. Perfusion imaging. Magn. Res. Med. 1992, 23, 37–45.
51. DIEHL, R.R., D. Linden, D. Lucke, P. Berlit. Phase relationship between cerebral blood flow velocity and blood pressure. A clinical test of autoregulation. Stroke. 1995, 26, 1801–4.
52. DIETERLE, T. Blood pressure measurement – an overview. Swiss Med. 2012, 142, 1–9.
53. DONNELLY, J., M.J. Aries, M. Czosnyka. Further understanding of cerebral autoregulation at the bedside: possible implications for future therapy. Expert Rev Neurother. 2015, 15(2), 169-85. doi: 10.1586/14737175.2015.996552.
54. DRUMMOND, J.C. The lower limit of autoregulation: time to revise our thinking? Anesthesiology. 1997, 86(6), 1431-3.
55. DRUMMOND, J.C. Popular misunderstandings in neuroanesthesia. Anesthesia & Analgesia. 2013, 117, 7-10.
56. DURDURAN, T. and A. G. Yodh. Diffuse correlation spectroscopy for non-invasive, micro-vascular cerebral blood flow measurement. NeuroImage. 2014, 85, 51–63.
57. DWL ELEKTRONISCHE SYSTEME GMBH (DE). Measurement of the intracranial pressure. Inventors: Klaus PAULAT, Jurgen ZOLONDZ. IPC: A61B5/03. European patent EP0933061 B1. 2004-10-20. European Patent Office [2014-11-20]. Link: https://www.google.com/patents/EP0933061B1.
58. EAMES, P.J., M. J. Blake, S. L. Dawson, R. B. Panerai, and J. F. Potter. Dynamic cerebral autoregulation and beat to beat blood pressure control are impaired in acute ischaemic stroke. J Neurol Neurosurg Psychiatry. 2002, 72, 467–473. doi: http://dx.doi.org/10.1136/jnnp.72.4.467.
59. ENDOH, H., T. Honda, N. Komura, C. Shibue, I. Watanabe, K. Shimoji. The effects of nicardipine on dynamic cerebral autoregulation in patients anesthetized with propofol and fentanyl. Anesth Analg. 2000, 91(3), 642-6.
60. ENDOH, H., T. Honda, S. Ohashi, S. Hida, C. Shibue, N. Komura. The influence of nitroglycerin and prostaglandin E1 on dynamic cerebral autoregulation in adult patients during propofol and fentanyl anaesthesia. Anaesthesia. 2001, 56(10), 947-52.
61. FANTINI, S., A. Sassaroli, K.T. Tgavalekos, et al. Cerebral blood flow and autoregulation: current measurement techniques and prospects for noninvasive optical methods. Neurophotonics. 2016, 3(3), 031411.

62. FIRSCHIN, R., D. Woischneck, S. Klein, S. Reissberg, W. Döhring, B. Peters. Classification of severe head injury based on magnetic resonance imaging. Acta Neurochir. 2001, 143 (3), 263–71.
63. FAUL, M., L. Xu, M.M. Wald, V.G. Coronado. Traumatic brain injury in the United States: emergency department visits, hospitalizations, and deaths. Atlanta (GA): Centers for Disease Control and Prevention, National Center for Injury Prevention and Control. 2010.
64. FINNERTY, F.A. Jr., Lloyd Witkin, and Joseph F. Fazekas. Cerebral Hemodynamics during Cerebral Ischemia Induced by Acute Hypotension. J Clin Invest. 1954, 33(9), 1227–1232. Available from URL: http://www.jci.org/articles/view/102997.
65. FRANK, A.M., C. Alexiou, P. Hulin, T. Janssen, W. Arnold, A.E. Trappe. Non-invasive measurement of intracranial pressure changes by otoacoustic emissions (OAEs)--a report of preliminary data. Zentralbl Neurochir. 2000, 61(4), 177-180.
66. FRERICHS, R.J., and H.A. Tuokko. A comparison of methods for measuring cognitive change in older adults. Arch Clin Neuropsychol. 2005, 20(3), 321-333.
67. GAO, L., R. Taha, D. Gauvin, et al. Post-operative cognitive dysfunction after cardiac surgery. Chest. 2005, 128(5), 3664-3670.
68. GERBER, L.M., Y.L. Chiu, N. Carney, R. Härtl, J. Ghajar. Marked reduction in mortality in patients with severe traumatic brain injury. J Neurosurg. 2013, 119(6), 1583–90.
69. GILLER, C.A., A.M. Giller, C.R. Cooper, M.R. Hatab. Evaluation of the cerebral hemodynamic response to rhythmic handgrip. J Appl Physiol. 2000, 88, 2205–13.
70. GJERRIS, F., J. Brennum. The cerebrospinal fluid, intracranial pressure and herniation of the brain. Clinical Neurology and Neurosurgery. 2004, 179–196, FADL's Forlag Aktieselskab, Copenhagen, Denmark.
71. GOSLING, R.G., G. Dunbar, D.H. King, D.L. Newman, C.D. Side, et al. The quantitative analysis of occlusive peripheral arterial disease by a non-intrusive ultrasonic technique. Angiology. 1971, 22, 52–5.
72. GREENBERG, M.S. (2010). Handbook of Neurosurgery. Thieme, New York, NY, USA, 7th edition.
73. HAMNER, J.W., M.A. Cohen, S. Mukai, L.A. Lipsitz, J.A. Taylor. Spectral indices of human cerebral blood flow control: responses to augmented blood pressure oscillations. J Physiol. 2004, 559, 965–73.
74. HANSON, E.J., R. E. Anderson, and T. M. Sundt. Comparison of 85 Kripton and 133 Xenon cerebral blood flow measurements before, during, and following focal, incomplete ischemia in the squirrel monkey. Circ Res. 1975, 36, 18–26.
75. HEADSENSE MEDICAL LTD (ISR). Apparatus and method for measuring intracranial pressure. Inventors: Guy WEINBERG, Surik PAPYAN. IPC: A61B5/03. US patent US20130197390 A1. 2013-08-01. United States Patent and Trademark Office [2014-11-21]. Link: http://www.google.ch/patents/US20130197390.

76. HERSCOVITCH, P., J. Markham, and M.E. Raichle. Brain blood flow measured with intravenous H2(15)O. I. Theory and error analysis. J. Nucl. Med. 1983, 24, 782–789.
77. HITACHI CONSTRUCTION MACHINERY CO., LTD., HIROJI KUCHIWAKI (JPN). Apparatus for recording intracranial pressure. Inventors: Naoki KAGEYAMA, Hiroji KUCHIWAKI, Junki ITO, Nobumitsu SAKUMA, Yukio OGURA, et al. IPC: A61B8/00. US patent US4971061 A1. 1990-11-20. United States Patent and Trademark Office [2014-11-22]. Link: https://www.google.com/patents/US4971061.
78. HITACHI CONSTRUCTION MACHINERY CO., LTD., HIROJI KUCHIWAKI (JPN). Method for recording intracranial pressure. Inventors: Naoki KAGEYAMA, Junki ITO, Nobumitsu SAKUMA, Yukio OGURA, et al. IPC: A61B8/08. European patent EP0413816 B1. 1994-12-07. European Patent Office [2014-11-10]. Link: https://google.com/patents/EP0413816B1.
79. HITACHI CONSTRUCTION MACHINERY CO., LTD., HIROJI KUCHIWAKI (JPN). Apparatus for measuring intracranial pressure. Inventors: Naoki KAGEYAMA, Junki ITO, Nobumitsu SAKUMA, Yukio OGURA. IPC: A61B5/00. European patent EP0327645 B1. 1994-08-10. European Patent Office [2014-11-10]. Link: http://google.com/patents/EP0327645B1.
80. HOLMAN, B.L., et al. Regional cerebral blood flow with the Anger camera. J. Nucl. Med. 1972, 13, 916–923.
81. HOEDT-RASMUSSEN, K., E. Sveinsdottir, and N.A. Lassen. Regional cerebral blood flow in man determined by intra-arterial injection of radioactive inert gas. Circ. Res. 1966, 18, 237–247.
82. HORI, D., C.W. Hogue, Jr., A. Shah, et al. Cerebral autoregulation monitoring with ultrasound-tagged near-infrared spectroscopy in cardiac surgery patients. Anesth Analg. 2015, 121(5), 1187-1193.
83. HUKKELHOVEN, C.W., E.W. Steyerberg, A.J. Rampen, et al. Patient age and outcome following severe traumatic brain injury: an analysis of 5600 patients. J Neurosurg. 2003, 99(4), 666–73.
84. HYNYNEN, K., and J. Sun. Trans-skull ultrasound therapy: the feasibility of using image-derived skull thickness information to correct the phase distortion. IEEE Trans Ultrason Ferroelectr Freq Control. 1999, 46(3), 752-5. doi: 10.1109/58.764862.
85. IMHOLZ, B.P.M., et al. Fifteen years experience with finger arterial pressure monitoring: assessment of the technology. Cardiovasc. Res. 1998, 38, 605–616.
86. INTA MEDICS, LTD (ISR). Noninvasive monitoring of intracranial pressure. Inventor: David MICHAELI. IPC: A61B5/00. European patent EP1182969A2. 2002-03-06. European Patent Office [2014-11-12]. Link: https://www.google.com/patents/EP1182969A2.
87. ISHIZU, K., et al. Extraction and retention of technetium-99m-ECD in human brain: dynamic SPECT and oxygen-15-water PET studies. J. Nucl. Med. 1996, 37, 1600–1604.

88. JOBES, D.R., E. Kennell, R. Bitner, E. Swenson, H. Wollman. Effects of Morphine-Nitrous Oxide Anesthesia on Cerebral Autoregulation. Anesthesiology. 1975, 42(1), 30-34.
89. JOHNSON, R., and QUIRK, W.H. (US). Apparatus and method for monitoring intracranial pressure. Inventors: Royce JOHNSON, William H. QUIRK, IV. IPC: A61B5/03. US patent US6231509 B1. 2001-05-15. United States Patent and Trademark Office [2014-11-22]. Link: https://www.google.com/patents/US6231509.
90. JOSHI, B. Predicting the limits of cerebral autoregulation during cardiopulmonary bypass. Anesth Analg. 2012, 114, 503-510.
91. KASHIF, F. (2011). Modeling and Estimation for Non-invasive Monitoring of Intracranial Pressure and Cerebrovascular Autoregulation. Doctoral thesis. Massachusetts Institute of Technology. Dept. of Electrical Engineering and Computer Science. Available from URL: http://hdl.handle.net/1721.1/66011.
92. KASPROWICZ, M., E. Schmidt, D.J. Kim, C. Haubrich, Z. Czosnyka, P. Smielewski, M. Czosnyka. Evaluation of the cerebrovascular pressure reactivity index using non-invasive finapres arterial blood pressure. Physiol Meas. 2010, 31, 1217–1228, 2010. Doi: http://dx.doi.org/10.1088/0967-3334/31/9/011.
93. KETY, S.S., and C.F. Schmidt. The determination of cerebral blood flow in man by the use of nitrous oxide in low concentrations. Am. J. Physiol. 1945, 143, 53–66.
94. KETY, S.S., and C.F. Schmidt, "The nitrous oxide method for the quantitative determination of cerebral blood flow in man: theory, procedure and normal values. J. Clin. Invest. 1948, 27, 476–483.
95. KNUDSEN, G.M., O.B. Paulson. Physiology of the brain. Clinical Neurology and Neurosurgery. 2004, 239–254. FADL's Forlag Aktieselskab, Copenhagen, Denmark.
96. LANG, E.W., J. Lagopoulos, J. Griffith, K. Yip, ET AL. Noninvasive cerebrovascular autoregulation assessment in traumatic brain injury: validation and utility. J Neurotrauma. 2003, 20, 69–75.
97. LANG, E.W., Y. Mudaliar, Y. Lagopoulos, N. Dorsch, et al. A review of cerebral autoregulation: assessment and measurements. Australasian Anaesthesia. 2005, 161–72. SOS Print and Media Group.
98. LASSEN, N.A. Cerebral blood flow and oxygen consumption in man. Physiol Rev. 1959, 39, 183–238.
99. LAVNIO, A., B. Ene-Iordache, I. Nodari, A. Girardini, et al. Cerebrovascular reactivity and autonomic drive following traumatic brain injury. Acta Neurochir Suppl. 2008, 102, 3–7.
100. LAZARIDIS, C., P. Smielewski, L.A. Steiner, K.M. Brady, P. Hutchinson, J.D. Pickard, M. Czosnyka. Optimal cerebral perfusion pressure: are we ready for it? Neurological Research. 2013, 35, 138-148.
101. LE ROUX, P. Invasive neurological and multimodality monitoring in the neuroICU in Textbook of Neurointensive Care, A. J. Layon, A. Gabrielli, and W. A. Friedman, Eds. 2013, 127–145, Springer, London.

102. LE ROUX, P., D.K. Menon, G. Citerio, P. Vespa, M.K. Bader, et al. Consensus summary statement of the International Multidisciplinary Consensus Conference on Multimodality Monitoring in Neurocritical Care : a statement for healthcare professionals from the Neurocritical Care Society and the European Society of Intensive Care Medicine. Intensive Care Med. 2014, 40(9), 1189-209. doi: 10.1007/s00134-014-3369-6.
103. LEAL-NOVAL, S.R., et al. Invasive and noninvasive assessment of cerebral oxygenation in patients with severe traumatic brain injury. Intens. Care Med. 2010, 36, 1309–1317.
104. LEVINE, B.D., C.A. Giller, L.D. Lane, J.C. Buckey, C.G. Blomqvist CG. Cerebral versus systemic hemodynamics during graded orthostatic stress in humans. Circulation. 1994, 90, 298–306.
105. LU, J., K.A. Mamum, and T. Chau. Online transcranial Doppler ultra-sonographic control of an onscreen keyboard. Front. Hum. Neurosci. 2014, 8, 199.
106. MADAN SAMUEL, M.M. Tympanic membrane displacement testing in regular assessment of intracranial pressure in eight children with shunted hydrocephalus. Journal of Neurosurgery. 1998, 88 (6), 983-995.
107. MARCHBANKS, J. (US). Method and apparatus for measuring intracranial fluid pressure. Inventor: Robert J. MARCHBANKS. US patent US4841986 A. 1989-06-27. United States Patent and Trademark Office [2014-11-26]. Link: https://www.google.com/patents/US4841986.
108. MARTIN, G.T., and H.F. Bowman. Validation of real-time continuous perfusion measurement. Med. Biol. Eng. Comput. 2000, 38, 319–325.
109. MASSACHUSETTS INSTITUTE OF TECHNOLOGY (US). Systems, devices and methods for noninvasive or minimally-invasive estimation of intracranial pressure and cerebrovascular autoregulation. Inventors: Faisal Mahmood KASHIF, Thomas HELDT, George Cheeran VARGHESE. IPC: A61B5/00. US patent US8366627 B2. 2013-02-05. United States Patent and Trademark Office [2014-11-22]. Link: https://www.google.com/patents/US8366627.
110. MASSACHUSETTS INSTITUTE OF TECHNOLOGY (US). Systems, devices and methods for noninvasive or minimally-invasive estimation of intracranial pressure and cerebrovascular autoregulation. Inventors: Faisal Mahmood KASHIF, Thomas HELDT, George Cheeran VARGHESE. IPC: A61B5/02. US patent US8821402 B2. 2014-09-02. United States Patent and Trademark Office [2014-11-22]. Link: https://www.google.com/patents/US8821402.
111. MENON, D.K. Procrustes, the traumatic penumbra, and perfusion pressure targets in closed head injury. Anesthesiology. 2003, 98(4), 805–7.
112. McCALL, M.L. Cerebral circulation and metabolism in toxemia of pregnancy; observations on the effects of veratrum viride and apresoline (1-hydrazinophthalazine). Am J Obstet Gynecol. 1953, 66(5), 1015-30.
113. MEDYS, INC. (US). Method and apparatus for measuring intracranial pressure. Inventor: Edwin C. MICK. IPC: A61B5/03. European patent EP0541671 A1.

1993-05-19. European Patent Office [2014-11-26]. Link: https://www.google.com/patents/EP0541671A1.
114. MELOT, C., et al. Estimation of cerebral blood flow at bedside by continuous jugular thermodiluation. J. Cereb. Blood Flow Metab. 1996, 16, 1263–1270.
115. MICIELI, G., C. Tassorelli, D. Bosone, A. Cavallini, E. Viotti, G. Nappi. Intracerebral vascular changes induced by cold pressor test: a model of sympathetic activation. Neurol Res. 1994, 16, 163–7.
116. MICHAELI, D., Z. Rappaport. Tissue resonance analysis; a novel method for noninvasive monitoring of intracranial pressure. Technical note. Journal of Neurosurgery. 2002, 96(6), 1132–1137.
117. MICK, E. C. Method and apparatus for the measurement of intracranial pressure. Inventor: Edwin C. MICK. IPC: A61B5/03. US patent US5074310 A. 1991-12-24. United States Patent and Trademark Office [2014-11-26]. Link: http://www.google.ch/patents/US5074310.
118. MICK, E. C. Method and apparatus for the measurement of intracranial pressure. Inventor: Edwin C. MICK. IPC: A61B5/03. US patent US5117835 A. 1992-06-02. United States Patent and Trademark Office [2014-11-26]. Link: https://www.google.ch/patents/US5117835.
119. MICRO-STAR INT'L CO, LTD (TW). Method and related system for measuring intracranial pressure. Inventors: Chung-You WU, Yi-Hong CHOU, Ta-Jung SU, Meng-Tsung LO. US patent US7682310 B2. 2010-03-23. United States Patent and Trademark Office [2014-11-21]. Link: https://www.google.com/patents/US7682310.
120. MOSS, S.M., et al. Long-term assessment of intracranial pressure using the tympanic membrane displacement measurement technique. European Journal of Pediatric Surgery. 1991, 1, 25-26.
121. MURPHY, G.S., E.A. Hessel,2nd, R.C. Groom. Optimal perfusion during cardiopulmonary bypass: an evidence-based approach. Anesth Analg. 2009, 108(5), 1394-1417.
122. NELSON, M.R., et al. Noninvasive measurement of central vascular pressures with arterial tonometry: clinical revival of the pulse pressure waveform? Mayo Clin. Proc. 2010, 85, 460–472.
123. NEURODX DEVELOPMENT LLC (US). Non-invasive intracranial pressure sensor. Inventor: Marek SWOBODA, Matias G. HOCHMAN, Frederick J. FRITZ. IPC: A61B5/021. US patent US20100204589 A1. 2010-08-12. United States Patent and Trademark Office [2014-11-21]. Link: https://www.google.com/patents/US20100204589.
124. NEW HEALTH SCIENCES, INC. (US). Systems and methods for investigating intracranial pressure. Inventors: Kevin E. CRUTCHFIELD, John DAVIDSON, Simon FITALL, Rakesh LALL, et al. IPC: A61B8/06. European patent EP1513451 A1. 2005-03-16. European Patent Office [2014-10-14]. Link: https://google.com/patents/EP1513451A1.
125. NEW HEALTH SCIENCES, INC. (US). Systems and methods for investigating intracranial pressure. Inventors: Kevin E. CRUTCHFIELD, B. Robert

MOZAYENI, John B. DAVIDSON, Simon FITALL, et al. IPC: A61B5/03. US Patent US7104958 B2. 2006-09-12. United States Patent and Trademark Office [2014-10-14]. Link: https://www.google.com/patents/US7104958.

126. NICOLET BIOMEDICAL INC. (US). Method and device for measuring the intra-cranial pressure in the skull of a test subject. Inventor: Klaus PAULAT. IPC: A61B5/05. US patent US6146336 A. 2000-11-14. United States Patent and Trademark Office [2014-11-20]. Link: https://www.google.com/patents/US6146336.
127. OBLAK, J.P., M. Zaletel, B. Zvan, T. Kiauta, T. Pogacnik. The effect of age on cerebrovascular reactivity to cold pressor test and head-up tilt. Acta Neurol Scand. 2002, 106, 30-3.
128. OGEDEGBE, G., and T. Pickering. Principles and techniques of blood pressure measurement. Cardiol. Clin. 2010, 28, 571–586.
129. OLIVEIRA, S.M. Non-invasive intracranial pressure system. Inventors: Sergio Mascarenhas OLIVEIRA, Gustavo Henrique Frigieri VILELA. IPC: A61B5/0205. US patent US20130085400 A1. 2013-04-04. United States Patent and Trademark Office [2014-11-19]. Link: https://www.google.com/patents/US20130085400.
130. OLSEN, K.S., L.B. Svendsen, F.S. Larsen, et al. Effect of labetalol on cerebral blood flow, oxygen metabolism and autoregulation in healthy humans. Br J Anaesth. 1995, 75(1), 51-54.
131. ONO, M., B. Joshi, K. Brady, et al. Risks for impaired cerebral autoregulation during cardiopulmonary bypass and postoperative stroke. Br J Anaesth. 2012, 109(3), 391- 398.
132. ONO, M., K. Brady, R.B. Easley, et al. Duration and magnitude of blood pressure below cerebral autoregulation threshold during cardiopulmonary bypass is associated with major morbidity and operative mortality. J Thorac Cardiovasc Surg. 2014, 147(1), 483-489.
133. ORSAN MEDICAL TECHNOLOGIES LTD (ISR). Non-invasive intracranial monitor. Inventors: Ben Zion POUPKO, Yosef REICHMAN, Alon RAPPAPORT, Shlomi BEN-ARI. IPC: A61B5/04. US patent US8211031 B2. 2012-07-03. United States Patent and Trademark Office [2014-11-27]. Link: https://www.google.tl/patents/US8211031.
134. PANERAI, R.B. The critical closing pressure of the cerebral circulation. Med Eng Phys. 2003, 25, 621–32.
135. PANERAI, R.B. Assessment of cerebral pressure autoregulation in humans—a review of measurement methods. Physiol Meas. 1998, 19, 305–38.
136. PAULSON, O.B., S. Strandgaard, L. Edvinsson. Cerebral autoregulation. Cerebrovasc Brain Metab Rev. 1990, 2, 161–92.
137. PAYNE, S. Cerebral autoregulation. Control of blood flow in the brain. Springer. 2016.
138. PETER, L., et al. A review of methods for non-invasive and continuous blood pressure monitoring: pulse transit time method is promising? 2014, 35, 271–282.

139. PETKUS, V., S. Krakauskaite, R. Chomskis, L. Bartusis, et al. Novel technology of non- invasive cerebrovascular autoregulation monitoring. Proc Comput-Based Med Syst. 2014, 427–30. Doi: 10.1109/CBMS. 2014.40.
140. PETKUS, V., A. Preiksaitis, S. Krakauskaite, R. Chomskis, et al. Novel Method and Device for Fully Non-Invasive Cerebrovascular Autoregulation Monitoring. Elektronika ir Elektrotechnika, 2014, 20, 8 (2014). Doi: http://dx.doi.org/10.5755/j01.eee.20.8.5464.
141. PETKUS, V., A. Ragauskas, A. Preiksaitis, S. Rocka, R. Chomskis, L. Bartusis. Innovative method of cerebrovascular autoregulation monitoring without ABP. Cerebrovasc Diseases. 2013, 35, 44.
142. PHYSIOSONICS, INC. (US). Methods for determining intracranial pressure non-invasively. Inventors: Pierre D. MOURAD, Brandt MOHR, Michel LIOT, Robert C.A. FREDERICKSON. IPC: A61B8/04. US patent No. US7547283 B2. 2009-06-16. United States Patent and Trademark Office [2014-11-21]. Link: https://www.google.com/patents/US7547283.
143. PRANEVICIUS, O., ET AL. (US). Noninvasive method to measure intracranial and effective cerebral outflow pressure. Inventors: Osvaldas PRANEVICIUS, Mindaugas PRANEVICIUS, Henrikas PRANEVICIUS et al. IPC: A61B5/02. US patent US8109880 B1. 2012-02-07. United States Patent and Trademark Office [2014-12-02]. Link: https://www.google.com/patents/US8109880.
144. RABOEL, P.H., J. Bartek, Jr., M. Andresen, B.M. Bellander, B. Romner. Intracranial Pressure Monitoring: Invasive versus Non-Invasive Methods—A Review. Crit Care Res Pract. 2012, 2012, ID 950393. doi: 10.1155/2012/950393.
145. PREIKSAITIS, A., S. Krakauskaite, V. Petkus, et al. Association of severe traumatic brain injury patient outcomes with duration of cerebrovascular autoregulation impairment events. Neurosurgery. 2016, 79(1), 75-82.
146. RAGAUSKAS, A., G. Daubaris, S. Rocka, and V. Petkus. Innovative technologies of head injury physiological monitoring. Ultragarsas. 2000, 4(37), 51-58.
147. RAGAUSKAS, A. ET AL. (LT). Method and Apparatus for Continuously Monitoring Intracranial Pressure. Inventors: Arminas RAGAUSKAS, Gediminas DAUBARIS, Vytautas PETKUS, Renaldas RAISUTIS. IPC: A61B8/14. US patent US20090287084 A1. 2009-11-19. United States Patent and Trademark Office [2014-12-01]. Link: https://www.google.com/patents/US20090287084.
148. RAGAUSKAS, A. (LT). Method and apparatus for noninvasive determination of the absolute value of intracranial pressure. Inventor: Arminas RAGAUSKAS. IPC: A61B5/03. US patent US20040087871 A1. 2004-05-06. United States Patent and Trademark Office [2014-12-01]. Link: https://www.google.ch/patents/US20040087871.
149. RAGAUSKAS, A., L. Bartusis, et al. Improved diagnostic value of a TCD-based non-invasive ICP measurement method compared with the sonographic ONSD method for detecting elevated intracranial pressure. Neurological Research. 2014, 36(7), 607-614.

150. RAGAUSKAS, A., G. Daubaris, A. Dziugys, V. Azelis, and V. Gedrimas. Innovative non-invasive method for absolute intracranial pressure measurement without calibration. Acta Neurochirurgica. 2005, 95, 357–361.
151. RAGAUSKAS, A., V. Petkus. Non-invasive technologies for intracranial pressure/volume measurement. IEEE/EMBS: 23rd Annual Conference-Proceedings. 2001, 1-4.
152. RAGAUSKAS, A., G. Daubaris, V. Petkus, R. Raisutis, R. Chomskis, et al. Non-invasive Technology for Monitoring of Cerebrovascular Autoregulation. Electronics and electrical engineering. 2008, 85, 93-96.
153. RAGAUSKAS, A., G. Daubaris, V. Ragaisis, V. Petkus. Implementation of non-invasive brain physiological monitoring concepts. Medical Engineering and Physics. 2003, 25, 667–678. doi: http://dx.doi.org/10.1016/S1350-4533(03)00082-1.
154. RASMUSSEN, L.S., K. Larsen, P. Houx, et al. The assessment of post-operative cognitive function. Acta Anaesthesiol Scand. 2001, 45(3), 275-289.
155. RASULO, F.A., A. Girardini, A. Lavinio, et al. Are optimal cerebral perfusion pressure and cerebrovascular autoregulation related to long-term outcome in patients with aneurysmal subarachnoid hemorrhage? J Neurosurg Anesthesiol. 2012, 24(1), 3-8.
156. REID, A., R.J. Marchbanks, D.M. Burge, A.M. Martin, D.E. Bateman, et al. The relationship between intracranial pressure and tympanic membrane displacement. British Journal of Audiology. 1990, 24 (2), 123-129. doi:10.3109/03005369009077853.
157. REINHARD, M., M. Roth, T. Muller, M. Czosnyka, J. Timmer, A. Hetzel. Cerebral autoregulation in carotid artery occlusive disease assessed from spontaneous blood pressure fluctuations by the correlation coefficient index. Stroke. 2003, 32, 2138–2144.
158. RICE CREEK MEDICAL, LLC (US). Non-invasive method and apparatus for monitoring intracranial pressure. Inventors: Scott C. MEYERSON, Paul Alexandre AVAN, Bela BUKI. US patent US6589189 B2. 2003-07-08. United States Patent and Trademark Office [2014-11-20]. Link: https://www.google.com/patents/US6589189.
159. ROATTA, S., G. Micieli, D. Bosone, G. Losano, R. Bini, et al. Effect of generalised sympathetic activation by cold pressor test on cerebral haemodynamics in healthy humans. J Auton Nerv Syst. 1998, 71, 159–66.
160. ROSENFELD, J., ET AL. (US). Method and apparatus for intracranial pressure estimation. Inventors: John G. ROSENFELD, Clark WATTS, Donald H. YORK. IPC: A61B5/03. US patent US4564022 A. 1986-01-14. United States Patent and Trademark Office [2014-11-21]. Link: http://www.google.ch/patents/US4564022.
161. RUNDSHAGEN, I. Post-operative cognitive dysfunction. Dtsch Arztebl Int. 2014, 111(8), 119-125.
162. SATO, T., et al. Accuracy of a continuous blood pressure monitor based on arterial tonometry. Hypertension. 1993, 21, 866–874.

163. SCHMIDT, B., ET AL. Non-invasive brain pressure determination system for human beings. Inventor: Bernhard SCHMIDT. IPC: A61B5/03. Deutch patent DE19600983 C1. 1997-05-28. Deutsches Patent- und Markenamt [2014-11-21]. Link: https://www.google.ch/patents/DE19600983C1?cl=en.
164. SCHMIDT, B., M. Czosnyka, A. Raabe, H. Yahya, et al. Adaptive non-invasive assessment of cerebral autoregulation and ICP. Stroke. 2003, 34, 84-89.
165. SCHMIDT, B., J.J. Schwarze, M. Weinhold, V. Lezaic, et al. Impaired autoregulation is associated with mortality in severe cerebral diseases. IJCNMH. 2014, 1(Suppl. 1), S18.
166. SCHOLKMANN, F., et al. A review on continuous wave functional near-infrared spectroscopy and imaging instrumentation and methodology. NeuroImage. 2014, 85, 6–27.
167. SCHONDORF, R., J. Benoit, T. Wein. Cerebrovascular and cardiovascular measurements during neurally mediated syncope induced by head-up tilt. Stroke. 1997, 28, 1564–8.
168. SHIMBLES, S., et al. Clinical comparison of tympanic membrane displacement with invasive intracranial pressure measurements. Physiological Measurement. 2005, 26 (6), 1085–1092. Doi:10.1088/0967-3334/26/6/017.
169. SCHUHMANN, M.U., J. Diedler, F. Neunhöfer, et al. Dose of cerebrovascular dysautoregulation, but not ICP/CPP, correlates to outcome in severe infant/pediatric traumatic brain injury. In Proc. of 16th International Symposium on Intracranial Pressure Neuromonitoring. 2016, 82-83.
170. SMITH, M. Monitoring intracranial pressure in traumatic brain injury. Anesthesia and Analgesia. 2008, 106, 240–248.
171. SMITH, M. Shedding light on the adult brain: a review of the clinical applications of near-infrared spectroscopy. Phil. Trans. R. Soc. 2011, 369, 4452–4469.
172. SMITH, N.B., and A. Webb (2011). Introduction to Medical Imaging: Physics, Engineering and Clinical Applications. Cambridge University Press, Cambridge, UK.
173. SORRENTINO, E., J. Diedler, M. Kasprowicz, K.P. Budohoski, et al. Critical thresholds for cerebrovascular reactivity after traumatic brain injury. Neurocrit Care. 2012, 16:258–66. doi: 10.1007/ s12028-011-9630-8.
174. SPRANGERS, R.L., K.H. Wesseling, A.L. Imholz, B.P. Imholz, W. Wieling. Initial blood pressure fall on stand up and exercise explained by changes in total peripheral resistance. J Appl Physiol. 1991, 70, 523–30.
175. STEINER, L.A., M. Czosnyka, S.K. Piechnik, et al. Continuous monitoring of cerebrovascular pressure reactivity allows determination of optimal cerebral perfusion pressure in patients with traumatic brain injury. Crit Care Med. 2002, 30(4), 733-738.
176. STETTIN, E., K. Paulat. Noninvasive intracranial pressure measurement using infrasonic emissions from the tympanic membrane. Journal of Clinical Monitoring and Computing. 2011, 25(3), 203-210.

177. STRANDGAARD, S. Autoregulation of cerebral blood flow in hypertensive patients. The modifying influence of prolonged antihypertensive treatment on the tolerance to acute, drug-induced hypotension. Circulation. 1976, 53(4), 720-7.
178. STRUMWASSER, A., et al. Sonographic Optic Nerve Sheath Diameter as an Estimate of Intracranial. Journal of Surgical Research. 2011, 170, 265–271.
179. SVIRI, G.E., D.W. Newell. Cerebral autoregulation following traumatic brain injury. Open Neurosurg J. 2010, 3, 6-9.
180. TBICARE PROJECT. Evidence based Diagnostic and Treatment Planning Solution for Traumatic Brain Injuries. From 2011-02-01 to 2014-07-31. Project ID: 270259. Funded under: FP7-ICT. [2017-04-03]. Available from URL: http://cordis.europa.eu/project/rcn/97956_en.html.
181. THIRD EYE DIAGNOSTICS, INC. Internet site. [2017-04-04]. Available from URL: http://www.3-e-d.com.
182. THIRD EYE DIAGNOSTICS, INC. (US). Methods and devices for assessing intracranial pressure. Inventors: BELLEZZA, Anthony and LAI, William. IPC: A61B5/00. US patent US9398861 B2. 2016-07-26. United States Patent and Trademark Office [2017-03-31]. Link: https://www.google.com/patents/US9398861.
183. THIRD EYE DIAGNOSTICS, INC. (US). Devices and methods for noninvasive measurement of intracranial pressure. Inventors: Terry A. FULLER, William LAI. IPC: A61B5/00. US patent US9585578 B2. 2017-03-07. United States Patent and Trademark Office [2017-03-31]. Link: https://www.google.com/patents/US9585578.
184. TIECKS, F.P., A.M. Lam, R. Aaslid, D. W. Newell. Comparison of static and dynamic cerebral autoregulation measurements. Stroke. 1995, 26, 1014–9.
185. TIECKS, F.P., A.M. Lam, B.F. Matta, S. Strebel, et al. Effects of the Valsalva maneuver on cerebral circulation in healthy adults. A transcranial Doppler Study. Stroke. 1995, 26, 1386–92.
186. TRAYSTMAN, R.J. The paper that completely altered our thinking about cerebral blood flow measurements. J. Appl. Physiol. 2004, 97, 1601–1602.
187. TREGGIARI, M.M., N. Schutz, N. D. Yanez, J. A. Romand. Role of intracranial pressure values and patterns in predicting outcome in traumatic brain injury: a systematic review. Neurocritical Care. 2007. 6, 104–112.
188. THE UNITED STATES OF AMERICA AS REPRESENTED BY THE ADMINISTRATION OF THE NATIONAL AERONAUTICS AND SPACE ADMINISTRATION (US). Non-invasive method and apparatus for monitoring intracranial pressure and pressure volume index in humans. Inventors: William T. YOST, John H. CANTRELL, Jr. IPC: A61B5/03. US patent US5617873 A. 1997-04-08. United States Patent and Trademark Office [2014-11-22]. Link: https://www.google.ch/patents/US5617873.
189. THE UNITED STATES OF AMERICA AS REPRESENTED BY THE ADMINISTRATION OF THE NATIONAL AERONAUTICS AND SPACE ADMINISTRATION (US). Method and apparatus for assessment of changes in intracranial pressure. Inventors: William T. YOST, John H. CANTRELL, Jr.

IPC: A61B8/08. US patent US6413227 B1. 2002-07-02. United States Patent and Trademark Office [2014-11-22]. Link: http://www.google.ch/patents/US6413227.

190. THE UNITED STATES OF AMERICA AS REPRESENTED BY THE ADMINISTRATION OF THE NATIONAL AERONAUTICS AND SPACE ADMINISTRATION (US). Method and apparatus for non-invasive measurement of changes in intracranial pressure. Inventors: William T. YOST, John H. CANTRELL, Jr. IPC: A61B5/021. US patent US6761695 B2. 2004-07-02. United States Patent and Trademark Office [2014-11-22]. Link: https://www.google.com/patents/US6761695.
191. THE UNITED STATES OF AMERICA AS REPRESENTED BY THE ADMINISTRATION OF THE NATIONAL AERONAUTICS AND SPACE ADMINISTRATION (US). Method and apparatus for determining changes in intracranial pressure utilizing measurement of the circumferential expansion or contraction of a patient's skull. Inventors: William T. YOST, John H. CANTRELL, Jr. IPC: A61B5/021. US patent US6746410 B2. 2004-06-08. United States Patent and Trademark Office [2014-11-22]. Link: https://www.google.ch/patents/US6746410.
192. THE REGENTS OF THE UNIVERSITY OF CALIFORNIA (US). Data mining system for noninvasive intracranial pressure assessment. Inventors: Xiao HU, Valeriy I. NENOV, Neil A. MARTIN. IPC: G05B13/02. US patent US8821408 B2. 2014-09-02. United States Patent and Trademark Office [2017-03-31]. Link: https://www.google.com/patents/US8821408.
193. THE REGENTS OF THE UNIVERSITY OF CALIFORNIA (US). Steady-state indicator of intracranial pressure using geodesic distance of icp pulse waveforms. Inventor: Xiao HU. IPC: A61B5/03. World patent WO2014055797 A1. 2014-04-10. World Intellectual Property Organization [2017-03-31]. Link: https://www.google.com/patents/WO2014055797A1.
194. THE REGENTS OF THE UNIVERSITY OF CALIFORNIA (US). Method for noninvasive intracranial pressure measurement. Inventor: Dipen N. SINHA. IPC: A61B5/03. US patent US6117089 A. 2000-09-12. United States Patent and Trademark Office [2014-11-21]. Link: https://www.google.com/patents/US6117089.
195. THE REGENTS OF THE UNIVERSITY OF COLORADO (US). Statistical, noninvasive measurement of intracranial pressure. Inventors: Gregory Zlatko GRUDIC and Steven Lee MOULTON. IPC: A61B5/03. European patent EP2536328 A1. 2012-12-26. European Patent Office [2014-11-10]. Link: https://encrypted.google.com/patents/EP2536328A1.
196. THE REGENTS OF THE UNIVERSITY OF COLORADO (US). Statistical, noninvasive measurement of intracranial pressure. Inventors: Gregory Zlatko GRUDIC, Steven Lee MOULTON, Isobe Jane MULLIGAN. IPC: A61B5/03. US patent US8512260 B2. United States Patent and Trademark Office [2014-11-20]. Link: https://www.google.com/patents/US8512260.

197. THE REGENTS OF THE UNIVERSITY OF MICHIGAN, Functional MRI Laboratory. [2017-03-17]. Available from URL: http://fmri.research.umich.edu/research/main_topics/asl.php.
198. THE UAB RESEARCH FOUNDATION (US). Oximetric tonometer with intracranial pressure monitoring capability. Inventor: Kurt R. DENNINGHOFF. IPC: A61B3/12. European patent EP1085835 A1. 2001-03-28. European Patent Office [2014-10-15]. Link: https://www.google.ch/patents/EP1085835A1.
199. THE UAB RESEARCH FOUNDATION (US). Oximetric tonometer with intracranial pressure monitoring capability. Inventor: Kurt R. DENNINGHOFF. IPC: A61B5/03. US patent US6390989 B1. 2002-05-21. United States Patent and Trademark Office [2014-10-14]. Link: https://www.google.com/patents/US6390989.
200. THE UNIVERSITY OF CAMBRIDGE, Department of Chemical Engineering and Biotechnology. [2017-03-15]. Available from URL: http://www.ceb.cam.ac.uk/research/groups/rg-p4g/archive-folder/pfg/inkjet-folder/droplet-formation
201. TUROWSKI, B., and P. Schramm. An appeal to standardize CT- and MR-perfusion. Clin. Neuroradiol. 2015, 25(Suppl 2), 205–210.
202. UAB VITTAMED (LT). Method and apparatus for non-invasively deriving and indicating of dynamic characteristics of the human and animal intracranial media. Inventors: Arminas RAGAUSKAS, Gediminas DAUBARIS. IPC: A61B8/04. US patent US5388583 A. 1995-02-14. United States Patent and Trademark Office [2014-12-01]. Link: https://www.google.ch/patents/US5388583.
203. UAB VITTAMED (LT). Method and apparatus for determining the pressure inside the brain. Inventors: Arminas RAGAUSKAS, Gediminas DAUBARIS, Algis DZIUGYS. IPC: A61B5/03. US patent US5951477 A. 1999-09-14. United States Patent and Trademark Office [2014-12-01]. Link: https://www.google.com/patents/US5951477.
204. UAB VITTAMED (LT). Method and apparatus for continuously monitoring intracranial pressure. Inventors: Arminas RAGAUSKAS, Gediminas DAUBARIS, Vytautas PETKUS, Renaldas RAISUTIS. IPC: A61B8/06. US patent US9168023 B2. 2015-10-27. United States Patent and Trademark Office [2017-04-01]. Link: https://www.google.com/patents/US9168023.
205. UAB VITTAMED (LT). Method and apparatus for determining the absolute value of intracranial pressure. Inventors: Arminas RAGAUSKAS, Vytautas PETKUS, Romanas CHOMSKIS, Rolandas ZAKELIS, et al. IPC: A61B8/00. US patent US8394025 B2. 2013-03-12. United States Patent and Trademark Office [2014-12-01]. Link: https://www.google.com/patents/US8394025.
206. UAB VITTAMED (LT). Method and apparatus for noninvasive determination of the absolute value of intracranial pressure. Inventor: Arminas RAGAUSKAS. IPC: A61B5/03. US patent US7147605 B2. 2006-12-12. United States Patent and Trademark Office [2014-12-01]. Link: https://www.google.com/patents/US7147605.

207. UAB VITTAMED TECHNOLOGIJOS (LT). Apparatus and method of non-invasive cerebrovascular autoregulation monitoring. Inventors: Arminas RAGAUSKAS, Gediminas DAUBARIS, Vytautas PETKUS, Renaldas RAISUTIS. IPC: A61B8/06. US Patent US7998075 B2. 2011-08-16. United States Patent and Trademark Office [2016-09-21]. Link: https://www.google.com/patents/US7998075.
208. URSINO, M. A mathematical study of human intracranial hydrodynamics part 1—The cerebrospinal fluid pulse pressure. Annals of Biomedical Engineering. 1988, 16(4), 379-401.
209. VILLRINGER, A., et al. Dynamic imaging with lanthanide chelates in normal brain: contrast due to magnetic susceptibility effects. Magn. Reson. Med. 1988, 6, 164–174.
210. VIRGINIA COMMONWEALTH UNIVERSITY (US). Method and apparatus for monitoring intra ocular and intra cranial pressure. Inventors: Martin M. LENHARDT, Kevin WARD. IPC: A61B. US Patent US8172769 B2. 2012-05-08. United States Patent and Trademark Office [2014-11-22]. Link: https://www.google.com/patents/US8172769.
211. VIRGINIA COMMONWEALTH UNIVERSITY (US). Sensor for non-invasively monitoring intracranial pressure. Inventors: Karla MOSSI, Vivek VIJAYWARGI, Pooma MANE, Richard Patrick PROFFIT et al. IPC: A61B8/04. World patent WO2010151734 A3. 2011-04-14. World Intellectual Property Organization [2015-03-31]. Link: https://www.google.com/patents/WO2010151734A3.
212. WAGNER, B.P., et al. Rapid assessment of cerebral autoregulation by near-infrared spectroscopy and a single dose of phenylephrine. Pediatr. Res. 2011, 69(5 Pt 1), 436–441.
213. WALOVITCH, R.C., et al. Characterization of technetium-99m-L, L- ECD for brain perfusion imaging, part 1: pharmacology of technetium-99m ECD in nonhuman primates. J. Nucl. Med. 1989, 30(11), 1892–1901.
214. WIELING, W., C.T. Krediet, et al. Initial orthostatic hypotension: review of a forgotten condition. Clin Sci (Lond). 2007, 112, 157–65.
215. WILSON, E.M., and J.H. Halsey. Bilateral jugular venous blood flow by thermal dilution. Stroke. 1970, 1, 348–355.
216. XIE, X.Z. Noninvasive intracranial pressure estimation by orbital subarachnoid space measurement: the Beijing Intracranial and Intraocular Pressure (iCOP) study. Critical Care. 2013, 17(4), 1-12.
217. XU, P., et al. Improved Noninvasive Intracranial Pressure Assessment With Nonlinear Kernel Regression. IEEE transactions on information technology in biomedicine. 2010, 14, 4.
218. YAM, A.T., E.W. Lang, J. Lagopoulos, K. Yip, et al. Cerebral autoregulation and ageing. J Clin Neurosci. 2005, 12, 643–6.
219. ZAKELIS, Rolandas (2012). Analysis of the electronic system for human intracranial pressure non-invasive monitoring. Kaunas University of Technology, Faculty of Telecommunications and Electronics, Departament of

Electronics and Measurements Systems, Departament of Telecommunications, Telematics Science Laboratory. [2017-01-24]. Available from URL: http://archive.ktu.lt/sites/default/files/zakelis_rolandas_santrauka_a5_2012_04_03k.pdf.
220. ZHANG, R., S. Witkowski, Q. Fu, J.A. Claassen, B.D. Levine. Cerebral hemodynamics after short- and long- term reduction in blood pressure in mild and moderate hypertension. Hypertension. 2007, 49(5), 1149–55.
221. ZWEIFEL, C., G. Castellani, M. Czosnyka, E. Carrera, et al. Continuous assessment of cerebral autoregulation with near-infrared spectroscopy in adults after subarachnoid haemorrhage. Stroke. 2010, 41, 1963–1968.

PUBLICATIONS

Articles published in scientific journals assigned to international databases

"ISI Web of Science" publications with citation index

1. Petkus, Vytautas; Preikšaitis, Aidanas; **Krakauskaitė, Solventa**; Zubaviciute, Erika; Ročka, Saulius; Rastenyte, Daiva; Vosylius, Saulius; Ragauskas, Arminas. Benefit on optimal cerebral perfusion pressure targeted treatment for traumatic brain injury patients // Journal of Critical Care. 2017, vol. 41, pg. 49-55. [MEDLINE; Science Citation Index Expanded (Web of Science)]. [IF: 2,191 (2013)]. [Indėlis: 0,125]. DOI: http://dx.doi.org/10.1016/j.jcrc.2017.04.029
2. Preikšaitis, Aidanas; **Krakauskaitė, Solventa**; Petkus, Vytautas; Ročka, Saulius; Chomskis, Romanas; Dagi, Teodoro Forcht; Ragauskas, Arminas. Association of severe traumatic brain injury patient outcomes with duration of cerebrovascular autoregulation impairment events // Neurosurgery. Hagerstown, MD: Lippincott Williams & Wilkins. ISSN 0148-396X. 2016, vol. 79, iss. 1, p. 75-82. [Science Citation Index Expanded (Web of Science); MEDLINE; PubMed; Index medicus]. [IF: 3,780, AIF: 2,715 (E, 2015)]. [M.kr. 02B]. [Indėlis: 0.571; Persk. indėlis: 0.571].
3. Petkus, Vytautas; **Krakauskaitė, Solventa**; Preikšaitis, Aidanas; Ročka, Saulius; Chomskis, Romanas; Ragauskas, Arminas. Association between the outcome of traumatic brain injury patients and cerebrovascular autoregulation, cerebral perfusion pressure, age, and injury grades // Medicina. Amsterdam: Elsevier. ISSN 1010-660X. 2016, vol. 52, iss. 1, p. 46-53. [Science Citation Index Expanded (Web of Science); MEDLINE; Science Direct; IndexCopernicus; Scopus]. [IF: 0,609, AIF: 4,043 (E, 2015)]. [M.kr. 02B]. [Indėlis: 0.667; Persk. indėlis: 0.667].
4. Petkus, Vytautas; Preikšaitis, Aidanas; **Krakauskaitė, Solventa**; Chomskis, Romanas; Ročka, Saulius; Kalasauskienė, Aurija; Kalvaitis, Evaldas; Ragauskas, Arminas. Novel method and device for fully non- invasive cerebrovascular autoregulation monitoring // Elektronika ir elektrotechnika = Electronics and electrical engineering. Kaunas: KTU. ISSN 1392-1215. 2014, Vol. 20, no. 8, p. 24-29. [Science Citation Index Expanded (Web of Science); Inspec; Computers & Applied Sciences Complete; Central & Eastern European Academic Source; Scopus]. [IF: 0,561, AIF: 1,798 (E, 2014)]. [M.kr. 01T]. [Indėlis: 0.625; Persk. indėlis: 0.625].

Articles published in other referenced international databases

1. **Krakauskaitė, Solventa**; Petkus, Vytautas; Bartušis, Laimonas; Žakelis, Rolandas; Chomskis, Romanas; Preikšaitis, Aidanas; Ragauskas, Arminas; Matijošaitis, Vaidas; Petrikonis, Kęstutis; Rastenytė, Daiva. Accuracy, precision, sensitivity, and specificity of noninvasive ICP absolute value measurements // Acta neurochirurgica supplementum : Intracranial pressure and brain monitoring XV : 15th international conference on intracranial pressure and brain monitoring (ICP), November 6-10, 2013 Singapore, Singapore / edited by Beng-Ti Ang.

Cham: Springer. ISSN 0065-1419. 2016, vol. 122, p. 317-321. [M.kr. 02B]. [Indėlis: 0.6; Persk. indėlis: 0.6].

2. Petkus, Vytautas; **Krakauskaitė, Solventa**; Žakelis, Rolandas; Bartušis, Laimonas; Chomskis, Romanas; Ragauskas, Arminas; Preikšaitis, Aidanas; Ročka, Saulius. Novel technology of non-invasive cerebrovascular autoregulation monitoring // 2014 IEEE 27th International symposium on computer-based medical systems (CBMS), 27-29 May, 2014, New York / IEEE Computer Society. Piscataway, NJ: IEEE, 2014, ISBN 9781479944354. p. 427-430. [M.kr. 01T]. [Indėlis: 0.75; Persk. indėlis: 0.75].
3. **Krakauskaitė, Solventa**; Petkus, Vytautas; Žakelis, Rolandas; Bartušis, Laimonas; Chomskis, Romanas; Ragauskas, Arminas. Innovative computerized non-invasive intracranial pressure measurement technology and its clinical validation // 2014 IEEE 27th International symposium on computer-based medical systems (CBMS), 27-29 May, 2014, New York / IEEE Computer Society. Piscataway, NJ: IEEE, 2014, ISBN 9781479944354. p. 451-454. [M.kr. 01T]. [Indėlis: 1; Persk. indėlis: 1].

Abstracts in international referenced scientific publications

In publications of international conferences

1. Preikšaitis, Aidanas; Petkus, Vytautas; Zubavičiūtė, Erika; **Krakauskaitė, Solventa**; Ročka, Saulius; Rastenytė, Daiva; Vosylius, Saulius; Ragauskas, Arminas. Benefit of optimal cerebral perfusion pressure targeted treatment for traumatic brain injury patients // Journal of cerebral blood flow & metabolism : Brain & Brain pet 2017 : abstract book. Thousands oaks, CA: SAGE. ISSN: 0271-678X, eISSN: 1559-7016. 2017, vol. 37, iss. 1, suppl, p. 441-442. [Indėlis: 0,125].
2. Petkus, Vytautas; Kumpaitienė, Birutė; Žakelis, Rolandas; **Krakauskaitė, Solventa**; Chomskis, Romanas; Švagždienė, Milda; Širvinskas, Edmundas; Benetis, Rimantas; Ragauskas, Arminas. Non-invasive cerebral autoregulation monitoring during cardiac surgery with cardiopulmonary bypass // Journal of cerebral blood flow & metabolism : Brain & Brain pet 2017 : abstract book. Thousands oaks, CA: SAGE. ISSN: 0271- 678X, eISSN: 1559-7016. 2017, vol. 37, iss. 1, suppl, p. 244-245. [Indėlis: 0,111].
3. Žakelis, Rolandas; Ragauskas, Arminas; Širvinskas, Edmundas; Benetis, Rimantas; Kumpaitienė, Birutė; Švagždienė, Milda; Chomskis, Romanas; **Krakauskaitė, Solventa**; Petkus, Vytautas. Mean arterial pressure and impaired cerebrovascular autoregulation // International journal of stroke : Abstracts for the 22nd Meeting of the European Society of Neurosonology and Cerebral Hemodynamics (ESNCH), 19–21 May 2017, Berlin. London: SAGE. ISSN: 1747-4930. 2017, vol. 12, iss. 1S, p. 53. [Indėlis: 0,111].
4. Petkus, Vytautas; Žakelis, Rolandas; Bartušis, Laimonas; **Krakauskaitė, Solventa**; Preikšaitis, Aidanas; Chomskis, Romanas; Ročka, Saulius; Ragauskas, Arminas. Prospective comparative clinical study of non-invasive cerebrovascular

autoregulation monitor // International journal of stroke : Abstracts for the 22nd Meeting of the European Society of Neurosonology and Cerebral Hemodynamics (ESNCH), 19–21 May 2017, Berlin. London: SAGE. ISSN: 1747-4930. 2017, vol. 12, iss. 1S, p. 54. [Indėlis: 0,125].

5. Preikšaitis, Aidanas; Petkus, Vytautas; **Krakauskaitė, Solventa**; Chomskis, Romanas; Ročka, Saulius; Vosylius, Saulius; Rastenytė, Daiva; Ragauskas, Arminas. Association of severe traumatic brain injury patients' outcomes with cerebrovascular autoregulation impairment events and optimal cerebral perfusion pressure // 16th International Symposium on Intracranial Pressure & Neuromonitoring (ICP) in conjunction with The 6th Annual Meeting of the Cerebral Autoregulation Research Network, June 28 - July 2, 2016, Cambridge, USA. [S.l.]: [s.n.], 2016. p. 81-82. [Indėlis: 0,125].
6. Žakelis, Rolandas; Kumpaitienė, Birutė; **Krakauskaitė, Solventa**; Petkus, Vytautas; Chomskis, Romanas; Švagždienė, Milda; Širvinskas, Edmundas; Benetis, Rimantas; Ragauskas, Arminas. Non-invasive cerebral autoregulation monitoring during cardiac surgery with cardiopulmonary bypass // 16th International Symposium on Intracranial Pressure & Neuromonitoring (ICP) in conjunction with the 6th Annual Meeting of the Cerebral Autoregulation Research Network, June 28 - July 2, 2016, Cambridge, USA. [S.l.]: [s.n.], 2016. p. 325-326. [Indėlis: 0,111].
7. Preikšaitis, Aidanas; Petkus, Vytautas; **Krakauskaitė, Solventa**; Chomskis, Romanas; Ročka, Saulius; Rastenytė, Daiva; Ragauskas, Arminas. Association of severe traumatic brain injury patients' outcomes with cerebrovascular autoregulation impairment events // Brain Injury : accepted abstracts from the International Brain Injury Association's Eleventh World Congress on Brain Injury. New York: Taylor & Francis. ISSN: 0269- 9052. 2016, vol. 30, no. 5-6, p. 640, no. 0416. [MEDLINE; Science Citation Index Expanded (Web of Science)] [Indėlis: 0,142].
8. Ragauskas, Arminas; Petkus, Vytautas; **Krakauskaitė, Solventa**; Chomskis, Romanas; Preikšaitis, Aidanas; Ročka, Saulius. Association of the outcome of traumatic brain injury patients with cerebrovascular autoregulation impairment events // IPEM conferences : 5th International Meeting on Cerebral Haemodynamic Regulation 13-14 July 2015, Chilworth Manor, Southampton / Organised by the Cerebral Autoregulation Research Network (CARNet). York: Institute of Physics and Engineering in Medicine, 2015. p. 78-83. [Indėlis: 0,166].
9. Ragauskas, Arminas; Petkus, Vytautas; **Krakauskaitė, Solventa**; Chomskis, Romanas; Preikšaitis, Aidanas. Prospective comparative clinical study of non-invasive cerebrovascular autoregulation monitor // IPEM conferences : 5th International Meeting on Cerebral Haemodynamic Regulation 13-14 July 2015, Chilworth Manor, Southampton / Organised by the Cerebral Autoregulation Research Network (CARNet). York: Institute of Physics and Engineering in Medicine, 2015. p. 102-103. [Indėlis: 0,200].

10. Ragauskas, Arminas; Bartušis, Laimonas; Žakelis, Rolandas; Daubaris, Gediminas; **Krakauskaitė, Solventa**; Matijošaitis, Vaidas; Petrikonis, Kęstutis; Rastenytė, Daiva. Accuracy, precision, sensitivity and specificity of non-invasive absolute intracranial pressure value measurement method // Cerebrovascular diseases. Basel: Karger. ISSN: 1015-9770. 2014, Vol. 37, suppl. 2, p. 52-53. [Indėlis: 0,125].
11. **Krakauskaitė, Solventa**. Accuracy, precision, sensitivity and specificity of non-invasive ICP absolute value measurements // Breaking boundaries of science, technology, medicine, art, and healthcare policy : 11th annual world congress of SBMT, 17-19 March, 2014, Sydney, Australia / Society for Brain Mapping and Therapeutics. [S.l: s.n, 2014. p. 86-87. [Indėlis: 1,000].

In publication of national conference

1. **Krakauskaitė, Solventa**; Žakelis, Rolandas; Petkus, Vytautas; Preikšaitis, Aidanas; Ragauskas, Arminas. Inovatyvus neinvazinis smegenų intrakranijinio slėgio matuoklis // Fizinių ir technologijos mokslų tarpdalykiniai tyrimai : 5-oji jaunųjų mokslininkų konferencija, 2015 m. vasario 10 d. : pranešimų tezės / Lietuvos mokslų akademija [elektroninis išteklius]. [S.l.: s.n.], 2015. p. 58-59. [Indėlis: 0,200].

SL344. 2017-06-28, 15,75 leidyb. apsk. l. Tiražas 32 egz. Užsakymas 217.
Išleido Kauno technologijos universitetas, K. Donelaičio g. 73, 44249 Kaunas
Spausdino leidyklos „Technologija“ spaustuvė, Studentų g. 54, 51424 Kaunas

ANNEX

Annex 1. A summary of the patients' clinical data

No.	Age	Sex	Trauma type	GCS	Diagnosis and CT findings	HCT score	Surgery type	GOS after hospitalisation	GOS 6m.
1	58y	M	Fall	8	ASDH, DAI	7	Craniotomy, evacuation of ASDH, subdural ICP	4	4
2	50y	M	Traffic accident	7	DAI	2	Intraparenchymal ICP	1	1
3	66y	M	Unknown	8	Traumatic ICH, DAI	8	Craniotomy, evacuation of ICH, subdural ICP	3	3
4	20y	M	Traffic accident	4	DAI	5	Intraparenchymal ICP	3	4
5	53y	F	Unknown	7	DAI	2	Intraparenchymal ICP	2	2
6	65y	M	Fall	7	DAI	5	Intraparenchymal ICP	2	1
7	58y	M	Fall	5	Traumatic ICH, DAI	9	Craniotomy, evacuation of ICH, subdural ICP	3	3
8	47y	M	Fall	5	ASDH, traumatic ICH	5	Craniotomy, evacuation of haematomas, subdural ICP	2	1
9	19y	M	Traffic accident	8	Depression fracture, DAI	0	Depression fracture elimination, subdural ICP	4	5
10	24y	F	Fall	8	DAI	5	Intraparenchymal ICP	4	4
11	30y	M	Violence	4	Traumatic ICH, EDH, SDH DAI	6	Craniotomy, evacuation of haematomas, subdural ICP	4	4
12	49y	M	Fall	4	Traumatic ICH, DAI	14	Craniotomy evacuation of haematomas, subdural ICP	3	3
13	18y	M	Traffic accident	3	DAI	5	Intraparenchymal ICP	2	3
14	20y	M	Traffic accident	7	DAI	0	Intraparenchymal ICP	3	4

15	53y	M	Fall	3	ASDH, DAI	14	Craniotomy, evacuation of SDH, subdural ICP	1	1
16	32y	M	Fall	7	Traumatic ICH, DAI	5	Craniotomy, evacuation of haematomas, subdural ICP	3	4
17	45y	M	Fall	3	Traumatic ICH, DAI	5	Craniotomy, evacuation of haematomas, subdural ICP	3	3
18	24y	M	Traffic accident	5	DAI	5	Intraparenchymal ICP	3	5
19	21y	M	Violence	5	DAI	0	Intraparenchymal ICP	3	4
20	18y	F	Traffic accident	4	DAI	5	Intraparenchymal ICP	2	2
21	19y	M	Traffic accident	5	DAI	5	Intraparenchymal ICP	3	4
22	36y	M	Unknown	6	DAI	8	Intraparenchymal ICP	1	1
23	20y	M	Traffic accident	4	DAI, posterior fossa EDH	0	Craniectomy of posterior fossa, evacuation of EDH, intraparenchymas ICP	3	4
24	47y	F	Violence	5	Traumatic ICH, DAI	4	Intraparenchymal ICP	2	1
25	21y	M	Fall	5	DAI	4	Intraparenchymal ICP	3	4
26	62y	M	Unknown	7	DAI	-	Intraparenchymal ICP	3	3
27	21y	M	Traffic accident	3	Traumatic EDH (including posterior fossa), SDH, DAI	6	Craniotomy, evacuation of haematomas, intraventricular ICP, posterior fossa decompression	3	4
28	48y	M	Unknown	6	Traumatic ICH, DAI	11	Craniotomy, evacuation of haematomas, subdural ICP	1	1
29	49y	M	Unknown	5	DAI	14	Intraparenchymal ICP	1	1
30	46y	M	Fall	4	DAI	2	Intraparenchymal ICP	2	1
31	21y	F	Traffic accident	6	DAI	-1	Intraparenchymal ICP	4	5
32	23y	M	Traffic accident	7	DAI	4	Intraparenchymal ICP	3	4
33	31y	F	Traffic accident	7	DAI	2	Intraparenchymal ICP	4	5

34	19y	M	Traffic accident	3	DAI	0	Intraparenchymal ICP	3	5
35	44y	M	Fall	7	Traumatic ICH, DAI	11	Craniotomy, intraparenchymal ICP	3	4
36	44y	M	Fall	6	DAI	1	Intraparenchymal ICP	3	4
37	49y	M	Unknown	13	Traumatic ICH, DAI	5	Evacuation of haematomas, intraparenchymal ICP	3	4
38	31y	M	Traffic accident	7	DAI	2	Intraparenchymal ICP	5	5
39	60y	F	Fall	3	DAI	4	Intraparenchymal ICP	1	1

HCT score – Helsinki computerized tomography scoring system.